

Role of the DREAM complex in mouse embryonic stem cells and identification of ZO-2 as a new LIN9 interacting protein

Dissertation zur Erlangung des
naturwissenschaftlichen Doktorgrades
der Bayerischen Julius-Maximilians-Universität Würzburg



vorgelegt von
Jasmina Esterlechner
aus
Starnberg

Würzburg 2013

Eingereicht am:

Mitglieder der Promotionskommission:

Vorsitzender:

Gutachter: Prof. Dr. Stefan Gaubatz

Gutachter: Prof. Dr. Georg Krohne

Tag des Promotionskolloquiums:

Doktorurkunde ausgehändigt am:

Abstract

The DREAM complex plays an important role in regulation of gene expression during the cell cycle. It was previously shown that the DREAM subunits LIN9 and B-MYB are required for early embryonic development and for the maintenance of the inner cell mass *in vitro*. In this work the effect of LIN9 or B-MYB depletion on embryonic stem cells (ESC) was examined. It demonstrates that LIN9 and B-MYB knock down changes the cell cycle distribution of ESCs and results in an accumulation of cells in G2 and M and in an increase of polyploid cells. By using genome-wide expression studies it was revealed that the depletion of LIN9 leads to downregulation of mitotic genes and to upregulation of differentiation-specific genes. ChIP-on chip experiments determined that mitotic genes are direct targets of LIN9 while lineage specific markers are regulated indirectly. Importantly, depletion of LIN9 does not alter the expression of the pluripotency markers Sox2 and Oct4 and LIN9 depleted ESCs retain alkaline phosphatase activity. I conclude that LIN9 is essential for proliferation and genome stability of ESCs by activating genes with important functions in mitosis and cytokinesis.

The exact molecular mechanisms behind this gene activation are still unclear as no DREAM subunit features a catalytically active domain. It is assumed that DREAM interacts with other proteins or co-factors for transcriptional activation. This study discovered potential binding proteins by combining *in vivo* isotope labeling of proteins with mass spectrometry (MS) and further analysed the identified interaction of the tight junction protein ZO-2 with DREAM which is cell cycle dependent and strongest in S-phase. ZO-2 depletion results in reduced cell proliferation and decreased G1 gene expression. As no G2/M genes, typical DREAM targets, are affected upon ZO-2 knock down, it is unlikely that ZO-2 binding is needed for a functional DREAM complex. However, this work demonstrates that with (MS)-based quantitative proteomics, DREAM interacting proteins can be identified which might help to elucidate the mechanisms underlying DREAM mediated gene activation.

Zusammenfassung

Der DREAM Komplex spielt eine bedeutende Rolle in der Genregulation im Verlauf des Zellzyklus. Es wurde gezeigt, dass die DREAM Untereinheiten LIN9 und B-MYB für die frühe Embryogenese und den *in vitro* Erhalt der inneren Zellmasse erforderlich sind. In der vorliegenden Arbeit wurde die Auswirkung von LIN9 und B-MYB Depletierung auf embryonale Stammzellen untersucht. Es zeigt sich, dass Depletion von LIN9 und B-MYB die Zellzyklus-Verteilung von embryonalen Stammzellen beeinflusst, zur Akkumulation der Zellen in G2 und M Phase und zu erhöhter Polyploidie führt. Genomweite Expressionsstudien ergaben, dass die Verringerung von LIN9 in der Runterregulierung von mitotischen und in der Hochregulierung von differenzierungsspezifischen Genen resultiert. ChIP-on-chip Experimente ermittelten, dass LIN9 Mitosegene als direkte Ziele hat, wohingegen entwicklungslinienspezifische Marker indirekt reguliert werden. Wesentlich ist, dass LIN9 Depletion nicht die Expression der Pluripotenzgene Oct4 oder Sox2 beeinflusst und embryonale Stammzellen ihre Alkaline Phosphatase Aktivität behalten. Daraus lässt schließen, dass LIN9 essentiell für die Proliferation und genomische Stabilität von embryonalen Stammzellen ist, in dem es Gene aktiviert, die wichtige Funktionen in Mitose und Zytokinese ausüben.

Der exakte Mechanismus hinter der Genaktivierung ist noch nicht geklärt, da keine DREAM Untereinheit eine katalytisch aktive Domäne aufweist. Vermutlich ist die Interaktion mit weiteren Proteinen oder Co-Faktoren für die Genaktivierung vonnöten. Diese Studie entdeckte mit *in vivo* Isotop-Markierung von Proteinen und Massenspektrometrie (MS) potentielle Bindungspartner und untersuchte die identifizierte Bindung mit dem Tight Junction Protein ZO-2 genauer. Diese Bindung ist zellzyklus-abhängig und ist am stärksten während der S-Phase. ZO-2 Depletion führt zu reduzierter Zellproliferation und verringerter G1-Genexpression. Da keine G2/M Gene, typische DREAM Ziele, von einer ZO-2 Depletion beeinflusst werden, ist es unwahrscheinlich, dass die ZO-2 Bindung für einen funktionellen DREAM Komplex benötigt wird. Jedoch demonstriert diese Studie, dass mit (MS)-basierender, quantitativer Proteomik DREAM interagierende Proteine identifiziert werden können. Dies ist hilfreich um die Mechanismen hinter der DREAM vermittelten Genaktivierung aufzuklären.

Contents

1. Introduction	2
1.1. The mammalian cell cycle	2
1.1.1. Cell cycle regulation	3
1.1.1.1. Cyclin-dependent kinases (CDKs) act as cell cycle regulators	3
1.1.1.2. Control of CDK Activation	3
1.1.1.3. pRB pathway	6
1.1.1.4. CDK inhibitors	8
1.2. The mammalian DREAM complex	8
1.2.1. G2/M gene regulation by CDE/CHR promoter elements	10
1.2.2. The subunit LIN9	11
1.2.3. The transcription factor B-MYB	12
1.3. Pluripotent stem cells and differentiation	15
1.3.1. Stem cells and pluripotency	15
1.3.1.1. Transcriptional regulation of pluripotency	16
1.3.1.2. Epigenetic control of pluripotency	17
1.3.2. The cell cycle in mouse stem cells and its change during differentiation	18
1.3.3. Differentiation	20
1.3.4. Aim of thesis	20
2. Materials and Methods	22
2.1. Materials	22
2.1.1. Devices	22
2.1.2. Chemical stocks	22
2.1.3. Transfection reagents	23
2.1.4. Enzymes	23
2.1.5. Molecular Kits & DNA/Protein Markers	24
2.1.5.1. Molecular Kits	24
2.1.5.2. Markers	24

2.1.6.	Buffers	24
2.1.6.1.	General Buffers	24
2.1.6.2.	Buffers for whole cell lysates and nuclear extracts	26
2.1.6.3.	Buffers for immunoprecipitation with BioTag-ES cells	27
2.1.6.4.	Buffers for immunoblotting	28
2.1.6.5.	Buffers for chromatin immunoprecipitation with BioTag ES cells (BioChIP)	30
2.1.6.6.	Buffers for flow cytometry (FACS)	30
2.1.7.	Antibodies	31
2.1.7.1.	Primary antibodies	31
2.1.7.2.	Secondary antibodies	32
2.1.7.3.	Beads	32
2.1.8.	Plasmids	33
2.1.8.1.	Plasmids for overexpression	33
2.1.8.2.	Plasmids for RNA knock down	33
2.1.9.	Primers	33
2.1.9.1.	Primers for quantitative RT-PCR	33
2.1.9.1.1.	Human primers	33
2.1.9.1.2.	Mouse primers	34
2.1.9.2.	Primers for chromatin immunoprecipitation	35
2.1.9.2.1.	Human primers for ChIP	35
2.1.9.2.2.	Mouse primers for ChIP	36
2.1.10.	siRNA sequences	37
2.1.11.	Cell lines, cell culture media and treatments	37
2.1.11.1.	Media and additives	37
2.1.11.2.	SILAC media and additives	37
2.1.11.3.	Cell lines / media	38
2.1.11.4.	Transfection reagents	38
2.2.	Methods	38
2.2.1.	Cell Culture	38
2.2.1.1.	Passaging of Cells	38
2.2.1.2.	Transient transfection	39
2.2.1.3.	Alkaline phosphatase activity test	39
2.2.1.4.	Embryoid Body (EB) formation	39
2.2.1.5.	SILAC cell culture	39

2.2.1.6.	Synchronisation of T98G cells	40
2.2.1.7.	Synchronisation of U2OS cells	40
2.2.1.8.	Synchronisation of ES cells	40
2.2.1.9.	Determination of cell cycle phases by flow cytometry (FACS)	40
2.2.1.10.	Determination of cells in S-phase by BrdU-FACS	40
2.2.1.11.	Determination of cells in M-phase by MPM2-FACS	41
2.2.1.12.	Growth Curve of U2OS and T98G cells	41
2.2.2.	Expression Analysis	42
2.2.2.1.	RNA isolation	42
2.2.2.2.	cDNA synthesis by reverse transcription	42
2.2.2.3.	Quantitative real-time PCR (qRT-PCR)	42
2.2.2.4.	Agilent Microarray	43
2.2.3.	Biochemical Methods	43
2.2.3.1.	Whole cell lysates	43
2.2.3.2.	Nuclear Extracts of ES cells	44
2.2.3.3.	Protein concentration (Bradford)	44
2.2.3.4.	Immunoprecipitation (IP)	44
2.2.3.5.	SDS-polyacrylamide gel electrophoresis (SDS-PAGE)	45
2.2.3.6.	Nupage [®] Bis-Tris gel electrophoresis	45
2.2.3.7.	Immunoblotting	45
2.2.3.8.	SILAC Immunoprecipitation for mass spectrometry	46
2.2.3.9.	Chromatin immunoprecipitation of biotinylated LIN9 ES cells (Bio-ChIP)	47
2.2.3.10.	Blocking beads for ChIP	48
2.2.3.11.	ChIP-on-chip	48
2.2.4.	Molecular Biology	49
2.2.4.1.	Analytical isolation of plasmid DNA from bacteria (DNA- Miniprep)	49
2.2.4.2.	Preparative isolation of plasmid DNA from bacteria (DNA- Maxiprep)	49
2.2.4.3.	Isolation of plasmid DNA fragments from agarose gels	49
2.2.4.4.	Isolation of PCR products after restriction	49
2.2.4.5.	Polymerase chain reaction (PCR)	50
2.2.4.6.	Agarose gel electrophoresis	51
2.2.4.7.	Enzymatic restriction	51

2.2.4.8.	Ligation	51
2.2.4.9.	Transformation of E.coli	52
3.	Results	53
3.1.	Role of the DREAM complex in murine ES cells	53
3.1.1.	Effects of LIN9 or B-MYB depletion on ES cell proliferation	53
3.1.1.1.	Depletion of LIN9 or B-MYB leads to G2/M arrest	54
3.1.1.2.	Impaired embryoid body formation after LIN9 or B-MYB depletion	55
3.1.2.	Gene regulation by the DREAM complex in ES cells	57
3.1.2.1.	DREAM binds promoters of G2/M target genes in ES cells but not the pluripotency gene Sox2	57
3.1.2.2.	LIN9 depletion causes downregulation of DREAM target genes	59
3.1.2.3.	Depletion of LIN9 in ES cells does not affect expression of pluripotency genes or pluripotency of ES cells	60
3.1.3.	Genome wide RNA expression analysis after LIN9 depletion to identify LIN9 regulated genes in ES cells	61
3.1.3.1.	Downregulated genes are involved in mitosis and cell cycle processes	62
3.1.3.2.	Early differentiation genes are amongst upregulated genes	62
3.1.3.3.	Synchronisation of mouse ES cells leads to enhanced expression of differentiation genes	65
3.1.4.	Genome wide ChIP approach to identify DREAM binding sites in ES cells	67
3.1.4.1.	ChIPchip analysis reveals that mainly G2/M genes are regulated	67
3.1.4.2.	Overlay of ChIPchip analysis and LIN9 kd RNA microarray	67
3.2.	Identification and characterisation of new DREAM binding partners	71
3.2.1.	Affinity purification reveals possible novel interaction partners of DREAM	71
3.2.2.	SILAC and MassSpec analysis reveals several potential binding partners	72
3.2.3.	ZO-2 also binds to DREAM in differentiated cells	74
3.2.4.	Binding of ZO-2 to DREAM is cell cycle dependent	74

3.2.5. Effects of ZO-2 depletion	76
3.2.5.1. ZO-2 depletion leads to proliferation defects	76
3.2.5.2. G1 but not G2/M gene expression is affected by ZO-2 depletion	76
3.2.5.3. ZO-2 depletion results in mitotic delay	79
4. Discussion	82
4.1. Only DREAM-B-MYB found in ES cells	82
4.2. DREAM-B-MYB responsible for G2/M progression, genomic stability and integrity in ES cells	83
4.3. DREAM is important for early embryonic development	85
4.4. DREAM-B-MYB in Pluripotency and Differentiation	86
4.4.1. DREAM does not influence pluripotency in ES cells	86
4.4.2. Differentiation genes indirectly affected by DREAM	87
4.5. Identification of possible DREAM interactors	90
4.5.1. The tight junction protein ZO-2	91
4.5.2. ZO-2 binding to DREAM is strongest in S-phase	92
4.5.2.1. ZO-2 affects G1 rather than G2/M gene expression	92
4.5.2.2. Reduced proliferation after ZO-2 depletion due to delayed progression through mitosis	93
4.5.3. ZO-2 might act as scaffold protein to support DREAM assembly	94
4.5.4. The mechanism of DREAM mediated gene regulation is still unclear	95
4.6. Conclusion	97
References	98
A. Appendix	112
A.1. Supplementary Data	112
A.2. Abbreviations	112
A.3. Own publications	115
A.4. Curriculum Vitae	116
A.5. Acknowledgments	117
A.6. Eidesstattliche Erklärung	118

List of Figures

1.1. Cell cycle regulation	5
1.2. pRB/E2F interaction	7
1.3. DREAM-B-MYB regulated G2/M genes	9
1.4. DREAM composition switches during the cell cycle	11
3.1. Knock down of LIN9 or B-MYB leads to accumulation in G2/M	54
3.2. EB formation is heavily impaired after DREAM LIN9 or B-MYB kd	56
3.3. DREAM composition and function in ES cells	58
3.4. ES cell line expressing biotinylated proteins	59
3.5. LIN9 depletion leads to reduction of DREAM target genes	60
3.6. Pluripotency is not affected by short term depletion of LIN9 or B-MYB	61
3.7. Genome-wide expression analysis of genes regulated upon LIN9 depletion in ES cells	63
3.8. Validation of upregulated genes after LIN9 depletion	64
3.9. Synchronisation of ES cells leads to upregulation of differentiation genes	66
3.10. GO term analysis of BioLIN9 ChIPchip	68
3.11. List of proteins found in MS analysis	73
3.12. ZO-2 binding to DREAM in HEK293T cells	74
3.13. DREAM-ZO-2 binding in synchronised T98G cells	75
3.14. Growth curves of cells after ZO-2 depletion	77
3.15. Expression analysis after ZO-2 knock down	78
3.16. BrdU-FACS analysis after ZO-2 depletion	80
3.17. MPM2-FACS analysis after ZO-2 depletion	81
4.1. Schematic representation of ZO-2	91

1. Introduction

1.1. The mammalian cell cycle

The mammalian cell cycle describes a series of complex processes which are dedicated to DNA replication and transmission of genetic material to daughter cells. Its strict regulation is fundamental to maintain the steady state between proliferation and cell death in the mammalian body to prevent from aberrant growth. Therefore many mechanisms are present to decide when a cell has to enter or to quit the cell cycle either by cell death, quiescence, differentiation or senescence.

The mammalian cell cycle can be separated into four distinct phases: During DNA synthesis phase (S-phase) DNA is replicated and the doubled chromosomes are distributed equally during mitosis (M-phase) to the two emerging daughter cells. The cell cycle also contains 'Gap' phases (figure 1.1). Gap1 (G1) connects the completion of M phase to the initiation of S-phase in the next cycle and Gap2 (G2) separates S-phase from mitosis. Those gap phases are important because they allow cells to prepare for the next cell cycle phase. In G1 and G2, proteins required for entering the next cell cycle step are synthesised. Furthermore, during gap phases different checkpoint mechanisms are activated. These surveillance mechanisms sense the replication state and genetic integrity of the cell and activate the DNA repair machinery if needed. Failure to enforce such controls results in genetic instability (Bartek and Lukas, 2001; Malumbres and Barbacid, 2001).

The time spanning G1-S-G2-phase is called interphase, during its course cells grow, duplicate their DNA and prepare for mitosis. Mitosis can also be subdivided into different phases. During prophase, chromatin gets condensed into chromosomes which align at the metaphase plate in metaphase. In anaphase, chromosomes are split and sister chromatids move to opposite ends of the cell whereas in telophase, the decondensing chromosomes are surrounded by the newly reformed nuclear membrane. Cell division is completed by cytokinesis. Between the two emerging daughter cells a contractile ring develops, con-

1. Introduction

stricting the cell membrane to form a cleavage furrow. Thus, the division into two cells gets completed.

Cells do not constantly undergo cell division. Dependent on environmental and developmental signals, cells in G1 may temporarily or permanently leave the cell cycle and enter a quiescent or arrested cell phase known as G0. Quiescent cells either retain the ability to re-enter the cell cycle after adequate stimulation or stay permanently in the resting state e.g. as result of differentiation or senescence. Cells often undergo senescence after DNA damage or incorrect mitosis to prevent cells from further aberrant cell cycles. In a cell population just a small proportion is actively dividing. Cells predominantly rest in G0 or G1. Cell external signals and intrinsic information together determine whether cells enter a division cycle. If a cell receives enough external mitogenic stimuli it can enter the cell cycle in G1 where it accumulates nutrients and increases in size as preparations for replication. When the cell reaches the 'Restriction point' in G1, it is bound to progress further in the cell cycle ('Point of no return'). From there on, progression through the cell cycle is controlled intrinsically by the cell cycle machinery (Pardee, 1974; Planas-Silva and Weinberg, 1997).

1.1.1. Cell cycle regulation

1.1.1.1. Cyclin-dependent kinases (CDKs) act as cell cycle regulators

It is fundamental for each round of cell division that each of the cell cycle phases is maintained in its correct temporal order. Otherwise even small alterations can lead to an aberrant cell division and therefore to apoptosis, DNA damage, mutations or aneuploidy which can contribute to tumour development. This regulation is coordinated by a family of enzymes known as Cyclin-dependent kinases (CDKs). The small serine/threonine kinases form complexes that consist of the catalytic CDK subunit and a regulatory cyclin subunit. Mammalian cells express a variety of CDKs of which the main four CDK1, CDK2, CDK4, and CDK6, are directly involved in cell cycle regulation upon binding their specific cyclin (Morgan, 2007).

1.1.1.2. Control of CDK Activation

CDK protein levels remain constant but the expression of cyclins occurs oscillating due to controlled degradation and resynthesis (Tyers and Jorgensen, 2000; Doree and Galas,

1. Introduction

1994; Morgan, 1997). Characteristic for the cell cycle are the overlapping waves of cell phase specific CDK activities which define the temporal order of each cell cycle (figure 1.1).

At the beginning of the cell cycle in early G1, cyclinD expression is induced by mitogenic stimuli like cytokines or growth factors (Hunter and Pines, 1994; Sherr, 1994). CyclinD forms complexes with CDK4 and CDK6 which promote the progression from G1 into S-phase (Matsushime et al., 1992; Meyerson and Harlow, 1994). The cyclinE-CDK2 complex is important during transition from G1 into S-phase. CyclinA-CDK2 complexes display their activity in later S-phase at the onset of G2. CyclinA also forms complexes with CDK1 to allow entry into M phase (Girard et al., 1991; Walker and Maller, 1991). To continue progress through mitosis, cyclinB-CDK1, also known as mitosis-promoting factor (MPF), is activated which controls the activation of different proteins important for proper chromosome segregation and mitotic spindle formation. APC-directed polyubiquitination of cyclinB and its subsequent degradation in late M-phase causes a rapid fall in MPF activity, permitting completion of mitosis and allow preparations for the next cell cycle (reviewed in Morgan, 1999).

CDKs promote cell cycle progression by phosphorylating critical downstream substrates to alter their activity. These events must happen at precise times during the cell cycle; to ensure this, CDK activities have to be tightly regulated. Many levels of regulation impinge upon the CDKs to execute tight control over cell cycle progression. The first step for cyclin-CDK activation is the assembly of the complex, which depends on the availability of the specific cyclin. Upon cyclin binding, the catalytical CDK subunit undergoes a series of conformational changes (reviewed in Morgan, 1995). This involves the addition of activating and the removal of inhibitory phosphorylations. Thus, complete CDK activation requires phosphorylation at a conserved threonine residue (e.g. Thr 161 in human CDK1) by a CDK activating kinase (CAK). Cyclin-CDK complexes can be inhibited by N-terminal phosphorylation (in human CDK1 at Thr14 and Tyr15) by Wee family proteins (Den Haese et al., 1995). Dephosphorylation at those sites by the CDC25 phosphatase contributes to the activation of cyclin-CDK complexes by stabilising cyclin-CDK interaction and therefore enhancing substrate binding (Russo et al., 1996).

1. Introduction

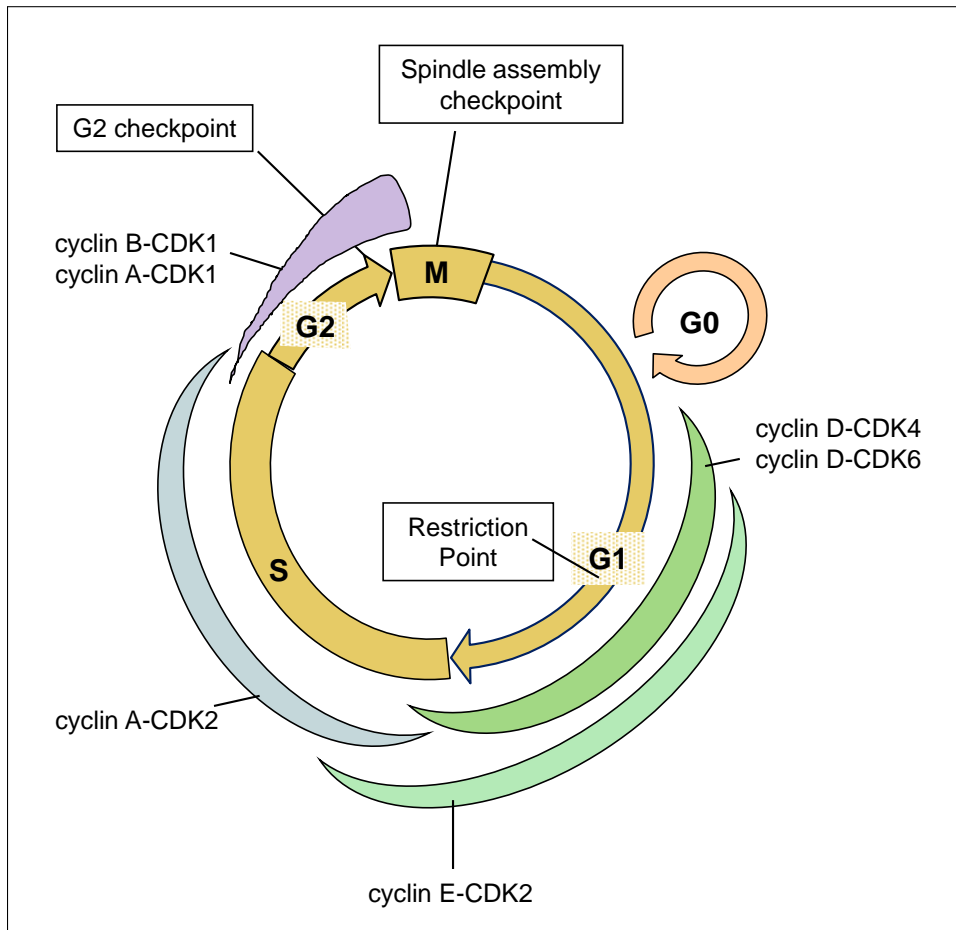


Figure 1.1.: **Cell cycle regulation** The somatic cell cycle is characterised by the doubling of DNA in synthesis (S) phase and the transmission of the genetic material to two emerging daughter cells in mitosis (M), separated by gap phases (G1, G2). Oscillating activity of different cyclin-CDK complexes guides the cell through the different phases of the cell cycle. Checkpoints (black boxes) are crucial instruments to affirm the correct progression through single cell cycle phases. They are constitutive active and have to be silenced for further cell cycle progression. Cells, no longer dividing, withdraw from cell cycle into G0 (Adapted and modified from Collier, 2007).

1. Introduction

1.1.1.3. pRB pathway

A major substrate of cyclinD-CDK4/6 is the tumour suppressor Retinoblastoma (pRB). pRB and its family members p107 and p130 are also called 'pocket proteins' because they share a common domain called pocket domain (Lipinski and Jacks, 1999) which consists of two highly conserved regions A & B, separated by a linker. The pocket domain mediates the interaction with E2F proteins and histone deacetylase (HDAC) (Felsani et al., 2006; Giacinti and Giordano, 2006). pRB and its family members play a crucial role in regulating G1 progression and act as negative regulators at the restriction point. Proteins of the pRB family conduct this role through association with transcription factors of the E2F family and by modulating their activity (Harbour and Dean, 2000).

E2F family

The members of the E2F family of transcription factors are the most important and best characterised pRB interacting proteins. In mammals, 8 family members (E2F1-8) are known, of which E2F1-6 form heterodimers with DP proteins (DP1 and DP2) for functional activity (Giacinti and Giordano, 2006). E2Fs can be divided into three functional groups (E2F1-3, E2F4-5 and E2F6-8).

- a) The transcriptional activators E2F1-3 are highly regulated in their expression during cell growth and cell cycle generally (Dyson, 1998) and bind predominantly to pRB. E2F1-3 regulate the expression of a host of genes needed for G1-S progression such as cyclinE. Upon binding of hypophosphorylated pRB to E2F1-3, the transactivating function is abolished, target gene expression silenced and cell cycle progression inhibited (Rayman et al., 2002). During G1, pRB sequentially gets phosphorylated by cyclinD-CDK4/6 complexes which leads to the partial release of E2Fs which allows the activation of cyclinE and Cdc25a transcription. The phosphatase CDC25A removes inhibitory phosphorylations from CDK2 which allows cyclinE-CDK2 formation that in return leads to full hyperphosphorylation of pRB and full release of E2Fs (fig 1.2). The activation of target genes enables progression into S-phase (Harbour and Dean, 2000; Harbour et al., 1999; Bartek and Lukas, 2001; Bracken et al., 2004).
- b) Contrary, E2F4-5 act as transcriptional repressors with E2F4 and E2F5 primarily binding p130 and p107 (Moberg et al., 1996; Beijersbergen et al., 1994; Ginsberg et al., 1994; Hijmans et al., 1995). During G0 and G1, pocket proteins and E2F4-5 bind to promoters with E2F consensus sites to repress gene transcription. Upon the subsequent hyperphosphorylation of the pocket proteins, the repressing E2Fs are released and relocated to the cytoplasm (Gaubatz et al., 2001; Verona et al., 1997).

1. Introduction

c) The third functional group consists of E2F6-8. They lack the N-terminal sequences of E2F1-3 as well as the C-terminal domain common to all the other E2F. Thus, the transactivation and the pocket protein binding domain are absent in E2F6-8 which marks them as RB independent transcriptional repressors (Cartwright et al., 1998; Di Stefano et al., 2003; Christensen et al., 2005; Bruin et al., 2003; Trimarchi et al., 1998; Gaubatz et al., 1998). E2F6 is the only member of this group that form heterodimers with DP proteins and it is supposed that it functions as a repressor of E2F-dependent transcription through interactions with Polycomb group of proteins (Attwooll et al., 2005; Cartwright et al., 1998; Trimarchi et al., 1998; Trimarchi et al., 2001; Ogawa et al., 2002; Gaubatz et al., 1998; Giangrande et al., 2004).

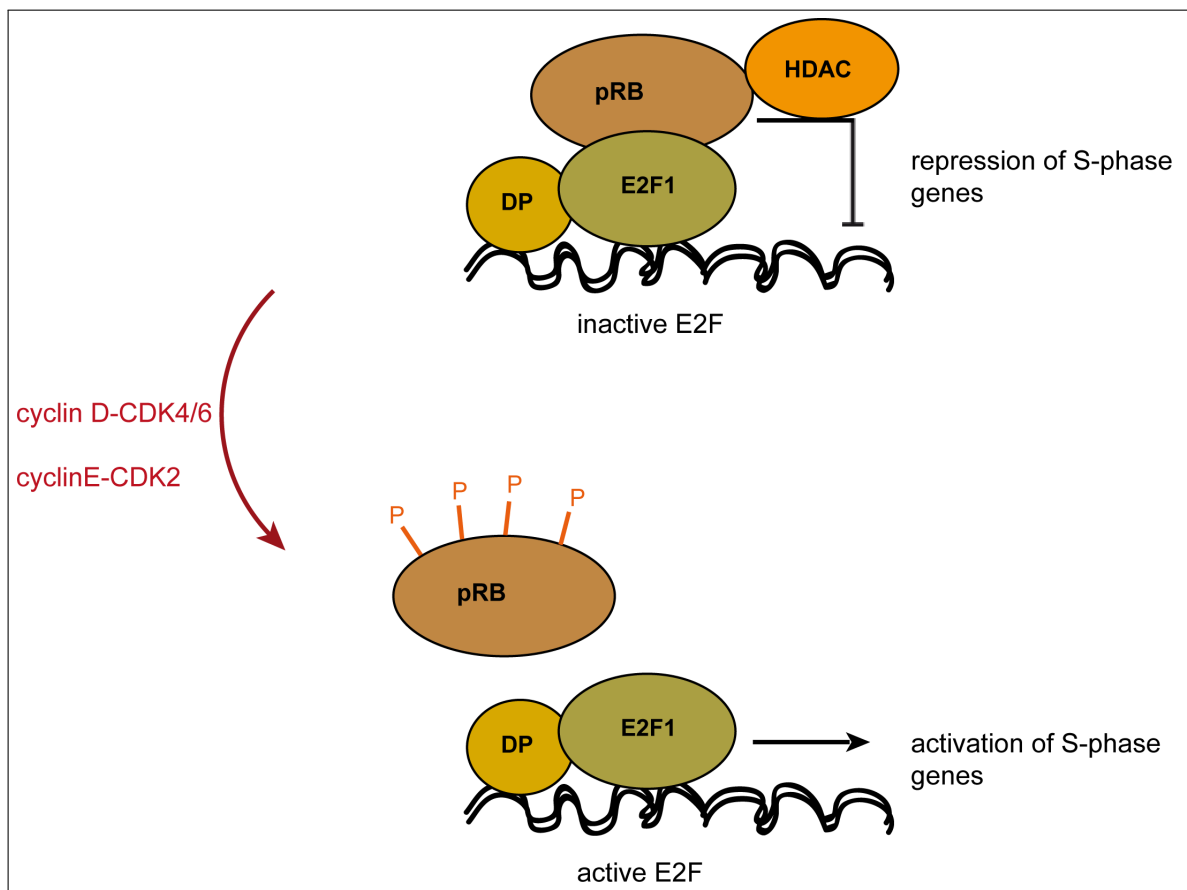


Figure 1.2.: **pRB/E2F interaction** Hyperphosphorylated pocket proteins (as shown for pRB) bind proteins of the E2F family and recruit HDAC to repress the expression of genes needed for G1/S transition. Upon subsequent phosphorylation by cyclin-CDK complexes, E2Fs are released and E2F-dependent gene transcription gets activated. Cells can now progress into S-phase.

1. Introduction

1.1.1.4. CDK inhibitors

CDK activity is additionally controlled by two classes of CDK inhibitors (CKIs) which act as brakes to stop cell cycle progression. Inhibition occurs after binding to cyclin-CDK complexes by steric inhibition, blocking access to the substrates or by destabilisation of the cyclin-CDK interaction (Pavletich, 1999). CKIs are induced after DNA damage, senescence, differentiation or in response to different cellular signals such as cytokines or cell-cell contact. The CKIs of the INK family, p16 (INK4a), p15 (INK4b), p18 (INK4c) and p19 (INK4d) specifically bind to CDK4 and CDK6, preventing their association with cyclinD and therefore lead to G1 arrest. CKIs are crucial for avoiding uncontrolled proliferation by inducing cell cycle arrest, as human tumours frequently harbour inactive p16 (Kamb et al., 1994). The second class of CKIs is composed of the three CIP/KIP family members, p21 (CIP1), p27 (KIP1) and p57 (Kip2) which can inhibit a wide range of CDK complexes (Vidal and Koff, 2000; Sherr and Roberts, 1999).

1.2. The mammalian DREAM complex

Correct cell cycle progression underlies tight regulation of periodic gene expression. E2F and pRB proteins are critical regulators for G1/S transition (section 1.1.1.3) due to their gene repressive function in G0/early G1 phase.

In 2004, an E2F/pRB repressor complex was identified in *Drosophila* named dREAM (Korenjak et al., 2004) or Myb-MuvB (Lewis et al., 2004) containing dE2F2 and dMyb together with the pRb homologues RBF1 or RBF2, Caf1p55, three Myb-interacting proteins (Mip40, Mip120 and Mip130) and other components such as dLin-52. It represses developmental gene expression but also positively regulates G2/M genes (Georgette et al., 2007). This complex is highly conserved as its homologue DRM was also found in *C. elegans* (Harrison et al., 2006) involved in vulva differentiation (Korenjak et al., 2004). In human cells DREAM was identified in 2007 (Schmit et al., 2007; Pilkinton et al., 2007; Litovchick et al., 2007) with the core components LIN9, LIN37, LIN54, LIN52 and RBAP48 (the human homologues of *Drosophila* Mip130, Mip40, Mip140, dLin52 and Caf1p55).

In G0-G1, DREAM binds to the pocket protein p130 and E2F4 to repress transcription of E2F target genes regulating the G1-S transition.

Genome wide location analysis in quiescent human cells showed that DREAM binds promoters of >800 cell cycle regulated genes indicating a repressing function in G0 (Litovchick et al., 2007). Upon S-phase entry, the DREAM core complex releases p130/E2F4 and associates with the transcription factor B-MYB instead (fig 1.4). This switch triggers the

1. Introduction

activation of G2/M gene expression (Schmit et al., 2007). This activator complex is named DREAM-B-MYB or Myb-MuvB (MMB) in contrast to the repressor DREAM (or MuvB).

To identify genes that are regulated by DREAM, RNA expression analyses were conducted in human and mouse fibroblasts after depletion of the core member LIN9 (Osterloh et al., 2007; Reichert et al., 2010). The majority of genes influenced by LIN9 are expressed during G2 or M-phase. They exert functions in G2/M transition and mitotic entry (e.g. cyclinA, cyclinB1, Cdc2), mitotic spindle checkpoint (Bub1, CenpE, Birc5), spindle assembly (AuroraA, Plk1), cytokinesis (Cep55), and exit from mitosis (Ubch10) (Osterloh et al., 2007) as shown in figure 1.3.

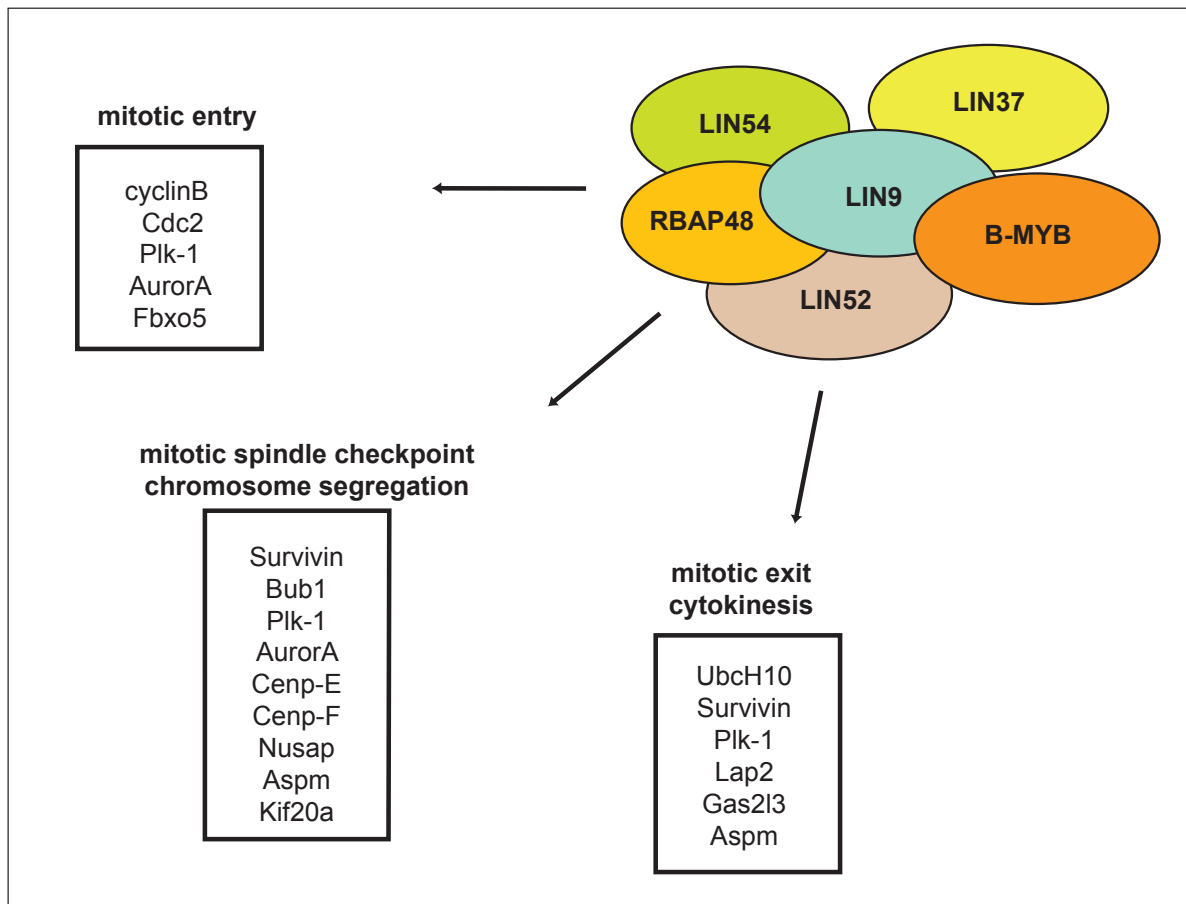


Figure 1.3.: **DREAM-B-MYB regulated G2/M genes** The DREAM-B-MYB complex activates a large set of G2/M genes. Among them are genes important for mitotic entry, spindle checkpoint, chromosome segregation or mitotic exit and cytokinesis.

1.2.1. G2/M gene regulation by CDE/CHR promoter elements

Correct entry and progression through mitosis is required to avoid failures in cell division which can lead to genomic instability. Genes needed in G2 or M phase must be provided on time and thus need precise regulation and coordination of expression.

G2/M genes are repressed during G0/G1 and are activated during S-phase. They often share some common features close to the transcription start in their promoters, namely CDE (cell cycle -dependent element), CHR (cell cycle genes homology region) and CCAAT-boxes. CDE and CHR are found in close proximity, separated by a 4 nucleotide spacer. CDE was first discovered in the human CDC25C promoter and found necessary for the repression of gene expression in G0/G1 (Lucibello et al., 1995). Shortly after, CHR was discovered. Mutation of CHR leads to the loss of transcriptional repression in G0/G1 as observed for CDE, affirming the repressive character of CDE/CHR elements (Zwicker et al., 1995). CDE is related to the TTGGCGC E2F binding consensus, which explains the binding of E2F and pocket proteins to several CDE-regulated promoters (Zwicker et al., 1995). There are two classes of CDE/CHR regulated genes. Class I genes require both sites for cell-cycle dependent repression whereas class II genes do not have a functional CDE site and are only regulated through a well-conserved CHR. Unlike the E2F-related CDE, which is needed for transcriptional repression, the CHR element participates in both repression and activation of genes. Genes regulated by CDE/CHR generally encode proteins with functions in S- or G2/M-phase (Zwicker et al., 1995). Binding of E2F4 and the pocket protein p130 was detected to several CDE-regulated promoters (e.g. CDC2, AurkB, cyclin A2) (Tommasi and Pfeifer, 1995; Kimura et al., 2004; Zhu et al., 2004). Also the DREAM subunit LIN54 was found to bind to a CHR and B-MYB binding site (with a CHR-like element) in the human CDC2 promoter (Schmit et al., 2009). Furthermore, DREAM binding to CHR was confirmed for human and mouse cyclinB promoter at which, in the human promoter, CDE is not required for DREAM binding (Müller et al., 2011). It is proposed that, in G0, DREAM-E2F4/p130 binding to CDE/CHR mediates gene repression (fig 1.4), whereas upon S-phase entry, the DREAM-B-MYB complex binds to CHR, as shown for cyclinB (Müller et al., 2011), or to alternative recognition sites outside CHR/CDE (Schmit et al., 2009) to activate gene expression. Analysis of a ChIPchip array showed that 18.8% of DREAM regulated promoters contain CHR elements (Müller et al., 2011). It is proposed that even more DREAM regulated genes contain CHR (or CHR-like elements) which underlines their important role in DREAM-mediated gene repression and activation.

1.2.2. The subunit LIN9

One of the best studied DREAM components is LIN9. It was first described in *C. elegans* where it is needed together with LIN35 (pRB) for vulva differentiation (Ferguson and Horvitz, 1989; Beitel et al., 2000). Further homologues were found in *Drosophila* (Mip130 and Aly) and *Arabidopsis thaliana* (Always Early) (Bhatt et al., 2004). Like the *Drosophila* Mip130 the mammalian LIN9 is part of the DREAM core complex.

LIN9 depletion in immortalised human BJ fibroblasts leads to inhibition of proliferation and accumulation of cells in G2/M resulting in a delayed entry into mitosis (Osterloh et al., 2007).

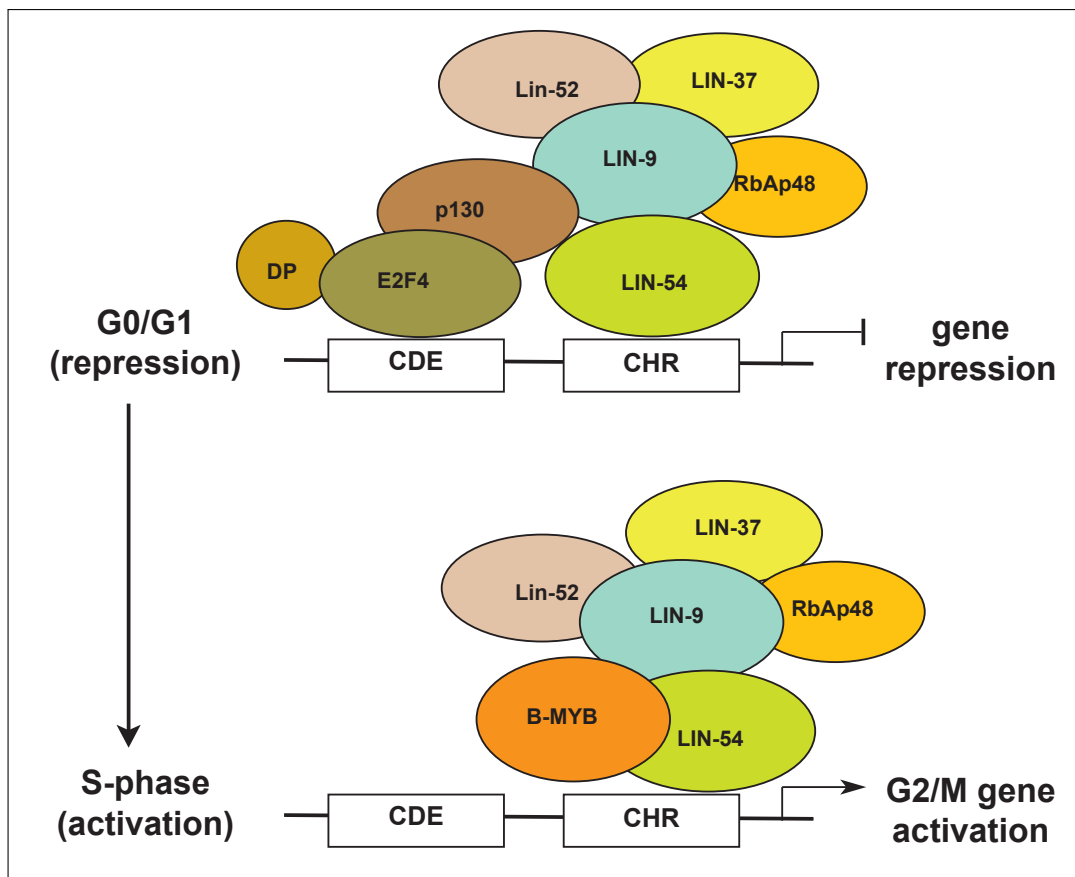


Figure 1.4.: **DREAM composition switches during the cell cycle** During G0/G1, the core unit associates with p130, E2F4 and DP1 to repress gene expression. Upon entry into S-phase, the incorporation of B-MYB allows the activation of G2/M genes. It is proposed that binding of E2F4/p130 and the core subunit LIN54 to CDE/CHR promoter elements is needed for gene repression whereas gene activation in S-phase is mediated by DREAM binding to CHR (or CHR-like elements) through LIN54 and B-MYB.

1. Introduction

Deletion of Lin9 in mice results in early embryonic lethality. Homozygous Lin9^{-/-} embryos die shortly after implantation due to failure of inner cell mass (ICM) proliferation (Reichert et al., 2010). To investigate Lin9 deletion phenotypes in adult mice, a conditional knock out mouse model was established in our lab which enabled the directed deletion of Lin9 upon repeated injection of tamoxifen. Mice died within 7 days of the first tamoxifen injection due to massive reduction of proliferating intestinal tissue (Reichert et al., 2010). Conditional knock out (ko) of Lin9 in mouse embryonic fibroblasts (MEFs) led to severe mitotic defects, abnormal shaped and multinucleated nuclei and senescence (Reichert et al., 2010).

Lin9-null cells that escape senescence are chromosomal instable because of compromised mitotic fidelity. This observation was made by experiments with MEFs expressing the SV40 large T antigen which binds to and disrupts the function of the tumour suppressors p53 and pRB. SV40 LT-expressing cells that adapt to the loss of Lin9 can grow anchorage-independently in soft agar, a hallmark of oncogenic transformation. This suggests an important role of LIN9 in mitotic gene regulation, the maintenance of genomic stability and tumour suppression (Hauser et al., 2012).

As mentioned, homozygous Lin9 ko leads to embryonic lethality in mice. In contrast, heterozygous Lin9^{+/-} mice develop normally, but establish more tumours and show reduced survival in a small cell lung tumour model which underlines the possibility that LIN9 functions as a haploinsufficient tumour suppressor (Reichert et al., 2010).

1.2.3. The transcription factor B-MYB

The Myb (**myeloblastosis**) gene family contains three members, the transcription factors A-Myb, B-Myb and c-Myb. The proto-oncogene c-Myb is the mammalian homologue of the v-Myb oncogene, carried by the Avian myeloblastosis virus and E26 retrovirus that cause acute leukaemia in birds (reviewed in Graf, 1992). Homology search led to the other family members A-, and B-Myb (Nomura et al., 1988). Besides high sequence homology, the Myb proteins have a similar structure. All Myb proteins harbour a conserved N-terminal DNA-binding domain and a central transcriptional transactivation domain. In A- and c-Myb the C-terminal domain act as a transcriptional repressor, whereas in B-Myb it seems to be a positive regulator of its transcriptional transactivation function (Oh and Reddy, 1998). Despite their similarities all Myb genes show distinct expression patterns. c-Myb is prevalently expressed in immature haematopoietic cells (Gonda and Metcalf, 1984), knock out studies showed its importance for haematopoiesis and T-cell development (Mucenski et al., 1991; Bender et al., 2004). A-Myb is expressed in germinal B-lymphocytes as well

1. Introduction

as in breast and testis where it fulfils its functions e.g. in spermatogenesis (Toscani et al., 1997; Trauth et al., 1994).

In contrast, B-MYB is ubiquitously expressed in all cell types (Nomura et al., 1988) and at all stages of mouse embryogenesis with protein levels stringently coupled to the proliferative state of the cells (Sitzmann et al., 1996). B-Myb knock out in mice leads to an early embryonic lethality (Tanaka et al., 1999) similar to Lin9 ko mice due to failure of ICM formation, supporting its important role in embryonic development.

Expression of B-Myb is cell cycle regulated. In G₀, B-Myb is repressed by E2F/pRB (Lam and Watson, 1993; Hurford et al., 1997) until its expression is induced at the G₁/S border (Lam et al., 1995). For activation, B-MYB undergoes several phosphorylations mediated by cyclinA-CDK1 (Robinson et al., 1996; Saville and Watson, 1998) which indicates a role in cell cycle control.

B-Myb is the most conserved member of the Myb gene family. Non-vertebrates such as *Drosophila* express only one Myb gene which is closely related to B-Myb (dMyb in *Drosophila*).

As described in 1.2, dMyb is a member of the dREAM complex which acts as a transcriptional repressor mainly of developmentally expressed genes (Lewis et al., 2004; Korenjak et al., 2004). dMyb was also shown to function as activator of DNA replication and trans-activator of G₂/M genes like cyclinB (Okada et al., 2002). dMyb mutants exhibit defects in cell cycle progression (Okada et al., 2002; Katzen et al., 1998) and genome instability (Manak et al., 2002; Fung et al., 2002).

Mammalian B-MYB is part of the DREAM complex in S-phase that acts as activator for G₂/M gene expression. Independently of its function in the DREAM complex, a direct role in mitotic spindle formation for B-MYB was implicated (Yamauchi et al., 2008). Yamauchi *et al.* report that B-MYB is integrated in a clathrin and filamin complex (Myb-Clafi complex) which is needed for stabilisation of kinetochores and localisation of clathrin at the mitotic spindle.

B-MYB in cancer

The deregulation of B-Myb can contribute to the development and/or maintenance of malignant tumours.

A direct role of B-MYB in cancer is not proven but there are many hints that B-MYB acts as tumour promoting factor. B-Myb is amplified in breast, liver, ovarian carcinomas and cutaneous T-cell lymphomas (Zondervan et al., 2000; Tanner et al., 2000; Mao et al., 2003; Thorner et al., 2009). Increased expression levels are also found in testicular and

1. Introduction

prostate malignancies (Nomura et al., 1988; Raschella et al., 1995). In neuroblastoma the constant expression of B-MYB represses the differentiation of cells into neurons (Raschella et al., 1995), high B-MYB levels correlate with a poor prognosis (Raschella et al., 1999). A recent study highlighted the connection between B-MYB and p53 (Mannefeld et al., 2009). Cells with a p53^{-/-} status lack a proper G1 arrest, therefore they are strongly dependent on a functional G2 checkpoint (Bunz et al., 1998). DNA damage results in p53-dependent binding of p130/E2F4 to DREAM and dissociation of B-MYB whereas, in p53^{-/-} cells, this dissociation fails which leads to the upregulation of G2/M genes. Furthermore, B-MYB is required for the recovery from the G2-DNA-damage checkpoint in p53^{-/-} cells. DNA damage overrides the checkpoint which leads to the premature entry into mitosis. Mannefeld *et al.* showed the important role of DREAM-B-MYB in the DNA damage response downstream of p53. Furthermore, reanalysis of microarray expression data sets revealed that high B-MYB levels not only correlate with the p53 status but also with an advanced tumour stage in primary human breast cancers.

B-MYB in ES cells

B-Myb is the only *Myb* family member expressed in ES cells (Sitzmann et al., 1996) with very high protein levels, up to 1000-fold greater than in adult cells (Tarasov et al., 2008). This abundance suggests a variety of functions of B-MYB in ES cells. Its important role in the organism is underlined by many depletion studies. Knock out of B-Myb results in early embryonic lethality shortly after implantation at day 4.5-5.5 due to failure of ICM formation (Tanaka et al., 1999). Approaches with inducible dominant-negative MYB mutants (MERT) suggested that this phenotype is based on defective cell cycle progression through G1 (Iwai et al., 2001). Further studies in ES cells showed that B-Myb depletion with short hairpin RNA (shRNA) led to cell cycle arrest in G2/M, mitotic spindle and centrosome defects. These aberrations seem to promote either the generation of aneuploid cells or the induction of differentiation coupled with apoptosis (Tarasov et al., 2008).

In 2010, another study demonstrated that the conditional knock out of B-Myb in ES cells results in disturbance of S-phase progression. Ablation of B-MYB led to stalled DNA replication forks which contributes to the increase of DNA doublestrand breaks (Lorvellec et al., 2010). B-MYB might therefore also be required in S-phase for proper DNA replication in S-phase.

In recent studies, B-MYB was implicated to function in the maintenance of pluripotency (Tarasov et al., 2008; Zhan et al., 2012). Tarasov *et al.* Falling B-MYB levels are observed 48-72 hours after differentiation initiation *in vitro*, slightly earlier than Oct4 levels start to

1. Introduction

decrease. Depletion of B-Myb by shRNA resulted in increased levels of early differentiation genes and to a slight decrease of the pluripotency markers Sox2 and Oct4. B-MYB was also found on the Pou5f1 promoter, suggesting B-MYB might be involved in Oct4 regulation and therefore participating in maintenance of pluripotency (Tarasov et al., 2008). However, a recent study could not confirm the binding of B-MYB to Pou5f1 promoter but to Nanog and Sox2 (Zhan et al., 2012). The assumed role of B-MYB in the maintenance of pluripotency therefore has still to be determined.

Overall, B-MYB seems to exert various functions in pluripotent cells such as cell cycle progression, proliferation, DNA synthesis and correct spindle formation in mitosis. Mutation or loss of function of B-MYB can contribute to cancer formation.

1.3. Pluripotent stem cells and differentiation

1.3.1. Stem cells and pluripotency

The capability of a cell to develop into all embryonic as well as extraembryonic tissues and therefore to generate a fully viable organism is called totipotency. Only the fertilised zygote and blastomere cells of the 2-8 cell stage possess this ability. Cells then proliferate and differentiate into the first two lineages, the pluripotent inner cell mass and the trophoectoderm.

Pluripotency describes the ability to differentiate into cells and tissues of any of the three germ layers (endoderm, mesoderm, ectoderm). Three types of pluripotent cells can be established from mammalian embryos: embryonic stem (ES), embryonic carcinoma (EC) and embryonic germ (EG) cells.

EC cell lines are derived of undifferentiated embryonic components of germ cell tumours. EG cell lines are derived from primordial germ cells (PGCs) and are usually isolated from the genital ridge of 9.5- to 12.5- days post coitum (dpc) embryos. After appropriate *in vivo* developmental pathways, ES and EG (but not EC) cells can contribute to all cells of a developing embryo, including the germ line (reviewed in Boheler, 2002).

ES cells are derived from epiblast cells within the inner cell mass of the pre-implantation blastocyst (Evans and Kaufman, 1981; Martin, 1981). Just as their *in vivo* counterparts from the epiblast, ES cells possess the capacity for self-renewal which allows for unlimited proliferation while retaining their pluripotent character. Under appropriate conditions ES cells can be maintained in cell culture in their pluripotent undifferentiated state. Murine ES cells can be propagated on a feeder layer of MEFs or under feeder-free conditions upon

1. Introduction

addition of the leukaemia inhibitor factor (LIF) which contributes to the maintenance of ES pluripotency and self-renewal. LIF is a soluble glycoprotein that acts via a membrane-bound gp130 signaling complex to control signal transduction and activation of the transcription factor STAT3 (Smith et al., 1988; Niwa et al., 1998; Matsuda et al., 1999)

1.3.1.1. Transcriptional regulation of pluripotency

The best studied proteins crucial for self-renewal are the homeodomain protein POU5F1 (OCT4), NANOG and SOX2 (Avilion et al., 2003; Pesce and Schöeler, 2001; Chambers et al., 2003; Mitsui et al., 2003). They are essential key regulators for the formation and maintenance of the ICM in early embryonic development and for self-renewal of pluripotent ES cells.

Oct4

Oct4 expression is restricted to pluripotent cells from the four- to eight- cell stage of the embryo until the epiblast begins to differentiate (Palmieri et al., 1994). The presence of OCT4 protein is essential for ICM and epiblast formation as mouse embryos lacking Oct4 die following implantation (Nichols et al., 1998). Appropriate Oct4 levels must be present to keep pluripotency. 2-fold increase of Oct4 expression induces differentiation into primitive endo- and mesoderm whereas downregulation of Oct4 leads to trophoectoderm formation and loss of pluripotency (Niwa et al., 2000).

Nanog

The homeobox transcription factor Nanog is expressed in the inner cells of a compacted morula and blastocyst and is downregulated just prior to implantation (Mitsui et al., 2003; Chambers et al., 2003). Overexpression of Nanog enables ES cells to self-renew independently from LIF/gp130/STAT3 signaling (Mitsui et al., 2003; Chambers et al., 2003) and allows culturing in serum-free medium in the absence of bone morphogenic protein (BMP) (Ying et al., 2003).

Sox2

The transcription factor Sox2 is expressed in the pluripotent lineages of early mouse embryos as well as in the multipotent cells of the extra-embryonic ectoderm. Deletion of Sox2 leads to early lethality after implantation (Avilion et al., 2003). Downregulation of Sox2 results in polyploidy in ES cells and in the induction of trophoectodermal differentiation similar to Oct4 depletion. This suggests a cooperation of both factors in preventing dif-

1. Introduction

ferentiation (Li et al., 2007).

Genome-wide location analyses were conducted to identify gene promoters regulated by these pluripotency markers in ES cells (Boyer et al., 2005; Loh et al., 2006). These analyses revealed that OCT4, SOX2 and NANOG form an interconnected autoregulatory loop by binding together at each of their promoters. Many gene promoters are co-occupied by OCT4, NANOG and SOX2, encoding important homeodomain proteins and transcription factors. Furthermore, OCT4 and NANOG were found on gene promoters which are involved in the maintenance of pluripotency and self-renewal.

1.3.1.2. Epigenetic control of pluripotency

Besides the influence of transcription factors on gene regulation, epigenetic control also plays a role in regulating the balance between pluripotency and differentiation.

DNA is packed into chromatin with nucleosomes as basic units. A nucleosome consists of DNA wrapped around a core of 8 proteins (two copies each of the histone proteins H2A, H2B, H3, and H4). These local structures get folded and compacted into higher chromatin structures and are then present either as transcriptional silent heterochromatin or active euchromatin (reviewed in Patterton and Wolffe, 1996; Horn and Peterson, 2006). Different forms of epigenetic controls, such as histone modifications and chromatin remodeling, modulate the chromatin to regulate the transcriptional activity in specific genomic regions.

(1) Different enzymes can transfer post-translational modifications on the amino-termini of histone proteins such as acetyl-, methyl-, phosphate-, sumo- or ubiquitin- residues (reviewed in Kouzarides, 2007). These modifications are marks that signal either transcriptional repression or activation. Activating modifications are acetylation of H3 and H4 or the tri-methylation of H3 at lysin4 (H3K4me3) whereas tri-methylation of H3 at lysin9 (H3K9me3) or tri-methylation at lysin27 (H3K27me3) signals repression by promoting the compaction of the chromatin structure (Ringrose et al., 2004).

(2) Another class of chromatin remodeling enzymes (e.g. complexes of the SWI/SNF or ISWI family) can hydrolyse ATP, resulting in contact disruption between DNA and histones. This change of nucleosome conformation leads to an alteration of the higher chromatin structure which influences DNA accessibility for the transcriptional machinery (reviewed in Gangaraju and Bartholomew, 2007).

1. Introduction

Chromatin organisation in ES cells

The global chromatin structure in ES cells is generally dynamic. Their DNA is predominantly present as euchromatin showing an abundance of histone acetylation and increased accessibility of nucleosomes (Efroni et al., 2008; Meshorer et al., 2006). Lineage specification at the beginning of differentiation is accompanied by the decrease of euchromatin and the concomitant increase of heterochromatin formation (Meshorer and Misteli, 2006; Dai and Rasmussen, 2007).

Characteristic for undifferentiated cells are bivalent domains consisting of large H3K27me3 and small H3K4me3 regions in promoters of many lineage specific genes (Bernstein et al., 2006; Azuara et al., 2006; Mikkelsen et al., 2007). While H3K27me3 might help to repress developmental genes in ES cells, the H3K4me3 poises genes for activation, preserving their potential to become activated upon initiation of specific differentiation programs. In differentiated cells, either regions with H3K27 methylation or H3K4 methylation are found instead of bivalent domains according to pathway-specific gene expression programs (Bernstein et al., 2006).

In ES cells, the chromatin remodeler proteins of the Polycomb group family (PcG) play an important role in embryonic development and have been implicated in pluripotency (reviewed in Margueron and Reinberg, 2011). PcG proteins function in two distinct repressor complexes PRC1 and PRC2. Genome wide location analysis showed that they occupy a set of genes composed of transcriptional regulators and signaling factors needed for development. Promoter regions of those lineage specific genes are rich in H3K27me3 marks, a silencing modification mediated by PRC2 (Boyer et al., 2006; Lee et al., 2006). Deletion of the PRC2 core members Eed1 or Suz12 result in derepression of many of those genes underlining the direct functional link of PRC2 in silencing differentiation genes in ES cells (Bernstein et al., 2006; Boyer et al., 2006).

1.3.2. The cell cycle in mouse stem cells and its change during differentiation

ES cells either undergo symmetric self-renewal which results in two identical stem cells or asymmetric cell cycle which gives rise to a stem cell and a cell dedicated to differentiation. Other than somatic cells, pluripotent ES cells display a different cell cycle structure. ES cells lack fully formed gap phases and show a rapid rate of cell division, typically in the order of ~10 h (Burdon et al., 2002). G1 phase lasts ~2h compared to 6-12 h in embryonic fibroblasts (Savatier et al., 1994); in ES cells a high proportion of time is devoted to

1. Introduction

S-phase (~60%) (Savatier et al., 1994; Mac Auley et al., 1993; Stead et al., 2002). During differentiation cell division times increase (>18 h) and cell cycle is remodeled with a prolonged G1 phase (White et al., 2005; Stead et al., 2002).

Pluripotent mouse ES cells show elevated CDK activities throughout the cell cycle, the highest is found for CDK2 which, together with a mostly inactive cyclinD, accounts for this high cell division rate. Characteristic is the absence of periodical waves of CDK activities, only the activity of the mitotic regulator cyclinB1-CDK1 occurs oscillating (White et al., 2005; Stead et al., 2002). Another reason for the constant activity of CDKs is the almost complete absence of CDK inhibitors (Stead et al., 2002; Savatier et al., 1996).

Another big difference applies the pRB pathway which is very important in the somatic cell cycle and inactive in ES cells. ES cells do not express the pocket protein p130, and pRB and p107 are held in an inactive hyperphosphorylated state because kinases that regulate pRB family members are constitutively active (LeCouter et al., 1996; Savatier et al., 1994). This means that E2F responsive genes are no longer cell cycle regulated (Faast et al., 2004).

Cell cycle changes during differentiation

Before changes in protein levels of the pluripotency markers OCT4, SOX2 or NANOG are detectable, the cell cycle structure gets remodeled. Increasing levels of the CDK inhibitors p21 and p27 as well as the reduction of cyclinA and cyclinE lead to a decreased and now cell cycle regulated CDK2 activity. Together with enhanced cyclinD expression this leads to the expansion of G1 and the activation of the pRB pathway (Savatier et al., 1996; Stead et al., 2002; White et al., 2005). Hypophosphorylation of pRB results in its complexing with the differentiation promoting transcription factors MyoD, myogenin or C/EBP which leads to the promotion of their activity (Novitch et al., 1999; Gu et al., 1993; Chen et al., 1996). Withdrawal of LIF induces differentiation of ES cells. Already 24 hours after LIF removal, cell cycle transit times are prolonged, a higher amount of cells is found in G1 and a more robust G1 checkpoint is established (Yamanaka et al., 2008). The upregulation of early mesodermal markers such as Brachyury (T) or Goosecoid demonstrate the beginning of differentiation (Savatier et al., 1996).

1.3.3. Differentiation

ES cells as model system for cell differentiation

Differentiation is defined by the loss of pluripotency. Thus, induction of differentiation has been used as a tool to reveal genes needed for pluripotency. Various cell culture methods were used to induce differentiation (Wobus and Boheler, 2005):

- culturing cells at low density
- withdrawal of LIF
- addition of BMP
- addition of retinoic acid.

Additionally, ES cells can be differentiated *in vitro* by cultivation in the absence of LIF as embryo-like aggregates, so-called embryoid bodies (EBs). EBs recapitulate a number of aspects of embryonic development similar to gastrulation of an epiblast-stage embryo *in vivo* (reviewed in Weitzer, 2006). Early EB formation at day 2-3 morphologically resembles morula compaction. On day 4, EBs show an endoderm exterior, a mesoderm and ectoderm-like interior surrounding a large cystic yolk sac-like cavity, analogue gastrulation-like development and axis formation.

Within 2-4 days, expression levels of pluripotency factors such as Sox2 and Rex1 drop, Nanog and Oct4 levels decrease slower. Expression of early differentiation markers increase, dependent on growth factor availability in the culture medium (Dang and Kyba, 2002). Different protocols were established to differentiate mouse ES cells directed into cardiogenic, myogenic, neuronal-, epithelial-, and vascular smooth muscle-like cells *in vitro* (reviewed by Guan et al., 1999; O'Shea, 2004).

1.3.4. Aim of thesis

Lin9 knock out studies provided many information about LIN9/DREAM function in differentiated cells. DREAM plays an important role in the regulation of the cell cycle by repressing as well as activating gene expression. Lin9 ko results in early embryonic lethality in mice which underlines its important role in embryonic development (Reichert et al., 2010). It might also hint to a function of LIN9 in regulating not also cell cycle relevant genes but also influencing genes involved in pluripotency or differentiation. Recent studies suggest such a role in maintaining pluripotency for the transcription factor B-MYB

1. Introduction

(Tarasov et al., 2008; Zhan et al., 2012) which is also part of the activating DREAM complex and that shows a similar ko phenotype in mice (Tanaka et al., 1999).

The first part of this project deals with the function of LIN9 and the DREAM-B-MYB complex in embryonic stem cells. By depleting the DREAM member LIN9 and the DREAM associating factor B-MYB their influence upon cell proliferation and a possible role in pluripotency and differentiation can be analysed. Furthermore, by conducting genome wide location analyses and RNA microarrays a better understanding which genes are directly regulated by DREAM-B-MYB in ES cells can be achieved.

The second part focuses on the analysis of the composition of the DREAM complex in ES cells. The DREAM complex and its basic composition is well characterised in cells. However, the mechanistic of activating or repressing gene activity is unknown as none of the DREAM members bear a catalytic domain. Hence it is of interest which proteins might function as possible DREAM interacting partners or co-factors contributing to DREAM-mediated gene activation. For the identification of DREAM binding proteins mass spectrometry analyses will be performed and the interaction with candidate proteins will be further characterised.

2. Materials and Methods

2.1. Materials

2.1.1. Devices

Device	Company
Bioruptor [®]	Diagenode
Mx3000	Agilent technologies
Novex [®] Nupage [®] Gel Electrophoresis System	Life Technologies

2.1.2. Chemical stocks

Chemical	Stock concentration
ammonium persulfate (APS)	10 % in H ₂ O
ampicillin	100 mg/ml in H ₂ O
Bovine serum albumin (BSA)	20 mg/ml
dNTPs	2 mM dATP, dCTP, dGTP, dTTP each
DMSO	Ready to use
DTT	1 M in H ₂ O
ethidium bromide	10 mg/ml in H ₂ O
luminol	250 mM in DMSO
Neomycin (G418)	200 mg/ml in H ₂ O
p-Coumaric acid	90 mM in DMSO
PMSF (Phenylmethylsulphonylfluoride) (Roche)	20 mg/ml in isopropanol
Ponceau S solution	0.1 % Ponceau S in 5 % acetic acid
propidium iodide (PI)	1 mg/ml in H ₂ O
Protease Inhibitor Cocktail (PIC) (Sigma)	Ready to use

2. Materials and Methods

Proteinase K	10 mg/ml in 50 mM Tris-HCl pH 8.0 / 1 mM CaCl ₂
ProtoGel 30 % (Biozym)	Ready to use
Random primer (Roche)	0.5 mg/ml in H ₂ O
RNase A	10 mg/ml in 10 mM Tris-HCl pH 7.4 / 150 mM NaCl
Sodium dodecyl sulfate (SDS)	10 % in H ₂ O
Temed 99 %	Ready to use
Trifast (total RNA isolation reagent) (Peqlab)	Ready to use
thymidine	200 mM in DMSO
Salmon sperm ssDNA	10 mg/ml in H ₂ O

2.1.3. Transfection reagents

Reagent	Company
Dharmafect2	Thermo Fisher
Lipofectamine2000	Life Technologies
Metafectene Pro	Biontix

2.1.4. Enzymes

Enzymes	Company
ABsolute QPCR SBR Green Mix	Thermo Fisher
M-MLV-RT Transcriptase (200 u/μl)	Promega
<i>Pfu</i> DNA Polymerase (2.5 u/μl)	Promega
Proteinase K (10 mg/ml)	Applichem
Restriction Endonucleases	New England Biolabs / Fermentas
RNase A (10 mg/ml)	Sigma-Aldrich®
RiboLock RNase-Inhibitor (40 u/μl)	Fermentas
T4-DNA-Ligase (400 u/μl)	New England Biolabs

2. Materials and Methods

2.1.5. Molecular Kits & DNA/Protein Markers

2.1.5.1. Molecular Kits

Absolute QPCR SYBR Green Mix	Thermo Fisher
Amicon Ultra - 0.5 ml Centrifugal Filters	Millipore
Colloidal Blue Staining Kit	Life Technologies
Jetstar Gel Extraction Kit	Genomed
Plasmid Mini/Midi/Maxi Kit	Life Technologies
QIAquick Gel Extraction Kit	Qiagen
QIAquick MinElute PCR Kit	Qiagen
QIAquick PCR Purification Kit	Qiagen
RNeasy Mini Kit	Qiagen

2.1.5.2. Markers

GeneRuler™ 1 kb DNA Ladder	Fermentas
PageRuler™ Prestained Protein Ladder	Fermentas

2.1.6. Buffers

All buffers are stored at room temperature unless otherwise noted.

2.1.6.1. General Buffers

5x Loading Dye (5x BX)	15 % Ficoll 0.05 % bromphenol blue 0.05 % xylene cyanol 0.05 M EDTA in 1X TAE
2x HBS	280 mM NaCl 1.5 mM Na ₂ HPO ₄ 50 mM HEPES-KOH, pH 7.05
Luria Bertani (LB) Agar	40 g powder in 1 l H ₂ O, autoclaved

2. Materials and Methods

Luria Bertani (LB) Medium	25 g powder in 1 l H ₂ O, autoclaved
Miniprep-Solution S1	25 mM Tris-HCl pH 8.0 10 mM EDTA
Miniprep-Solution S2	200 mM NaOH 1 % SDS
Miniprep-Solution S3	29.44 g potassium acetate 11.5 ml acetic acid 28.5 ml H ₂ O
Phosphate buffered saline (PBS)(1x)	13.7 mM NaCl 0.3 mM KCl 0.64 mM Na ₂ HPO ₄ adjust pH to 7.4 with HCl
TAE buffer (1x)	40 mM Tris base 5 mM glacial acetic acid 10 mM EDTA, pH 8.0
TBS (1x)	50 mM Tris-HCl, pH 7.4 150 mM NaCl
TE	10 mM Tris-HCl, pH 7.5 1 mM EDTA

2. Materials and Methods

2.1.6.2. Buffers for whole cell lysates and nuclear extracts

TNN buffer	50 mM Tris-HCl, pH 7.5 120 mM NaCl 5 mM EDTA 0.5 % NP-40 10 mM $\text{Na}_4\text{H}_2\text{PO}_7$ 2 mM Na_3VO_4 100 mM NaF PIC (Sigma) 1:1000 (add freshly) 1 mM PMSF
Nuclear extract buffer A (NebA)	20 mM HEPES 10 mM KCl 1 mM EDTA 0.1 mM Na_3VO_4 0.2 % (v/v) Nonidet P40 (NP-40) 10 % (v/v) glycerol add fresh 1 mM DTT 1 mM PMSF PIC (Sigma) 1:1000 store at 4°C without PIC for several months
Nuclear extract buffer B (NebB)	20 mM HEPES 10 mM KCl 1 mM EDTA 0.1 mM Na_3VO_4 350 mM NaCl 20 % (v/v) glycerol add fresh 1 mM DTT 1 mM PMSF PIC (Sigma) 1:1000 store at 4°C without PIC for several months

2. Materials and Methods

Bradford Solution	50 mg Coomassie Brilliant Blue G 23.75 ml ethanol 50 ml 85 % (v/v) ortho-phosphoric acid ad 500 ml H ₂ O filter twice
-------------------	--

2.1.6.3. Buffers for immunoprecipitation with BioTag-ES cells

IPO buffer	20 mM Tris-HCl, pH 7.5 1 mM EDTA 10 % (v/v) glycerol add fresh 1 mM DTT 0.2 mM PMSF PIC (Sigma) 1:1000 store at 4°C without PIC for several months
------------	---

IP350 buffer (0.5 % (v/v) NP-40)	350 mM NaCl 20 mM Tris-HCl, pH 7.5 1 mM EDTA 0.5 % NP-40 10 % (v/v) glycerol add fresh 1 mM DTT 0.2 mM PMSF PIC (Sigma) 1:1000 store at 4°C without PIC for several months
----------------------------------	---

2. Materials and Methods

IP350 buffer (0.3 % (v/v) NP-40)	350 mM NaCl 20 mM Tris-HCl, pH 7.5 1 mM EDTA 0.3 % NP-40 10 % (v/v) glycerol add fresh 1 mM DTT 0.2 mM PMSF PIC (Sigma) 1:1000 store at 4°C without PIC for several months
IP150 buffer (0.3 % (v/v) NP-40)	150 mM NaCl 20 mM Tris-HCl, pH 7.5 1 mM EDTA 0.3 % NP-40 10 % (v/v) glycerol add fresh 1 mM DTT 0.2 mM PMSF PIC (Sigma) 1:1000 store at 4°C without PIC for several months

2.1.6.4. Buffers for immunoblotting

NuPAGE [®] MOPS SDS Running Buffer (20 x)	Life Technologies
4 x Upper Stock for SDS gels	33 g Tris 10 ml SDS(20 %) ad to 500 ml H ₂ O, adjust to pH 6.8
4 x Lower Stock for SDS gels	90.85 g Tris 10 ml SDS(20 %) ad to 500 ml H ₂ O, adjust to pH 8.8

2. Materials and Methods

Acrylamide buffer for SDS-gels (Protogel)	30 % /w/v) acrylamide 0.8 % (w/v) N,N'-methylenebisacrylamide
Blotting buffer (1x)	0.6 g Tris base 2.258 g glycine 150 ml methanol ad to 1 l H ₂ O
Blocking solution	5 % (w/v) milk powder in TBST
3x Electrophoresis sample buffer (3xESB)	300 mM Tris-HCl, pH 6.8 15 mM EDTA 150 mM DTT 12 % (w/v) SDS 15 % (w/v) glycerol 0.03 % (w/v) bromphenol blue
Ponceau S	0.1 % Ponceau S 5 % glacial acetic acid
TBST	0.05 % Tween 20 in 1xTBS
Substrate Solution	10 ml 100 mM Tris-HCl, pH 8.5 50 µl 250 mM luminol 22 µl 90 mM p-coumaric acid 3 µl 30 % H ₂ O ₂

2. Materials and Methods

2.1.6.5. Buffers for chromatin immunoprecipitation with BioTag ES cells (BioChIP)

SDS ChIP buffer	0.1 % SDS 1 % Triton X-100 2 mM EDTA 20 mM Tris-HCl, pH 8.1 150 mM NaCl
Washing buffer 1	2 % SDS
Washing buffer 2	0.1 % sodium deoxycholate (DOC) 1 % Triton X-100 1 mM EDTA 50 mM HEPES, pH 7.5 500 mM NaCl
Washing buffer 3	0.25 M LiCl 0.5 % Nonidet P-40 0.5 % sodium deoxycholate (DOC) 1 mM EDTA 10 mM Tris-HCl, pH 8.1
SDS elution buffer	50 mM Tris-HCl, pH 8.1 1 % SDS 10 mM EDTA

2.1.6.6. Buffers for flow cytometry (FACS)

Sodium citrate	38 mM in H ₂ O
Blocking buffer (made fresh)	1 ml ChIP lysis buffer 50 µl BSA (20 mg/ml) 10 µl ssDNA (10 mg/ml)

2.1.7. Antibodies

2.1.7.1. Primary antibodies

Internal No.	Antibody	Company	Origin	Application	Dilution
# 136	LIN9	(Osterloh <i>et al.</i> 2007)	rabbit polyclonal	IP ChIP (purified)	1:50 10 µg
# 137	LIN9	(Osterloh <i>et al.</i> 2007)	rabbit polyclonal	WB	1:500
# 163	LIN9	abcam ab62329	rabbit polyclonal	IP WB	1 µg/mg protein 1:1000
# 131	Lin37	(Schmit <i>et al.</i> 2007)	rabbit polyclonal	WB	1:500
# 129	Lin54	(Schmit <i>et al.</i> 2007)	rabbit polyclonal	WB	1:500
# 79	B-MYB (N-19)	Santa Cruz sc-724	rabbit polyclonal	IP	1:50
# 149	B-MYB LX015.1	(Tavner <i>et al.</i> 2007)	mouse monoclonal	WB	1:10
# 32	p107 (C-18)	Santa Cruz sc-318	rabbit polyclonal	WB	1:1000
# 33	p130 (C-20)	Santa Cruz sc-317	rabbit polyclonal	IP WB	1:100 1:1000
# 6	E2F4 (C-20)	Santa Cruz sc-866	rabbit polyclonal	WB	1:1000
# 152	RbAp48 (15G12)	(gift from IRIC / Montreal)	mouse monoclonal	WB	1:1000
# 158	a-Tubulin	Sigma T6074	mouse monoclonal	WB	1:10000

2. Materials and Methods

# 196	b-actin	Santa Cruz sc-47778	mouse monoclonal	WB	1:10000
# 104	IgG (15006)	Sigma	rabbit polyclonal	ChIP	4 µg

Internal No.	Antibody	Company	Origin	Application	Dilution
# 93	cyclinB1 (GNS1)	Santa Cruz sc-245	mouse monoclonal	WB	1:5000
# 219	ZO-2 (H-110)	Santa Cruz sc-11448	rabbit polyclonal	IP WB	1:50 1:1000
# 92	HA	Covance MMS-101	mouse monoclonal	WB	1:2000
# 93	Flag M2	Sigma F3165	mouse monoclonal	WB	1:5000
# 213	MPM2	Millipore 05-368	mouse monoclonal	FACS	
	BrdU-FITC	Becton Dickinson 347583	mouse monoclonal	FACS	

2.1.7.2. Secondary antibodies

Antibody	Company	Application
anti-mouse HRP linked	GE Healthcare	WB 1:5000
anti-protein A HRP linked	BD Biosciences	WB 1:5000
anti-mouse Alexa 488	Invitrogen	FACS

2.1.7.3. Beads

Protein A Agarose	Pierce
Protein G Agarose	Millipore
Dynabeads® Protein G	Life Technologies
Dynabeads® M-270 Streptavidin	Life Technologies

2.1.8. Plasmids

2.1.8.1. Plasmids for overexpression

Internal number	Plasmid name	Description
# 375	pCDNA3-Flag hlin9	Overexpression of human LIN9

2.1.8.2. Plasmids for RNA knock down

Internal number	Plasmid name	Description
# 572	pSuper.puro	Empty vector control for knock-down constructs
# 1164	pSuper.puro.shLin9	Expression vector for mouse LIN9-shRNA
# 1165	pSuper.puro.shBMyb # 1	Expression vector for mouse B-MYB-shRNA
# 1211	pSuper.puro.shBMyb # 2	Expression vector for mouse B-MYB-shRNA

shRNA sequences:

shRNA against

shLin9

shBMyb # 1

shBMyb # 2

Sequences 5' to 3'

GCU ACU UAC AGA GUA ACU UUC
(Knight *et al.* 2009)

GCC CAU AAA GUC CUG GGU AAC
(Knight *et al.* 2009)

GGU GCG ACC UGA GUA AAU U
(Tarasov *et al.* 2008)

2.1.9. Primers

2.1.9.1. Primers for quantitative RT-PCR

2.1.9.1.1. Human primers

Number	Application	Sequence	
SG 645	GAPDH	GCC CAA TAC GAC CAA ATC C	sense
SG 656		AGC CAC ATC GCT CAG ACA C	antisense
SG 620	S14	GGC AGA CCG AGA TGA ATC CTC A	sense
SG 621		CAG GTC CAG GGG TCT TGG TCC	antisense

2. Materials and Methods

SG 572	cyclinA2	GGT ACT GAA GTC CGG GAA CC	sense
SG 573		GAA GAT CCT TAA GGG GTG CAA	antisense
SG 574	ccnb1 (cyclinB1)	CGC CTG AGC CTA TTT TGG T	sense
SG 575		GCA CAT CCA GAT GTT TCC ATT	antisense
SG 576	cdc2 (cdk1)	TGG ATC TGA AGA AAT ACT TGG ATT CTA	sense
SG 577		CAA TCC CCT GTA GGA TTT GG	antisense
SG 568	Birc5	GCC CAG TGT TTC TTC TGC TT	sense
SG 569		CCG GAC GAA TGC TTT TTA TG	antisense
SG 590	Ubch10	TGC CGA GCT CTG GAA AAA	sense
SG 591		AAA AGA CGA CAC AAG GAC AGG	antisense
SG 630	B-Myb	TCC ACA CTG CCC AAG TCT CT	sense
SG 631		AGC AAG CTG TTG TCT TCT TTG A	antisense
SG 731	cdc6	CCT GTT CTC CTC GTG TAA AAG C	sense
SG 732		GTG TTG CAT AGG TTG TCA TCG	antisense
SG 1535	ZO-2	GTC CCA GAG ACC AAC AAG GA	sense
SG 1536		AAA GTT CTC GGG GCT GCT	antisense

2.1.9.1.2. Mouse primers

Number	Application	Sequence	
SG 1282	b-actin	CTA AGG CCA ACC GTG AAA AG	sense
SG 1283		ACC AGA GGC ATA CAG GGA CA	antisense
SG 785	Lin9	TTG GGA CTC ACA CCA TTC CT	sense
SG 786		GAA GGC CGC TGT TTT TGT C	antisense
SG 820	B-Myb	TTA AAT GGA CCC ACG AGG AG	sense
SG 821		TTC CAG TCT TGC TGT CCA AA	antisense
SG 1005	ccnb1 (cyclinB1)	CGC TGA AAA TTC TTG ACA ACG	sense
SG 1006		TCT TAG CCA GGT GCT GCA TA	antisense
SG 1026	Aspm	GAT GGA GGC CGA GAG AGG	sense
SG 1027		CAG CTT CCA CTT TGG ATA AGT ATT TC	antisense
SG 1030	Nusap	TCT AAA CTT GGG AAC AAT AAA AGG A	sense
SG 1031		TGG ATT CCA TTT TCT TAA AAC GA	antisense

2. Materials and Methods

SG 1009	Aurka	GGG ACA TGG CTG TTG AGG	sense
SG 1010		GTT TTC TTT ACA TCT GTC CAT GTC A	antisense
SG 965	Oct4	GTT GGA GAA GGT GGA ACC AA AG	sense
SG 966		CTC CTT CTG CAG GGC TTT C	antisense
SG 1200	Kif20a	AAG GAC CTG TTG TCA GAC TGC	sense
SG 1201		TGA GGT GTC CGC CAG TCG AGC	antisense
SG 1290	Flk1	CAG TGG TAC TGG CAG CTA GAA G	sense
SG 1291		ACA AGC ATA CGG GCT TGT TT	antisense
SG 1306	Vax2	ACT GAG TTG GCC CGA CAG	sense
SG 1307		CCC GCT TCT CCA GGT CTC	antisense
SG 1308	NeuroD1	CGC AGA AGG CAA GGT GTC	sense
SG 1309		TTT GGT CAT GTT TCC ACT TCC	antisense
SG 1312	Gm11487	AGC TCA GGA GAC AAA ATG CAG	sense
SG 1313		CTG AGG AAC TTT GGC CTT CTT	antisense
SG 1314	AFP	CAT GCT GCA AAG CTG ACA A	sense
SG 1315		CTT TGC AAT GGA TGC TCT CTT	antisense
SG 1316	Pcdh8	GAA GTT CAG TGG GAA AGA CAG C	sense
SG 1317		GTA CAC GCC CAC AGT CCA C	antisense
SG 1318	Pdgfra	GTC GTT GAC CTG CAG TGG A	sense
SG 1319		GTC GTT GAC CTG CAG TGG A	antisense
SG 1320	Stmn3	CTG AGG AGC GGA GGA AGA	sense
SG 1321		CCT CCC GTT CAT GCT CAC	antisense
SG 1322	Id4	AGG GTG ACA GCA TTC TCT GC	sense
SG 1323		CCG GTG GCT TGT TTC TCT TA	antisense

2.1.9.2. Primers for chromatin immunoprecipitation

2.1.9.2.1. Human primers for ChIP

Number	Application	Sequence	
SG 540	GAPDH2	GGC AGC AAG AGT CAC TCC A	sense
SG 541		TGT CTC TTG AAG CAT GTC TCT TGA AGC ACA CAG GTT	antisense
SG 548	cyclinB1	AGT GAG TGC CAC GAA CAG G	sense

2. Materials and Methods

SG 549		GCC AGC CTA GCC TCA GAT TT	antisense
SG 612	Birc5	CCA TTA ACC GCC AGA TTT GA	sense
SG 613		GCG GTG GTC CTT GAG AAA G	antisense
SG 552	Ubch10	GCC CTT TAA TGG TTA GCG TTT	sense
SG 553		GCT GCC ATT AAC TAA CGA ATC C	antisense
SG 1513	cyclinD1	CTG CCG GCC TTC CTA GTT	sense
SG 1514		GGA TTT AGG GGG TGA GGT G	antisense
SG 614	AurkA	TGG GAC TGC CAC AGG TCT	sense
SG 615		CGC ACT TGC TCC CTA AGA AC	antisense

2.1.9.2.2. Mouse primers for ChIP

Number	Application	Sequence	
SG 976	GAPDH	ATT TCC CCT GTT CTC CCA TT	sense
SG 977		GAC ATC CAG GAC CCA GAG AC	antisense
SG 1180	Mutyh	GAG CTT GTC CCT CAC CAG TT	sense
SG 1181		AGC CTG AAT CTG CCC TCT TT	antisense
SG 1207	Kif20a	CAG ACA GTC TTC GGG TGA GTG	sense
SG 1208		CTT CTA CGG ACG CGC AAG	antisense
SG 1209	Hmmr	TCG CCT GAA TTC AAA TTT ACC	sense
SG 1210		CAG GAT TGG CCA GAT AGG TT	antisense
SG 1211	AurkA	AGA AGG CTG CGG GAA GAG	sense
SG 1212		GTC TGT GGA TGA ACG GGA GT	antisense
SG 1257	b-actin	AAA TGC TGC ACT GTG CGG CG	sense
SG 1258		AGG CAA CTT TCG GAA CGG CG	antisense
SG 1050	Aspm	GCT GTA GCG AGG AGG TTC C	sense
SG 1051		TTT TGC TCG GTT CAA ATA TCG	antisense
SG 1568	CyclinD1	CCA GCG AGG AGG AAT AGA TG	sense
SG 1569		CGA AAA TCT CCA GCA ACA GC	antisense
SG 1576	Kif20a	CCA AGA CCT GCC ACT CTG A	sense
SG 1577	downstream	TAT GGT GGG GGA AAG ATG G	antisense

2.1.10. siRNA sequences

siRNA against	Sequences 5' to 3'	Target
ctrl	UAG CGA CUA AAC ACA UCA A	non targeting
B-Myb# 1 (mouse)	GCC CAU AAA GUC CUG GGU AAC	Knight <i>et al.</i> 2009
B-Myb# 2 (mouse)	GGU GCG ACC UGA GUA AAU U	Tarasov <i>et al.</i> 2008
Lin9 (mouse)	GCU ACU UAC AGA GUA ACU UUC	Knight <i>et al.</i> 2009
Lin54 (mouse)	GCA AAU GCA UCG GCU GUA AGA	Knight <i>et al.</i> 2009
ZO-2 (human)	UGG GAG UCA GAU CUU CGU AAA	Kusch <i>et al.</i> , 2009

2.1.11. Cell lines, cell culture media and treatments

2.1.11.1. Media and additives

DMEM (4.5 g Glucose/L-Glutamine)	Gibco [®] , Life Technologies
Penicillin/Streptomycin (10 u/μl each)	Cambrex / Lonza
TrypLE™	Gibco [®] , Life Technologies
Fetal calf serum (FCS)	Gibco [®] , Life Technologies
MEM Non essential amino acids (100 X) (NEAA)	Gibco [®] , Life Technologies
Sodium-Pyruvate MEM 100 mM	Gibco [®] , Life Technologies

2.1.11.2. SILAC media and additives

Mouse Stem Cell Expansion DMEM for SILAC	PIERCE (Thermo Scientific)
Stem Cell Screened Dialyzed FBS for SILAC	PIERCE (Thermo Scientific)
¹³ C labeled L-Lysine HCl	Silantes
¹³ C ¹⁵ N labeled L-Arginine HCl	Silantes
L-Lysin-HCl	Sigma
L-Arginine	Sigma
L-Proline	Sigma

2. Materials and Methods

2.1.11.3. Cell lines / media

ES cells	15 % FCS / 1 % PenStrep / NEAA (1X) / 1 mM Na-Pyruvate / 0.1 mM β -mercaptoethanol / 1000 u/ml LIF
Embryoid bodies	15 % FCS / 1 % PenStrep / NEAA (1X)/ / 1 mM Na-Pyruvate / 0.1 mM β -mercaptoethanol
293T	10 % FCS / 1 % PenStrep
T98G	10 % FCS / 1 % PenStrep / NEAA (1X)
U2OS	10 % FCS / 1 % PenStrep

The different ES cell lines were used:

Cell line	feature	usage
D3	wildtype	siRNA / Embryoid Bodies
E14	wildtype	siRNA / Embryoid Bodies
HaBirA	BirA ligase	SILAC / ChIPchip
Bio-B-Myb	BirA ligase / FlagBio-B-MYB	SILAC / ChIPchip
Bio-Lin9	BirA ligase / FlagBio-LIN9	SILAC / ChIPchip
Bio-ZO2	BirA ligase / FlagBio-ZO2	SILAC / ChIPchip

2.1.11.4. Transfection reagents

ES cells	Lipofectamine2000 (Life Technologies)
T98G	MetafectenePro (Biontex) Dharmafect2 (ThermoScientific)
U2OS	Dharmafect1 (ThermoScientific)
293T	Calcium phosphate

2.2. Methods

2.2.1. Cell Culture

2.2.1.1. Passaging of Cells

Eukaryotic cells were cultured in a tissue culture incubator at 37°C and 5% CO₂. For passaging, cells were washed once with 1x PBS and incubated with TrypLE at 37°C until the cells detach. After detachment, cells were plated onto new cell culture dishes.

2. Materials and Methods

2.2.1.2. Transient transfection

Mouse ES cells were transfected using Lipofectamine2000. 1×10^6 cells were plated on a 6-cm dish the day before transfection. 400 μ l OptiMEM were mixed with 10 μ l Lipofectamine2000, incubated for 5 min at RT and transferred to a tube containing 400 μ l OptiMEM with 3 μ g plasmid. After 20 min the transfection mix was added to the cells washed once with OptiMEM. After 4 h the transfection mix was replaced with fresh complete medium.

T98G cells were transfected with Dharmafect2 according to the manufacturer's protocol with 75 nM siRNA and 3 μ l Dharmafect2 per 6-well.

2.2.1.3. Alkaline phosphatase activity test

Characteristic for undifferentiated cells is the high expression and activity of alkaline phosphatase (AP). To test the pluripotency of ES cells, AP activity was determined with the Alkaline Phosphatase Detection Kit (Millipore). AP positive cells show a violet staining.

2.2.1.4. Embryoid Body (EB) formation

To study undirected differentiation of ES cells *in vitro* the Hanging-Drop method was used to achieve EB cultures (Wang and Yang, 2008). To do so, an ES cell suspension was prepared with 1×10^4 cells/ml. Drops of 20 μ l were placed on the lid of cell culture dishes and carefully placed on the dish filled with 1xPBS to prevent drying of the cells. Cells were incubated for two days to induce EB formation, then washed from the lids and kept in suspension on poly-HEMA coated plates.

2.2.1.5. SILAC cell culture

For SILAC (stable isotope labeling by amino acids in cell culture) cell culture, the control cell line (HA BirA) was cultured in 'light' medium without labeled amino acids. The tested cell line was cultured in 'heavy' medium containing the labeled amino acids. For sufficient incorporation of the amino acids, cells at least underwent 4 passages.

SILAC medium consisted of special DMEM medium without lysine and arginine, dialysed FCS and the additives usually used for ES cell culture. The 'light' medium was enriched with L-lysine (100 mg/500 ml), L-arginine (50 mg/500 ml) and L-proline (115 mg/500 ml), whereas 'heavy' medium was enriched with the labeled amino acids and L-lysine.

2. Materials and Methods

2.2.1.6. Synchronisation of T98G cells

T98G cells were synchronised in G0 phase by serum starvation. To do so, cells were washed twice with 1xPBS and fed with medium containing 0% FCS. After 72 h cells were released into cell cycle by replacing the starvation medium with medium containing 20% FCS. Progress through the cell cycle was monitored by PI-FACS staining. Cells were harvested at different time points between 0 h (G0-phase) and 32 hours after release.

To synchronise T98G cells in G1 phase of the cell cycle a thymidine block was used. Cells were blocked with 2 mM thymidine for 24 hours, washed twice with PBS and released into the cell cycle with fresh medium.

2.2.1.7. Synchronisation of U2OS cells

For synchronisation of U2OS cells in late G1 phase they were treated for 24 h with 2.5 mM thymidine. After washing twice with 1x PBS cells were released into the cell cycle with normal growth medium.

2.2.1.8. Synchronisation of ES cells

To synchronise ES cells in G1 phase they were treated with 2 mM hydroxyurea (HU) for 12 hours. After washing 3 times with PBS they were released into the cell cycle with fresh medium.

Synchronisation in mitosis was achieved by treatment with 45 ng/ml nocodazole for 12 hours.

2.2.1.9. Determination of cell cycle phases by flow cytometry (FACS)

For FACS analysis cells were harvested by trypsinisation, washed with ice cold 1x PBS and fixed with 1 ml ice cold 80% ethanol over night at -20°C . On the next day, cells were washed again with 1x PBS and resuspended in 500 μl 38 mM sodium citrate and 25 μl RNaseA [10 mg/ml] and incubated for at least 30 min at 37°C . Cells were stained by addition of 15 μl propidium-iodide (PI) [1 mg/ml] and measured by FACS.

2.2.1.10. Determination of cells in S-phase by BrdU-FACS

FACS analysis with Bromodeoxyuridine (BrdU) staining was used to determine the amount of cells that are in S-phase of the cell cycle. 10 μM BrdU was added 30 min before cell harvesting and fixation in ice cold 80% ethanol over night at -20°C . DNA was denatured

2. Materials and Methods

by resuspending the cells in 1 ml 2 M HCl / 0.5 % Triton-X-100 and incubation at RT for 30 min. Cells were pelleted for 10 min at 1000×g (RT) and resuspended in 200 µl 0.1 M Na₂B₄O₇ to neutralise the acid. 1 × 10⁶ cells were transferred to a new tube, pelleted at 10,000×g for 10 sec and resuspended in 50 µl PBS / 0.5 % Tween20 / 1 % BSA. 20 µl of an α-BrdU-FITC antibody was added and incubated for 60 min in the dark. After washing with 50 µl PBS / 0.5 % Tween20 / 1 % BSA cells were resuspended in 500 µl PBS + 25 µl RNaseA [10 mg/ml] and incubated for at least 3 min at 37°C. Cells were stained by addition of 15 µl PI [1 mg/ml] and measured by FACS.

2.2.1.11. Determination of cells in M-phase by MPM2-FACS

To determine the amount of mitotic cells by FACS-analysis, cells were stained with an antibody that recognises the phosphorylated form of the Mitotic protein #2 (MPM2) which is an marker for mitotic cells. Cells were fixed with ice cold 80 % ethanol over night at -20°C. On the next day cells were pelleted for 10 min at 1000×g and washed with 1× PBS. Cell pellets were resuspended in 1.5 ml 'MPM2 Wash Buffer' (0.05 % Triton X-100 in PBS), pelleted for 5 min at 1200×g (4°C) and resuspended in 90 µl 'MPM2 Staining Solution' (0.05 % BSA, 0.2 % Triton X-100 in PBS). MPM- antibody was diluted 1:50 in PBS (25 µl PBS + 0.5 µl MPM2 antibody) and 16.8 µl were added to the cell solution. After incubation for at least for 2 h on ice, cells were washed twice with 1 ml MPM2 Wash Buffer and resuspended in 90 µl MPM2 Staining Solution. The second antibody was diluted 1:50 in PBS (25 µl PBS + 0.5 µl Anti mouse Alexa-Fluor488 antibody) and 1.9 µl were added to the cells. After incubation for 1 h in the dark on ice, cells were washed once with 1 ml MPM2 Wash Buffer and once with PBS. Cells were resuspended in 500 µl PBS + 35 µl RNaseA [10 mg/ml] + 25 µl PI [1 mg/ml], incubated for at least 30 min at 37°C and measured by FACS.

2.2.1.12. Growth Curve of U2OS and T98G cells

24 h after siRNA transfection 1 × 10⁴ cells were plated in wells of a 24-well plate in triplicates. Every day cells were counted using a Neubauer Chamber. The number of cells per ml in suspension was calculated using the following formula:

$$\text{Cells/ml} = (\text{Cells counted} / \text{number of counted large squares}) \times 1 \times 10^4.$$

Mean values of the cell numbers were plotted against time.

2.2.2. Expression Analysis

2.2.2.1. RNA isolation

RNA was isolated by using the RNA isolation reagent Trifast (Peqlab). After removing the medium from the cells 0.5 ml (for 6-well) Trifast was added to the cells under a fume hood. Cells were scraped off the plate, transferred to 1.5 ml Eppendorf tubes and incubated for a maximum of 5 min at room temperature (RT). 100 μ l chloroform was added and mixed by shaking (not vortexing). After 1-2 min samples were centrifuged for 10 min at 12,000 \times g and 4°C in a table top centrifuge. The upper aqueous phase was carefully transferred to a new tube containing 250 μ l isopropanol. After vortexing the samples and incubation at RT for 15 min the samples were centrifuged for 15 min, at 12000 \times g (RT). The RNA pellet was washed with 1 ml 75 % ethanol and centrifuged again for 5 min at 7000 \times g. The pellet was resolved in 25 μ l DEPC-H₂O.

2.2.2.2. cDNA synthesis by reverse transcription

For transcribing RNA into cDNA 1-2 μ g RNA were brought up to 9.5 μ l with ddH₂O and mixed with 0.5 μ l random primers [0.5 μ g/ μ l]. After incubation for 5 min at 70°C and cooling on ice for 1 min the following mixture was added:

5 μ l M-MLV 5x reaction buffer
6.25 μ l dNTPs [2 mM]
0.5 μ l Ribolock RNase inhibitor [40 U/ μ l]
0.5 μ l M-MLV-RT [200 U]
2.75 μ l H₂O

The mixture was incubated at 37°C for 60 min and inactivated for 15 min at 70°C.

2.2.2.3. Quantitative real-time PCR (qRT-PCR)

To determine the quantitative amount of specific mRNA compared to a housekeeping gene, the following reaction was prepared:

12.5 μ l Absolute QPCR SYBR Green Mix
10.5 μ l H₂O
1 μ l fw/rv primer mix (10 pmol/ μ l each)
1 μ l cDNA or precipitated chromatin

2. Materials and Methods

PCR program (40 cycles):

95°C 15 min

95°C 15 sec

60°C 1 min

The relative expression of a gene compared to a housekeeping gene was calculated with this formula:

$$2^{-\Delta\Delta Ct}$$

with $\Delta\Delta Ct = \Delta Ct$ (sample) - ΔCt (reference)

and $\Delta Ct = CT$ (gene of interest) - CT (housekeeping gene)

The standard deviation of $\Delta\Delta Ct$ was calculated with:

$$s = \sqrt{s_1^2 + s_2^2}$$

with s_1 = standard deviation (gene of interest)

and s_2 = standard deviation (housekeeping gene)

The margin of error for $2^{-\Delta\Delta Ct}$ was determined by this formula: $2^{-\Delta\Delta Ct \pm s}$

and the error used for the error bars was calculated with: $2^{-\Delta\Delta Ct \pm s} - 2^{-\Delta\Delta Ct}$

2.2.2.4. Agilent Microarray

For gene expression analysis the Agilent Two-Color Microarray-Based Gene Expression Analysis v.5.7 was used. 100 ng of total RNA was labeled and amplified with the Quick Amp Labeling Kit, 2-color and hybridised on the mouse chip Agilent 44K Whole Mouse Genome Array according to the manufactures instructions. The gene expression analysis in ES cells after LIN9 depletion was performed at the IMT in Marburg.

2.2.3. Biochemical Methods

2.2.3.1. Whole cell lysates

Cells were scraped in PBS, centrifuged for 5 min at 3000 rpm and 4°C. The pellet was resuspended in 10 times the amount of TNN buffer (with freshly added PMSF [1 µM] + proteasome inhibitor cocktail (PIC) (1:500) + DTT [1 µM]) for 20 min on ice. Lysates were pelleted for 10 min at 12,000 × g (4°C) and the supernatant was transferred to a new reaction tube. Lysates were used immediately or stored frozen at -80°C.

2. Materials and Methods

2.2.3.2. Nuclear Extracts of ES cells

ES cells were harvested by trypsinisation and pelleted for 5 min at 2400×g (4°C). After washing once with ice-cold 1× PBS and determining the cell number, cells were resuspended in 5× packaged cell volume (PCV) of NebA (1 mM DTT, 1 mM PMSF, PIC 1:1000) and pelleted for 5 min at 2400×g (4°C). Again cells were resuspended in 3× PCV of NebA (1 mM DTT, 1 mM PMSF, PIC 1:100) and incubated on ice for swelling. Cells were transferred to a 15 ml Glass Douncer (pre-rinsed with NebA) and homogenised slowly with 10 strokes (Pestle A - loose) to achieve a minimum of 95 % lysis (checked with Trypan Blue staining). Lysates were centrifuged for 15 min at 2400×g (4°C) and pellets were quickly resuspended with 3 ml (per 1×10^8 cells) of ice cold NebB. Cell nuclei were homogenised in a 15 ml Glass Douncer (pre-rinsed with NebB) with 10 strokes (Pestle A - loose). Lysates were transferred to 1.5 ml Eppendorf tubes and rotated end-over-end for 30 min in the cold room. Nuclear extracts were obtained by centrifugation of the lysates for 30 min at 14,000×g (4°C). Extracts could also be stored after flash-freezing in N₂ at –80°C.

2.2.3.3. Protein concentration (Bradford)

The protein concentration was determined with the method described by Bradford (Bradford, 1976). 1 µl of the lysate was mixed with 100 µl of 150 mM NaCl and 1 ml Bradford solution. After an incubation of 3 - 5 min the extinction at 595 nm was measured and compared to a standard BSA dilution series.

2.2.3.4. Immunoprecipitation (IP)

For immunoprecipitation 1-2 mg of whole cell lysate or nuclear extracts were incubated with the desired antibody for 3 h to over night at 4°C on a rotating wheel. 30 µl of Protein-G sepharose or Protein-G Dynabeads were added and incubated for 30 min (Dynabeads) to 60 min (Sepharose) at 4°C on a rotating wheel. The beads were washed 5 times with TNN buffer. With the last wash beads were transferred to a new tube. After the last wash the supernatant was completely removed. Protein was eluted by adding 30 µl 2× ESB and boiling at 95°C for 3 - 5 min. Optional, the samples were stored at –20°C.

In parallel, 5 - 10 % of the protein amount used for immunoprecipitation was boiled with 3× ESB at 95°C for 3 - 5 min and loaded onto a SDS-gel or optionally stored at –20°C.

2. Materials and Methods

2.2.3.5. SDS-polyacrylamide gel electrophoresis (SDS-PAGE)

SDS-PAGE analysis was performed using the discontinuous method (Laemmli, 1970). For electrophoretic separation, an 8-12 % SDS-acrylamide gel was prepared and, after polymerisation, a stacking gel was poured on top. The gels were prepared as follows (for 2 mini gels):

Separating gel (8 %)	Stacking gel (4 %)
7.25 ml H ₂ O	2.95 ml H ₂ O
3.75 ml Lower Stock (4x)	1.95 ml Upper Stock (4x)
4 ml Protogel (30 %)	0.8 ml Protogel (30 %)
100 µl APS (10 %)	50 µl APS (10 %)
10 µl Temed	10 µl Temed

Gels were run in 1xSDS running buffer for 30 min at 80 V to allow proteins to migrate through the stacking gel and then for another 1 h at 150 V.

2.2.3.6. Nupage[®] Bis-Tris gel electrophoresis

For MassSpec analysis protein samples were separated by the Novex[®] Nupage[®] SDS-PAGE Gel System (Life Technologies). Precast NuPAGE[®] 4-12 % Bis-Tris gels were used according to the manufactures manual under reducing conditions. Proteins were visualised by colloidal coomassie staining (Life Technologies).

2.2.3.7. Immunoblotting

The transfer of proteins onto a PVDF membranes was done via electroblotting. The PVDF membrane was pre-incubated with methanol and rinsed with blotting buffer. The SDS gel was equilibrated for 10 min in blotting buffer before blotting. The gel was laid onto a layer of Whatman filter paper (soaked with blotting buffer) and the PVDF membrane was placed on the SDS gel, followed by a second layer of filter paper. This 'sandwich' was enclosed on both sides by sponges (soaked in blotting buffer) and placed in a BioRad Wet Blot gadget filled with 1x blotting buffer. The transfer occurred for 60-90 min at 100 V in 1x blotting buffer. Successful and equal transfer of proteins was visualised by staining the membrane with a Ponceau S solution and destaining with H₂O.

For blocking, the membrane was transferred into blocking solution and incubated at RT for 1 h. The desired antibodies were added to fresh blocking solution in the required dilution

2. Materials and Methods

and incubated with the membrane over night at 4°C or alternatively for 2 h at RT. After washing the membrane 4 times with TBST for 5 min, the appropriate secondary HRP-conjugated antibody (in blocking solution) was added and incubated for 1 h at RT. The membrane was washed 6 times for 5 - 10 min with TBST and specific bands were then detected using a luminol-substrate-solution. The membrane was wrapped in plastic foil and exposed to an ECL-film.

2.2.3.8. SILAC Immunoprecipitation for mass spectrometry

To identify proteins associated with the DREAM complex, SILAC experiments with ES-cells expressing biotinylated LIN9 or B-MYB and subsequent mass spectrometry analysis were performed.

For one SILAC experiment 15-20 15-cm dishes of the ES-cell lines ('heavy' and 'light') were grown (section 2.2.1.5) and nuclear extracts were prepared as described in section 2.2.3.2. To reduce non-specific binding, nuclear extracts were precleared by adding ProteinG-Dynabeads and incubation on a rotating wheel for 1-2 hours at 4°C.

To remove the beads from the lysates, beads were collected on a magnet for 2 minutes and the supernatant was carried over to new 15-ml falcons. Nuclear extracts were adjusted to a concentration of 2 mg/ml protein and 0.025 % NP-40 by diluting with IP(0) buffer and NP-40. The salt concentration was adjusted to 150 mM NaCl.

For the IP 40 µl of Streptavidin-Dynabeads were used per mg protein (same amounts of protein were used for control and biotin-sample). Samples were incubated for 4 hours at 4°C on an end-over-end rotator. Beads were washed 5 times with IP(150) buffer (protease inhibitor cocktail added freshly). With the last wash the beads were transferred to 1.5 ml tubes and the buffer was completely removed. Proteins were eluted from the beads by adding 1×LDS sample buffer (reducing) and heating for 10 min at 70°C. Beads were captured by the magnet and the eluates were combined. To reduce the volume of the eluate, proteins were concentrated with 'Amicon Ultra-0.5 ml centrifugal filters' (Millipore). The concentrated eluate was sent to the Max Planck Institute for Biophysical Chemistry for further procedure and MassSpec analysis. Samples were used for SDS gel electrophoresis (section 2.2.3.6), protein bands were visualised by colloidal coomassie staining (Life Technologies) and cut out. Proteins were digested with trypsin to achieve small peptides and the samples analysed by liquid chromatography coupled with tandem MS (LC-MS/MS) for protein identification. Since metabolic incorporation of the labeled 'heavy' amino acids into the proteins results in a mass shift of the corresponding peptides, pairs of chemically identical peptides of different stable-isotope composition ('heavy' and 'light') can be distin-

2. Materials and Methods

guished in a mass spectrometer. The ratio of intensities for such peptide pairs accurately reflects the abundance ratio for the two proteins. Thus, proteins can be identified that show enriched binding to the biotinylated LIN9 or B-MYB.

2.2.3.9. Chromatin immunoprecipitation of biotinylated LIN9 ES cells (Bio-ChIP)

Proteins were crosslinked to DNA by adding 540 μ l 37 % formaldehyde dropwise to the 20 ml medium of a 15-cm dish. After 10 minutes, the reaction was stopped by addition of 2.5 ml 1M Glycine and incubation of 5 minutes. Cells were placed on ice, washed twice in PBS and scraped with ice cold PBS (+ PIC 1:1000 + 1 mM PMSF) into 15-ml falcons. The cell number per dish was determined by trypsinising and counting cells from a separate dish. Cells were aliquoted in 2×10^7 cell portions, frozen in liquid nitrogen and stored at -80°C or used immediately.

For sonification cells were lysed in 1 ml of ChIP lysis buffer (1 mM PMSF and PIC 1:1000), transferred to 15-ml polystyrole falcons and incubated for 10 min on ice. Chromatin was sheared with the BioRuptor sonicator from Diagenode. For ChIP sequencing analysis fragments of around 250 bp were needed. Therefore cells were sonicated as follows:

30 sec pulse on
20 sec pulse off
High amplitude
20 min total

Chromatin was spun at 14,000 rpm for 10 minutes (4°C). 50 μ l were used for chromatin size check.

For immunoprecipitation 1 % of the chromatin was used as input and set aside on ice for further use. The remaining chromatin was added to 50 μ l pre-blocked streptavidin M250 Dynabeads[®] (Life Technologies) and incubated for 5 h on a rotating wheel (4°C). For washing beads were collected on a magnet for 2 min and the supernatant was discarded. 1 ml of ChIP washing buffer 1 was added and the beads were transferred to a new tube and rotated at 4°C for 10 min to reduce background. Beads were washed once with ChIP washing buffer 1 and once each with ChIP washing buffer 2 and washing buffer 3. This was followed by two washing steps with TE buffer. After complete removal of TE, 250 μ l elution buffer was added to the beads and to the input samples. Reverse cross-linking was done over night at 65°C with shaking at 600 rpm.

On the next day, beads were removed, 1 μ l RNaseA [10 mg/ml] was added to the eluate

2. Materials and Methods

and incubated for 30 min at 37°C. Finally, a proteinase K (2 µl of [10 mg/ml] stock) digest was performed at 55°C for 2 hours.

DNA was purified with the Qiagen PCR Purification Kit according to the manufacturer's protocol, eluted in 50 µl EB buffer and stored at -20°C until further use.

2 µl of purified chromatin was used for analysis by quantitative PCR and enrichment of the precipitated samples on the tested promoters were compared to input chromatin.

2.2.3.10. Blocking beads for ChIP

ProteinG or M-270 Streptavidin Dynabeads® were blocked with BSA and ssDNA. To do so, 50 µl beads per IP were once washed with ChIP lysis or ChIP dilution buffer and incubated for at least 1 hour on an end-over-end rotator at 4°C with 1 ml blocking buffer.

2.2.3.11. ChIP-on-chip

For ChIP-on-chip, crosslinked chromatin was prepared from 2×10^8 BioLin9 cells and precipitated with streptavidin-coupled Dynabeads as described above. The crosslink was reversed, the DNA eluted and purified. Precipitated samples and input DNA were amplified using the WGA2 kit (Sigma). 4 µg amplified DNA was labeled with Cy5 and Cy3 and hybridised to a MM8 385k NimbleGen Mouse ChIP 385k RefSeq promoter array containing oligonucleotide probes that cover the region -2 to +0.5 kb relative to the transcriptional start sites for 19,489 annotated transcripts. Probes consisted of 50- to 75-mers at approximately 100 bp spacing. DNA labeling, hybridisation, detection and data analysis were performed using the services of Imagenes (Berlin). Signal intensity data were extracted from the scanned images of each array using NimbleScan data extraction software. Log₂ ratio of experimental and input signals was then computed and scaled and peak data files were generated (.gff) by identifying four or more consecutive probes, whose signals are above a cutoff value (a percentage of the hypothetical maximum (mean +6 standard deviation) using a 500 bp sliding window. The probability of false discovery is calculated by randomising the data 20 times and each peak is given a false discovery rate (FDR), where the lower the FDR score, the higher the probability that peak represents a true binding site. Enriched peaks were visualised using SignalMap. Promoters with a FDR < 0.1 and a peak score > 1 were considered positive LIN9 targets.

2.2.4. **Molecular Biology**

2.2.4.1. **Analytical isolation of plasmid DNA from bacteria (DNA-Miniprep)**

Single colonies were picked from a LB-agar plate after transformation and incubated in 4 ml LB containing ampicillin over night in a shaker at 37°C. 1.5 ml bacterial solution was pelleted and resuspended in 200 µl S1. The bacteria were lysed by adding 200 µl S2 for 5 minutes. This reaction was neutralised with 200 µl S3, mixing and incubation for 10 min on ice. The bacterial debris was pelleted for 5 minutes at full speed and plasmid DNA in the supernatant was precipitated with 600 µl isopropanol. After centrifugation for 10 min at room temperature, the pellet was washed with 1 ml 70 % ethanol. The pellet was air-dried and resuspended in 30 µl TE. Correct bacterial clones were identified by restriction digest (2.2.4.7).

2.2.4.2. **Preparative isolation of plasmid DNA from bacteria (DNA-Maxiprep)**

A pre-culture was prepared by inoculating 5 ml LB medium (containing ampicillin) with a single colony and growing for 8 hours to over night in a shaker at 37°C. 2.5 ml of this culture was used to inoculate 250 ml LB medium (containing ampicillin) which was incubated over night (max. 16 hours) at 37°C. Bacteria were harvested by centrifugation for 10 min at 4300 rpm (4°C). The pellet was resuspended with 10 ml resuspension buffer and further processed with the Plasmid Maxi Kit (Life Technologies) according the manufacturer's protocol.

The DNA pellet was resuspended with TE buffer and set up to 1 mg/ml concentration.

2.2.4.3. **Isolation of plasmid DNA fragments from agarose gels**

Plasmid DNA was digested with the appropriate enzymes and incubated at 37°C for at least 2 h. The restriction was loaded on a 0.8-1.2 % agarose gel and fragments were separated by electrophoresis at 120 V for 30 min. The desired bands were cut out and isolated with the JetStar Gel Extraction Kit (Genomed) according to the manufacturer's instructions.

2.2.4.4. **Isolation of PCR products after restriction**

To purify PCR products after restriction, the QIAquick PCR purification kit from Qiagen was used according to the manufacturer's protocol.

2. Materials and Methods

2.2.4.5. Polymerase chain reaction (PCR)

To amplify DNA fragments for cloning, the Pfu polymerase (Fermentas) was used, which is a special proof reading polymerase and has a 3'-5' proof reading / exonuclease activity.

Standard reaction mix:

template DNA	2-5 μ l
polymerase buffer	5 μ l
<i>Pfu</i> DNA polymerase	1 μ l
dNTPs [2 mM]	5 μ l
primer fw [10 μ M]	3 μ l
primer rev [10 μ M]	3 μ l
ddH ₂ O	add to 50 μ l

Primers should have an annealing temperature of between 55-70°C. The first cycle annealing temperature was calculated with just the base pairs that overlap with the DNA without the additional restriction site. The second annealing temperature was calculated with the whole primer and used for the remaining cycles. The annealing temperature of the PCR was set 3-5°C lower than the lowest calculated one of the primer pair. For most reactions, 25-35 cycles were sufficient.

Standard PCR conditions:

Step	Temperature	Time	No. of cycles
1) Initial denaturation	95°C	30 sec	1 cycle
2) Denaturation first cycle	95°C	30 sec	
3) Annealing first cycle		30 sec	1 cycle
4) Extension first cycle		2 min per kb	
5) Denaturation	95°C	30 sec	
6) Annealing		30 sec	25-35 cycles
7) Extension		2 min per kb	
8) Final Extension	72°C	5 min	1 cycle
9) Soak	4°C	Indefinite	1 cycle

2. Materials and Methods

2.2.4.6. Agarose gel electrophoresis

To separate DNA fragments according to their size, agarose gel electrophoresis was used. Agarose (0.8-1.4 %) was dissolved in 1x TAE by heating in a microwave. Ethidium bromide was added in the concentration of 1 µg/100 ml to enable the visibility of the DNA fragments under UV light. DNA samples were mixed with 6x DNA-loading buffer and loaded into the pockets of the gel. As size marker, the 1 kb DNA ladder from Fermentas was used. Electrophoresis was performed at 90-120 V for about 45 min. DNA bands were visualised under UV light, photographed and/or excised (section 2.2.4.3).

2.2.4.7. Enzymatic restriction

Restriction of plasmid DNA and PCR fragments was performed with an adequate restriction endonuclease and its recommended buffer for 1 - 3 h at 37°C.

Standard reaction mix

DNA	0.5-5 µg
10x buffer	5 µl
enzyme	0.5 µl
ddH ₂ O	add to 50 µl

Digested DNA fragments from vectors were separated and analysed by agarose gelelectrophoresis (section 2.2.4.6). Digested PCR products were purified with the QIAquick PCR purification kit.

2.2.4.8. Ligation

DNA fragments were mixed with a molar ratio 1:3 (vector to insert). To ligation mix was set up in a 10 µl volume containing 1 µl T4-Ligase buffer, 1 µl T4-Ligase (New England Biolabs) and ~ 25 ng vector DNA. Ligation was performed for 45 min at RT followed by an incubation for 15 min at 65°C to inactivate the enzyme.

2. Materials and Methods

2.2.4.9. Transformation of E.coli

For transformation chemical competent DH5 α were used. Cells were removed from -80°C and thawed on ice for 5 min. 200 ng of plasmid DNA or 10 μl ligation mix were mixed with 80 μl competent bacteria and incubated on ice for 10 min. Next the mix was heat shocked at 42°C for 45 sec and placed back on ice for 2 min. 1 ml of LB-medium (without antibiotics, pre-warmed to 37°C) was added to the transformation mix and incubated for 30 min at 37°C (shaking). Cells were pelleted for 1 min at 6000 rpm and resuspended after removing most of the supernatant. Bacteria were plated onto LB-agar plates (with proper antibiotics) and incubated over night at 37°C . Colonies were picked for plasmid isolation (section 2.2.4.1).

3. Results

3.1. Role of the DREAM complex in murine ES cells

The DREAM complex is essential for proper cell cycle progression and proliferation. Deletion of Lin9 or the associating transcription factor B-Myb leads to a peri-implantational lethality in mice (Reichert et al., 2010; Tanaka et al., 1999). They report that ES cells lacking Lin9 or B-Myb fail to build up inner cell mass which is the origin of embryonal stem cells. DREAM function is well characterised in differentiated cells but whether it fulfils more functions during differentiation is so far unknown. Aim of this work is to elucidate the role of LIN9 and the DREAM complex in mouse ES cells by the use of depletion assays as well as genome wide expression and promoter binding studies. This will help to achieve a better understanding about DREAM function in stem cell proliferation, cell cycle regulation and a possible role in cell differentiation or the maintenance of pluripotency.

3.1.1. Effects of LIN9 or B-MYB depletion on ES cell proliferation

Deletion of Lin9 in differentiated cells like mouse embryonic fibroblasts (MEFs) leads, besides abnormal mitosis or senescence, to accumulation and arrest of cells in G2/M phase of the cell cycle (Reichert et al., 2010). Since embryonal stem cells exhibit a different cell cycle behaviour with predominantly S-phase and mitosis and short gap phases, it would be interesting to know whether mouse ES cells show similar behaviour as differentiated cells upon DREAM disruption. To test the outcome of DREAM depletion in ES cells, the core component Lin9 or the associated factor B-Myb were targeted by short-hairpin RNA (shRNA).

ES cells then were either prepared for PI-FACS analysis to determine the cell cycle distribution, or used for differentiation assays to examine whether LIN9 or B-MYB depletion affects embryoid body (EB) formation, a method for *in vitro* differentiation.

3. Results

3.1.1.1. Depletion of LIN9 or B-MYB leads to G2/M arrest

The mouse ES cell lines D3 and E14 were used for these assays. Cells were transfected with the control vector pSuper.puro or the vector including a shRNA sequence against Lin9 or B-Myb (Knight and Watson, 2009) and selected with puromycin. 72 hours post transfection (hpt) cells were harvested for PI-FACS analysis. The efficient reduction of LIN9 down to 9% and B-MYB down to 13% on mRNA and protein level is shown in fig. 3.1 A & B. The percentage of cells in G2/M phase increased after depletion of Lin9 (42.5%) or B-Myb (56.4%) compared to control cells (33%) (fig. 3.1 C). Likewise, the amount of polyploid cells enlarged after LIN9 (14.3%) and B-MYB depletion (8.9%).

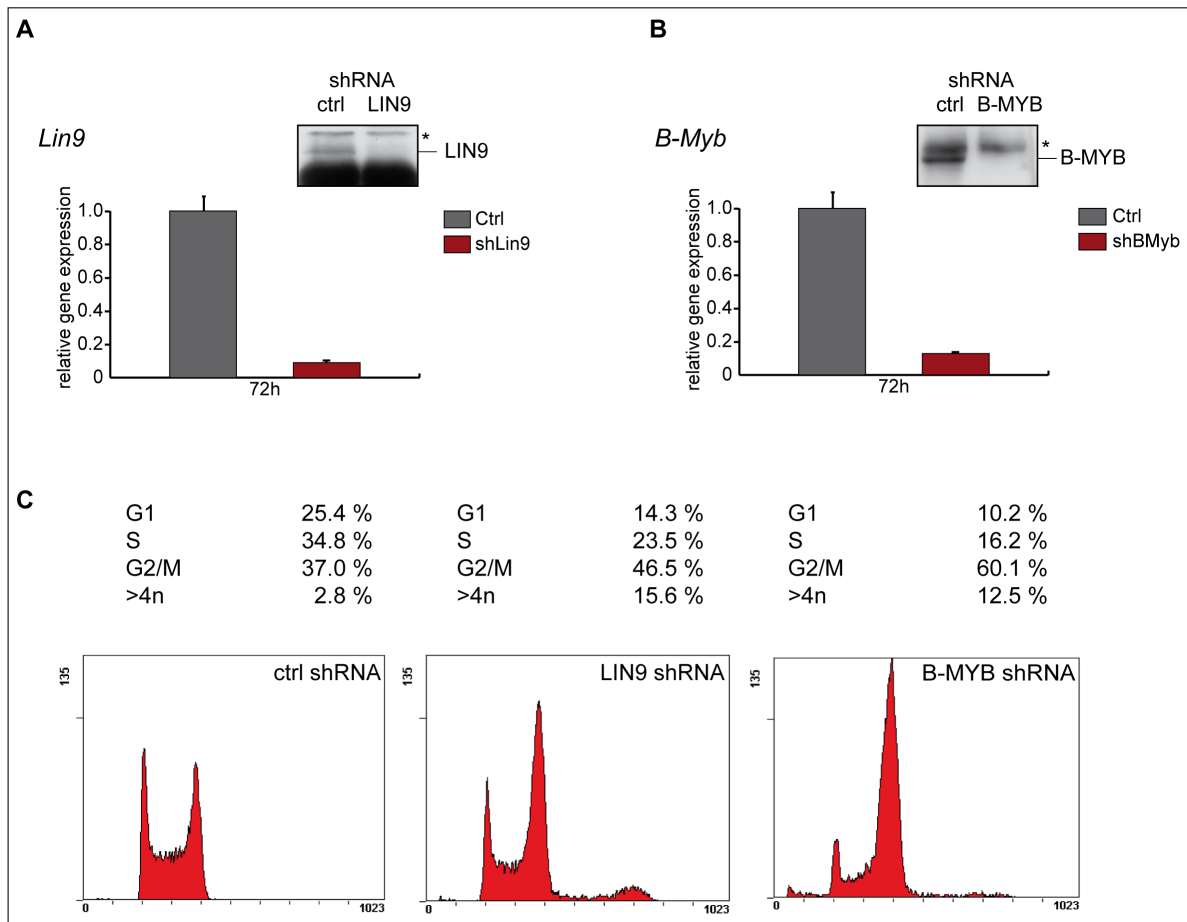


Figure 3.1.: **Knock down of LIN9 or B-MYB leads to accumulation in G2/M** ES cells (E14) were depleted by shRNA against Lin9 (A) and B-Myb (B) for 72h and selected with puromycin (1 μ g / ml). Knock down efficiency was determined on mRNA level by qRT-PCR as well as on protein level by immunoblotting. "*" marks unspecific bands. (C) PI-FACS profiles of ES cells after shRNA transfection exhibit an increased fraction of G2/M cells.

3. Results

3.1.1.2. Impaired embryoid body formation after LIN9 or B-MYB depletion

It was reported that LIN9 (Reichert et al., 2010) as well as B-MYB (Tanaka et al., 1999) are important for the development of mice and loss of one of those genes lead to an early lethality in mouse embryos.

Whether this dramatic knock out effect is only due to mitosis and proliferation defects or whether the DREAM complex also influences cell differentiation directly is so far not understood. Therefore, I next performed experiments to study the ability of ES cells to differentiate after LIN9 or B-MYB depletion. A good model to study undirected cell differentiation *in vitro* is the formation of embryoid bodies which resemble gastrulation *in vivo*. EBs form three-dimensional aggregates and undergo differentiation along all three germ lineages (ectoderm, endoderm, mesoderm).

Different methods are described to produce EBs. Here the 'Hanging Drop' method was used (Wang and Yang, 2008). Hence, drops consisting of 200 cells were placed on the inner lid of a cell culture dish. After 2 days, small EBs built on the tip of the drops and were collected in a 10-cm dish containing EB-medium for further growth (see EB formation scheme fig. 3.2 **A**). To prevent EB adhesion to the surface, dishes were coated with poly(2-hydroxyethyl methacrylate) (poly-HEMA).

To monitor EB formation after LIN9 or B-MYB depletion, E14 ES cells were transfected with shRNA against Lin9 or B-Myb or control vector (section 3.1.1) and selected with puromycin. 72 hpt cells were used for EB culture. Every day EB formation was monitored under the microscope. As shown in fig. 3.2 **B**, the ability to form and grow as EBs is strongly impaired after knock down of LIN9 or B-MYB. Control EBs exhibit a distinct outline, enlarge in size and form cavities after 4 days of culture whereas LIN9 and B-MYB depleted EBs stay small and have an irregular shape.

Thus, inhibition of the activating DREAM complex by depletion of LIN9 or B-MYB leads to a defect in correct stem cell differentiation. Whether this observation is caused by proliferation defects due to reduced G2/M gene expression or by direct deregulation of differentiation genes was topic of the following experiments.

3. Results

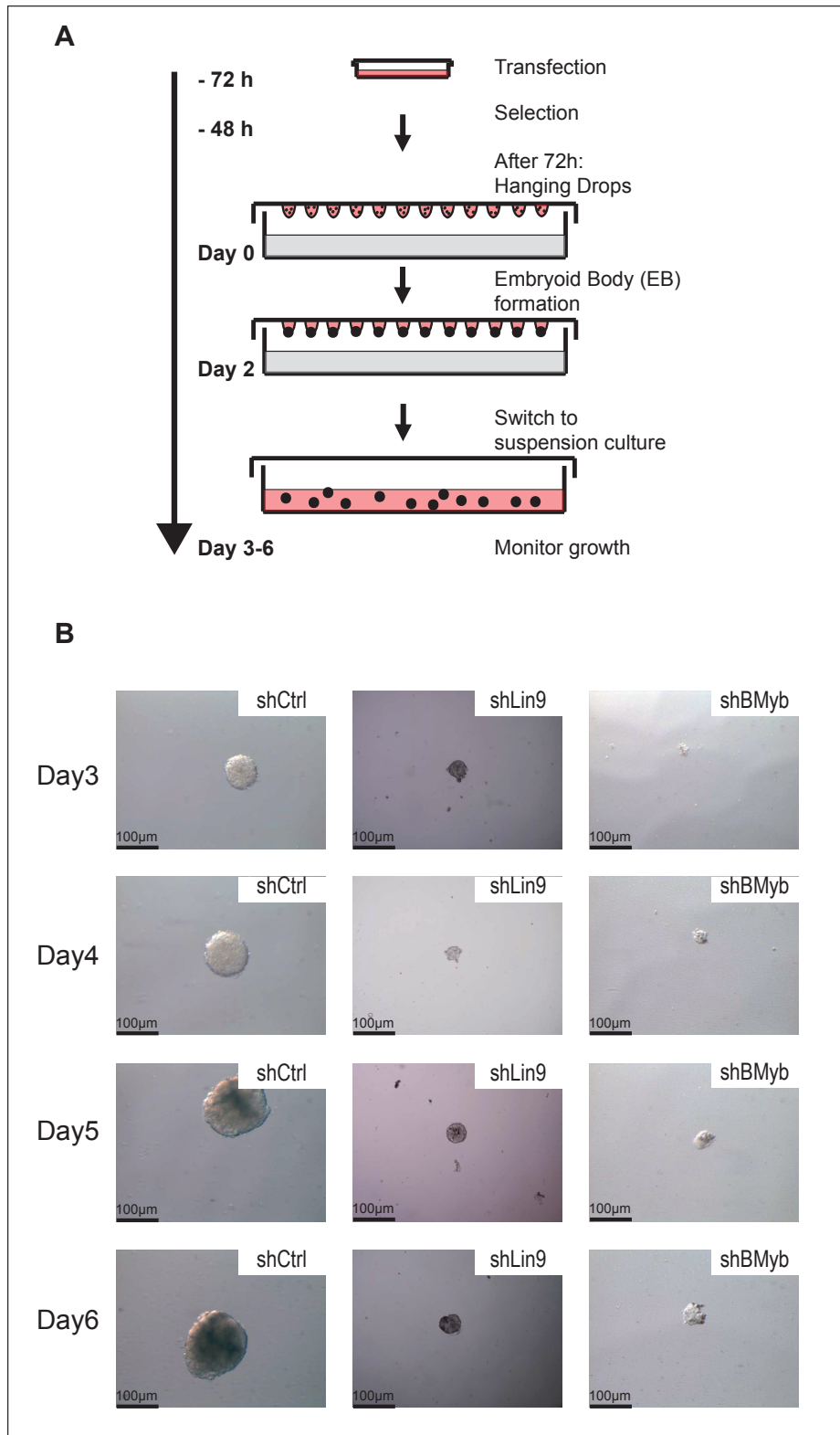


Figure 3.2.: **Embryoid body formation is heavily impaired after DREAM LIN9 or B-MYB kd** Embryoid bodies (EBs) were formed by the 'hanging drop' method after LIN9 and B-MYB depletion and their growth monitored for up to 6 days (A). EB formation is severely affected upon LIN9 or B-MYB depletion (B) compared to control.

3.1.2. Gene regulation by the DREAM complex in ES cells

Former studies about the DREAM complex were performed in somatic cells of different origin. During the cell cycle, the complex composition changes from its gene repressing state with p130 & E2F4 in G0/G1 to its activating form in S-phase when the transcription factor B-MYB gets incorporated to activate G2/M gene expression. Since ES cells have rather short gap-phases (G1, G2) and no cyclic expression of the cyclin-CDK complexes, it is possible that they exhibit a different DREAM composition. The pocket protein p130 which binds to DREAM in G0/G1 is not expressed in ES cells (LeCouter et al., 1996). This opens the possibility that the repressive DREAM complex might be absent or different in undifferentiated cells.

To address this question I performed LIN9 Co-immunoprecipitations (Co-IPs) with nuclear extracts from the mouse ES cell line E14. The IP was performed with a polyclonal antibody against the LIN9 protein. Bound proteins were detected by immunoblotting. As seen in fig. 3.3 A LIN9 binds to the other DREAM core components LIN37, LIN54 and to B-MYB which indicates the presence of the active complex. The pocket protein p130 is not expressed in mouse ES cells (see Input lane) (LeCouter et al., 1996) and p107, which is reported to associate to DREAM (Schmit et al., 2007; Pilkinton et al., 2007) shows no binding to LIN9. Thus, the known repressive DREAM complex might be absent in mouse ES cells. Binding of the other DREAM subunits LIN52 and RBAP48 could not be verified due to the lack of antibodies suitable for the use in mouse cells.

3.1.2.1. DREAM binds promoters of G2/M target genes in ES cells but not the pluripotency gene Sox2

With chromatin immunoprecipitation (ChIP) analysis the direct binding of DREAM subunits on target gene promoters can be studied.

To do so, I generated mouse ES cell lines based on HABirA ES cells (Driegen et al., 2005) which express the bacterial BirA ligase. This ligase, derived from *E.coli*, site-specifically biotinylates a lysine side chain within a 15-amino acid acceptor peptide (also known as Avi-tag) (fig. 3.4 A). Into those cells an expression vector with a double tagged LIN9 was stably inserted by transfection and neomycin selection. BirA activity leads to the generation of ES cells expressing N-terminally biotinylated and Flag-tagged LIN9 protein. This cell line was named Biotag-LIN9 (BioLIN9). In the same way a Biotag-B-MYB (BioB-MYB) cell line was established.

Immunoprecipitation with LIN9 / B-MYB -antibodies or streptavidin dynabeads and West-

3. Results

ern blot analyses proved the expression of the tagged proteins at endogenous levels (fig. 3.4 B and C). To see whether the tagged proteins get incorporated into the intact DREAM complex, an immunoprecipitation with magnetic streptavidin beads was performed with nuclear extracts of BioLIN9 ES cells. As seen in fig. 3.4 C, BioLIN9 is able to immunoprecipitate the DREAM core proteins LIN37 and LIN54 as well as the associated transcription factor B-MYB. Thus, the biotinylated proteins are incorporated into the DREAM complex and are suitable for the use in the following ChIP experiments.

With magnetic streptavidin dynabeads DNA-LIN9 complexes could be immunoprecipitated and analysed for bound gene promoters by qRT-PCR. As expected, DREAM binds the promoters of G2/M genes. Fig. 3.3 B shows the enrichment of biotinylated LIN9 on the promoters of the DREAM target genes *Aspm*, *AuroraA* (*Aurka*), *Hmnr*, and *Kif20a* but not on the pluripotency gene *Sox2*.

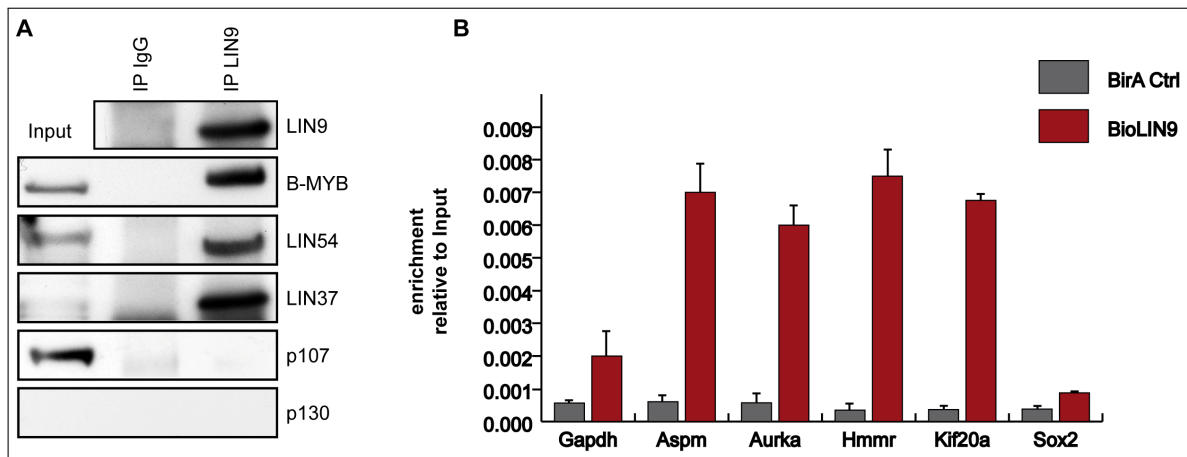


Figure 3.3.: **DREAM composition and function in ES cells**(A) LIN9 IP was performed with nuclear extracts of E14 ES cells. Immunoblotting against known DREAM subunits confirmed the existence of the DREAM complex with bound B-MYB. No p130 is expressed. (B) Promoters of known DREAM targets but the pluripotency gene *Sox2* is not bound by LIN9 in ES cells as investigated by ChIP analysis.

3. Results

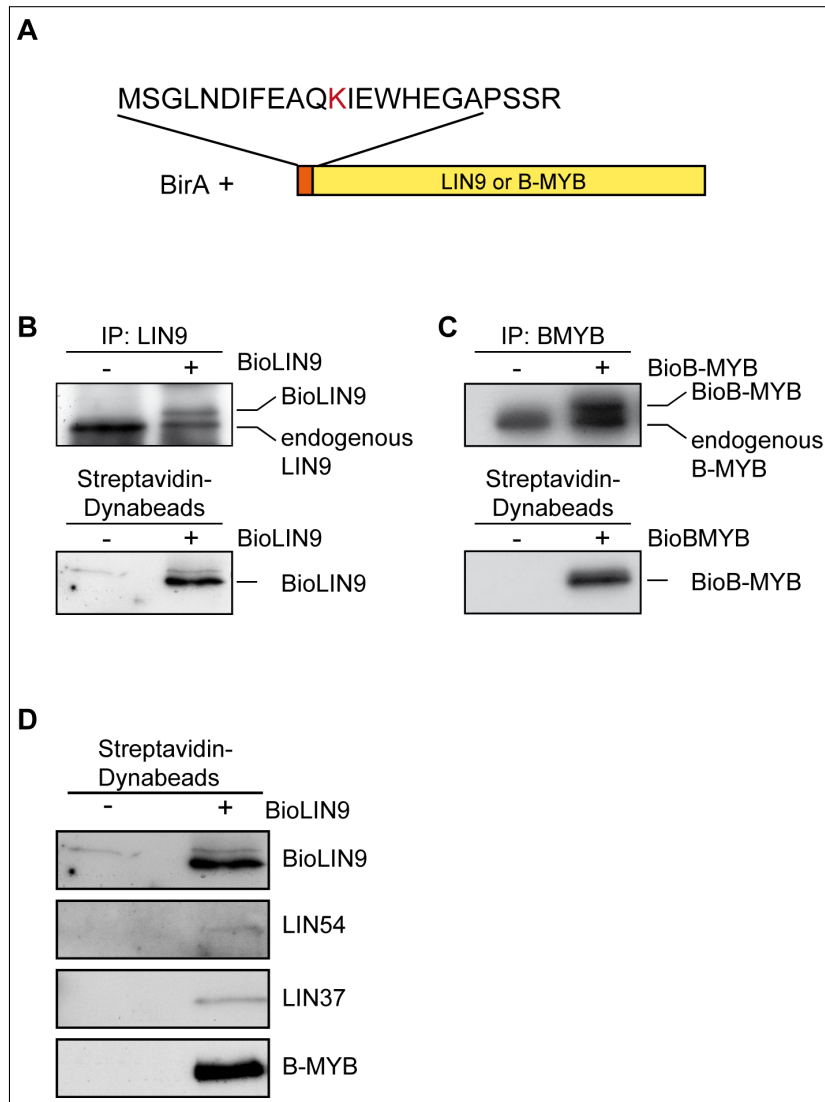


Figure 3.4.: **ES cell line expressing biotinylated proteins** (A) ES cell lines were generated that express LIN9 or B-MYB with a N-terminal Flag-tag and a biotinylation signal. Additionally, cells express the bacterial BirA ligase that attaches biotin on the lysin (K) residue in the biotinylation tag. (B) (C) ES cells express bio-tagged LIN9 or B-MYB at endogenous levels, the tagged protein can be immunoprecipitated by streptavidin dynabeads. (D) Biotin-LIN9 gets incorporated into the DREAM complex. Nuclear extracts were immunoprecipitated with magnetic streptavidin dynabeads and immunoblotted with antibodies against DREAM subunits.

3.1.2.2. LIN9 depletion causes downregulation of DREAM target genes

To test whether the expression of known DREAM target genes, many of them necessary for entry into proper mitosis, are affected in ES cells, cells were treated with shRNA against

3. Results

Lin9. 72 hpt cells were harvested for mRNA gene expression and Western blot analysis to analyse protein levels. As depicted in fig. 3.5 **A**, mRNA level of AuroraA (Aurka), a kinase that plays a critical role in various events during mitosis and which expression peaks during G2/M transition, is reduced by 54 % upon LIN9 depletion. Further DREAM target genes are also downregulated to 61 % (Aspm), 40 % (Ccnb1) and 23 % (Nusap). This negative regulation is not just seen on mRNA expression level but also on protein level as displayed for cyclinB (fig. 3.5 **B**). CyclinB expression peaks during G2/M phase and associates with the cyclin-dependent kinase1 (CDK1) necessary for the progression of cells into and out of M phase.

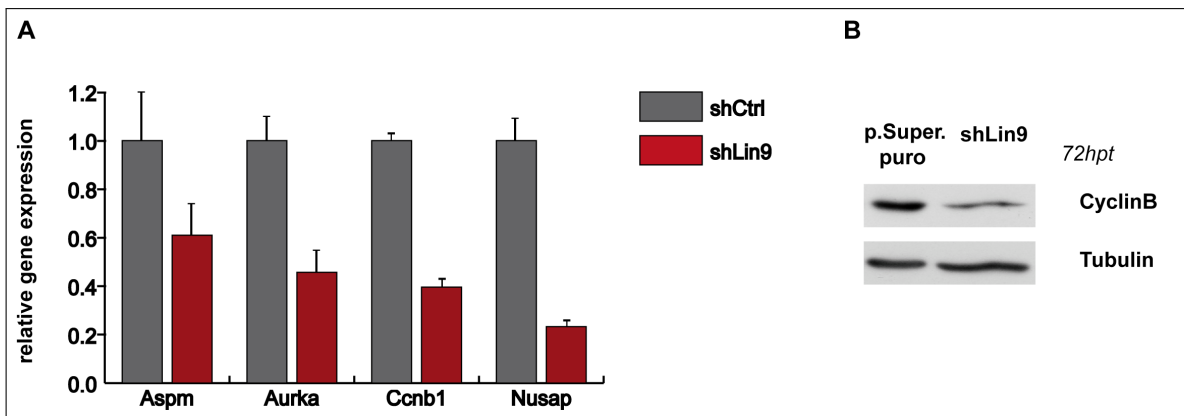


Figure 3.5.: **LIN9 depletion leads to reduced expression of DREAM target genes**
Expression analysis by qRT-PCR demonstrates reduced G2/M gene expression after LIN9 kd (**A**). Reduced mRNA levels also lead to lower protein levels as displayed for the DREAM target cyclinB (**B**).

3.1.2.3. Depletion of LIN9 in ES cells does not affect expression of pluripotency genes or pluripotency of ES cells

Reichert et al. (Reichert et al., 2010) reported that in embryos of Lin9 knock out mice the inner cell mass is not able to proliferate. Whether LIN9 has a direct influence on stem cell identity and pluripotency has not been studied. To address this question, ES cells were transfected with shRNA against Lin9 for 72 hours and the expression of the stem cell markers Oct4 and Sox2 was tested. Together with Nanog those three genes are core regulators of ES pluripotency (Pesce and Schöeler, 2001; Chambers et al., 2003; Mitsui et al., 2003; Avilion et al., 2003). During differentiation, expression of those markers is downregulated. As seen in fig. 3.6 **A**, after reducing Lin9 mRNA levels by 78 % there is no decrease in Oct4 or Sox2 expression levels.

3. Results

Another way to analyse whether LIN9 or B-MYB depletion affects the pluripotency potential of ES cells is the staining for alkaline phosphatase (AP) activity. Characteristic for undifferentiated cells is the high expression and activity of AP. AP positive cells exhibit a violet staining. After depletion of the DREAM members LIN9 or B-MYB AP expression was maintained when compared to control ES cells (fig. 3.6 B).

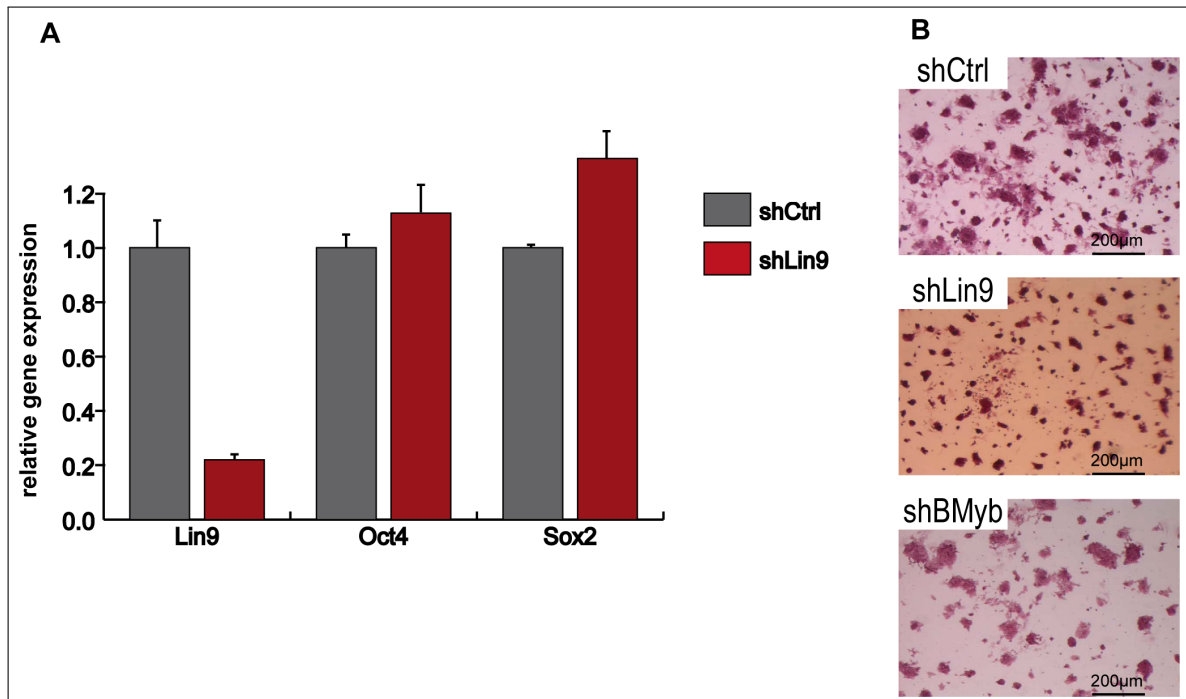


Figure 3.6.: **Pluripotency is not affected by short term depletion of LIN9 or B-MYB (A)** 72 h of LIN9 kd in ES cells does not reduce the expression of the pluripotency genes Oct4 or Sox2 as determined by qRT-PCR. **(B)** Alkaline phosphatase (AP) activity is a marker of pluripotent cells. AP staining is not altered upon LIN9 or B-MYB reduction compared to control cells.

3.1.3. Genome wide RNA expression analysis after LIN9 depletion to identify LIN9 regulated genes in ES cells

To identify changes in gene expression that could be responsible for altered cell cycle progression after depletion of LIN9 in ES cells, expression profiling using microarray analysis was performed. To do so, mouse ES cells (D3) were transfected with control plasmid or with the LIN9 specific shRNA plasmid. After 72 h, RNA was isolated and subjected to Agilent DNA microarrays monitoring more than 39,000 transcripts.

3. Results

581 genes were found with an at least 1.5 fold changed expression. Thereof 233 genes (19 genes > 2fold) were down- and 348 (55 > 2fold) were upregulated (fig. 3.7 A, supplementary S1).

3.1.3.1. Downregulated genes are involved in mitosis and cell cycle processes

The gene expression array after LIN9 depletion produced 233 genes which were downregulated at least 1.5 fold. With Gene Ontology (GO) analysis genes were annotated and functionally clustered. GO-term analysis produced that most downregulated genes, according to fold-change, are involved in cell cycle processes especially in M phase (fig. 3.7 B). Many regulated genes are needed for proper cell cycle progression like Aurora A (Aurka), cyclinB (Ccnb1), Cyclin dependent kinase 1 (Cdk1) or Polo-like kinase 1 (Plk1). 21.5 % of downregulated genes have functions in M phase like Aurora B (Aurkb) and Incenp - both components of the chromosomal passenger complex (CPC)-, Bub3 or Cenpf. Other functional clusters include genes for chromatin assembly (3.9 %) and DNA packaging (5.1 %) like topoisomerase (DNA) II alpha (Top2A), as well as different histone cluster and histone family proteins.

3.1.3.2. Early differentiation genes are amongst upregulated genes

With the array 348 genes >1.5 fold up-regulated were identified. Clustering by GO-term analysis showed that many upregulated genes were overrepresented in different developmental processes (fig. 3.7 C). Such are the clusters 'lung development' (2.6 %) with genes like Platelet-derived-growth factor receptor A (Pdgfra), HOP homeobox (Hopx), Epas1, Kdr (also known as Flk1), Gata6, Tbox4 or 'neuron differentiation' (4.6 %), represented for example by stathmin-like 3 (Stmn3) or neuronal differentiation 1 (NeuroD1). Furthermore, genes involved in 'angiogenesis' (2.6%) or 'cellular component morphogenesis' are overrepresented.

To validate the upregulation, mRNA levels of several genes were analysed in LIN9 depleted ES cells by qRT-PCR. Genes investigated include early differentiation markers for mesodermal- (alpha feto protein (Afp)) and exodermal development (Flk1 and NeuroD1) and the most upregulated gene Gm11487 with a so far unknown function. As depicted in fig. 3.8 A, all of the tested genes were upregulated after LIN9 depletion (78 % Lin9 kd). As in the array, Gm11487 showed the strongest effect with an > 8-fold expression. Pcdh8 (6.7-fold), Pdgfra (4-fold) and NeuroD1 (3.7-fold) also had an increased mRNA expression level. To investigate whether this is a direct effect of DREAM, the enrichment of LIN9 on

3. Results

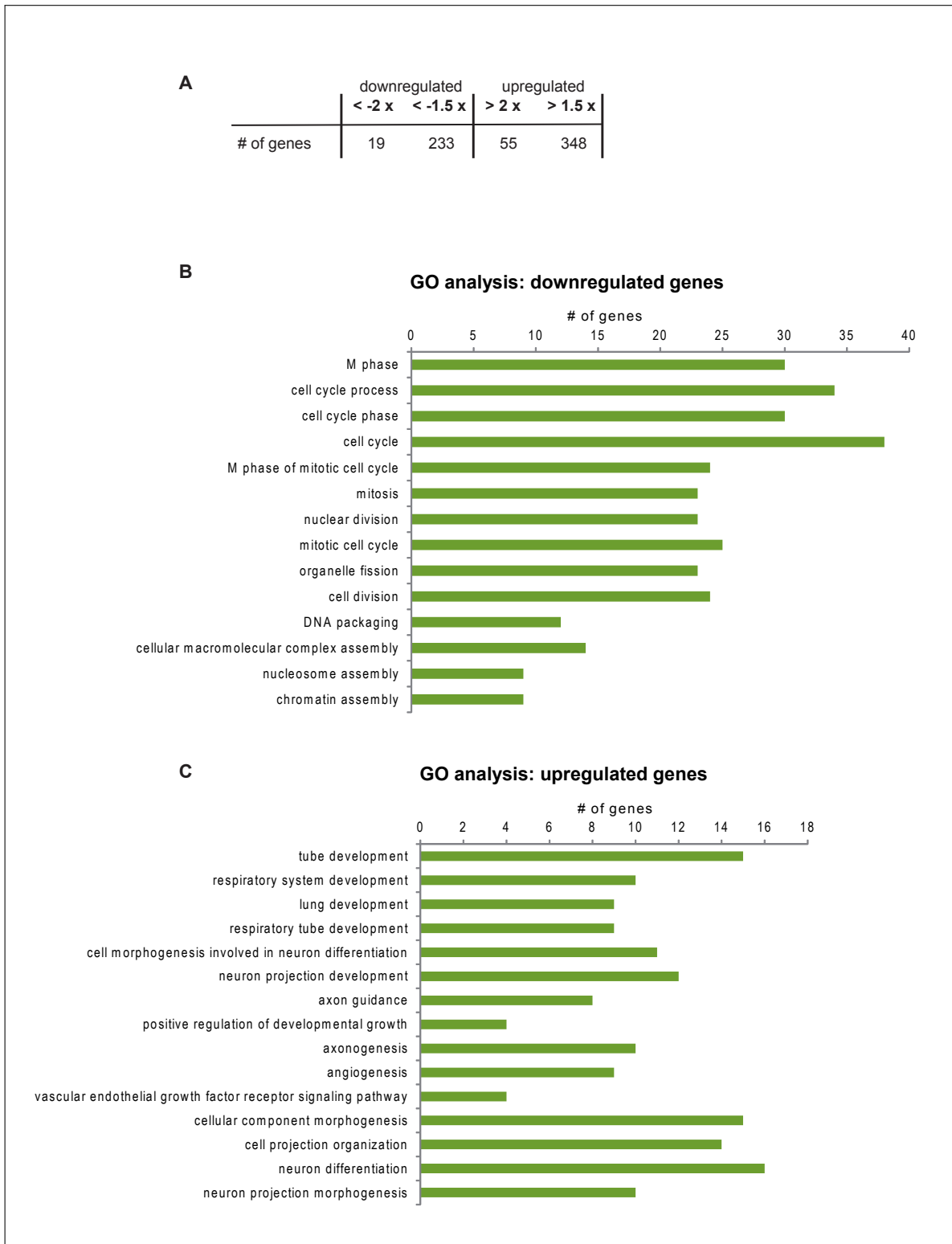


Figure 3.7.: **Genome-wide expression analysis of genes regulated upon LIN9 depletion in ES cells.** (A) 581 genes showed an expression regulation of at least 1.5-fold after LIN9 depletion. (B) GO analysis of up- and downregulated genes. Shown are the top fifteen overrepresented GO terms according to the p-value.

3. Results

the promoters of the Gm11487, NeuroD1 and Vax2 was tested with ChIP analysis. As no binding of LIN9 to the promoters of those genes could be detected (fig. 3.8 B), it seems that DREAM is not actively repressing those differentiation genes and that their enhanced expression is an indirect effect.

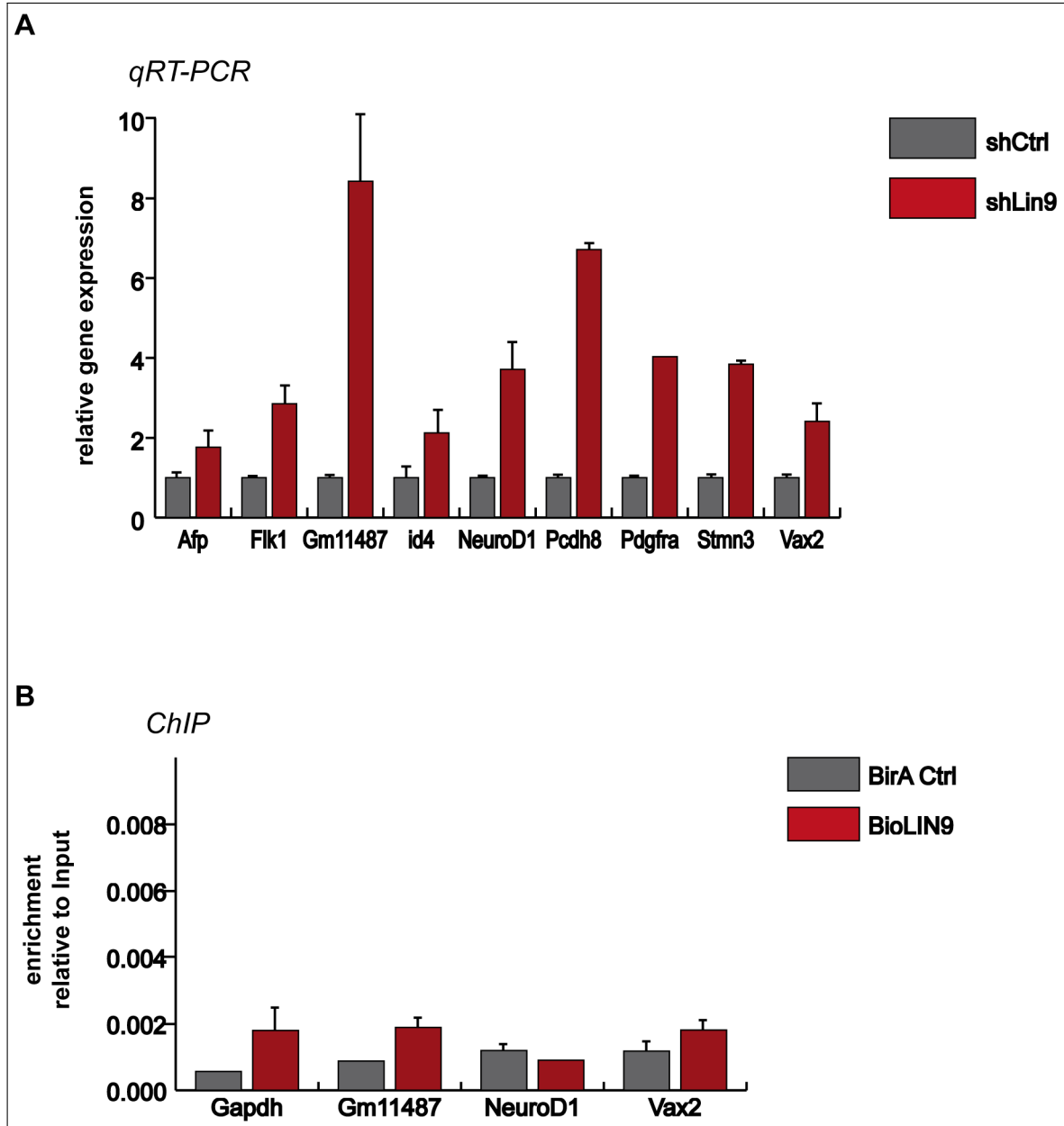


Figure 3.8.: Validation of upregulated genes after LIN9 depletion (A) Genes with high upregulation in the microarray were chosen for validation by qRT-PCR in ES cells after LIN9 depletion. (B) By ChIP analysis no enrichment of LIN9 on the upregulated genes Gm11487, NeuroD1 or Vax2 could be detected.

3. Results

3.1.3.3. Synchronisation of mouse ES cells leads to enhanced expression of differentiation genes

As shown in section 3.1.1.1, depletion of LIN9 or B-MYB leads to an increase of cells in G2/M phase which hints to an arrest in the cell cycle. This means that the transit time into mitosis is prolonged compared to control cells. It is possible that this cell cycle elongation leads to the observed upregulation of differentiation genes. To address this possibility, ES cells were synchronised either with hydroxyurea (HU) in G1-phase or trapped in mitosis with nocodazole (fig. 3.9 **A**). Then mRNA expression of some genes that were found upregulated after LIN9 depletion was analysed and compared with asynchronous growing cells. Both synchronisations led to a high upregulation of mRNA levels of the neuronal differentiation genes *Flk1*, *Pcdh8*, *Pdgfra* and *NeuroD1* as depicted in fig. 3.9 **B** and **C**.

This upregulation of differentiation genes upon cell cycle delay declines with time after release from cell cycle block. As displayed in fig. 3.9 **D** for HU synchronisation, mRNA expression levels decreased to normal levels 12 hours after drug removal, indicating that the upregulation is a transient result of the cell cycle block.

3. Results

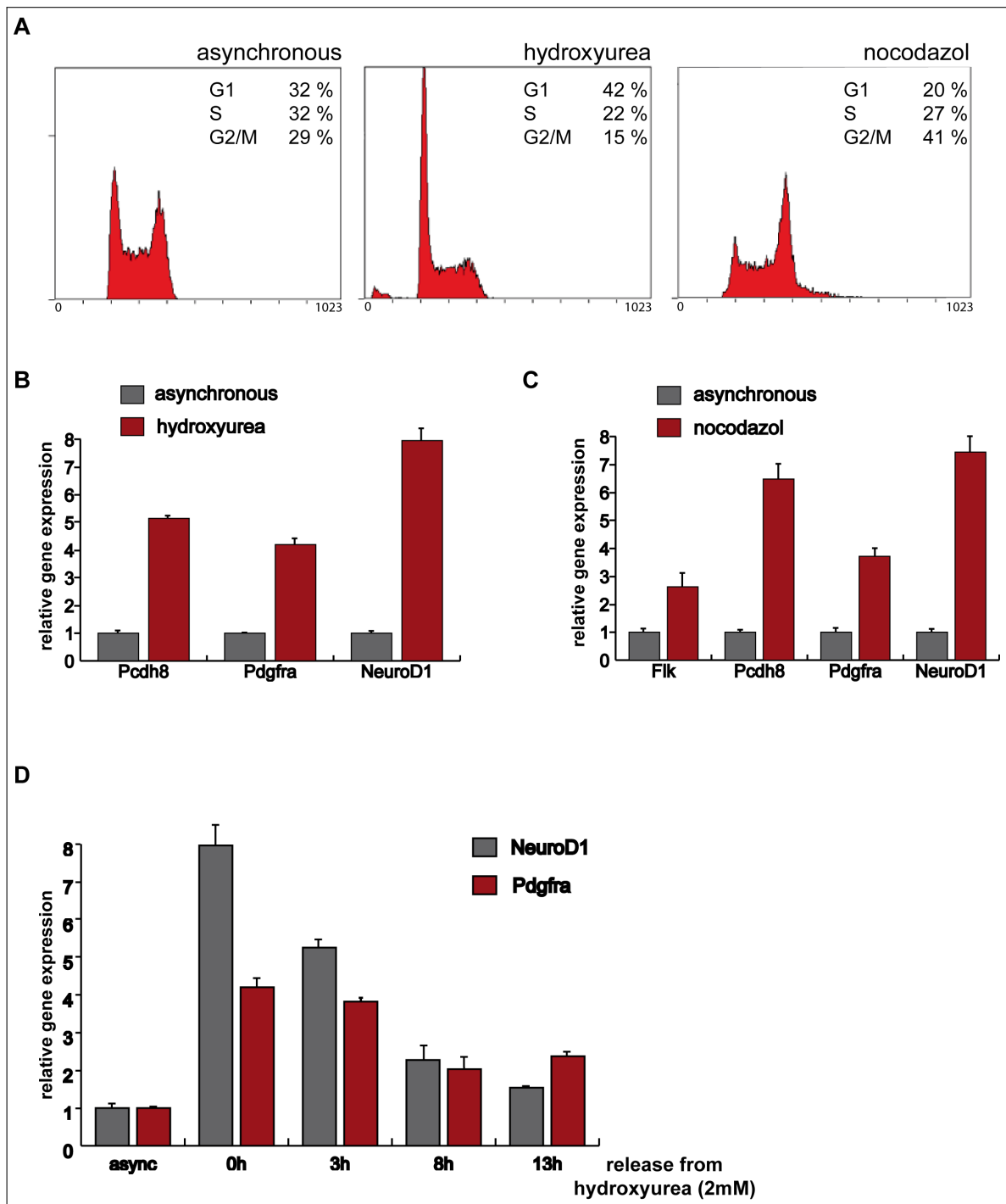


Figure 3.9.: **Synchronisation of ES cells leads to upregulation of differentiation genes** (A) ES cells were synchronised in G1 (hydroxyurea) or mitosis (nocodazole) and analysed by PI-FACS. (B) (C) Cells were treated as in (A) and gene expression was analysed by qRT-PCR. In both cases cell cycle arrest leads to an increase of mRNA levels of early differentiation genes that were also found deregulated after LIN9 depletion (fig. 3.8 A). (D) Cells were synchronised with HU in G1 and re-released into the cell cycle. qRT-PCR of Pdgfra and NeuroD1 at different time points shows that with further progression from the hydroxyurea - induced cell cycle block mRNA levels drop to normal levels.

3.1.4. Genome wide ChIP approach to identify DREAM binding sites in ES cells

The genome-wide expression study after LIN9 knock down revealed a long list of genes which were up- and downregulated (see supplementary S1). This could be the result of a direct binding of DREAM to the promoters of these genes or an indirect effect e.g. due to the disturbance of proliferation and cell cycle progression. To determine which promoters are directly bound by the DREAM complex a ChIP-on-chip (ChIPchip) technique was used which combines chromatin immunoprecipitation ('ChIP') with microarray technology ('chip').

For this approach, the ES cell line expressing biotinylated LIN9 (BioLIN9) was used. Chromatin from cells expressing biotin-tagged LIN9 was precipitated with streptavidin coupled magnetic beads, amplified, labeled and hybridised to a microarray that contains oligonucleotide probes covering the region -2 to +0.5 kb relative to the transcriptional start sites of 19,489 annotated mouse genes.

3.1.4.1. ChIPchip analysis reveals that mainly G2/M genes are regulated

ChIPchip analysis was performed by NimbleGen. The received data was filtered by Enrichment peaks >1 and FDR value <0.1 . Overall, LIN9 bound to 1605 (8.1%) of the promoter regions analysed.

Functional annotation analysis based on GO terms revealed a significant enrichment on promoters of genes that are involved in regulation of mitosis, cell cycle processes, transcription, translation and mRNA processing (fig. 3.10 **A**, supplementary S5).

3.1.4.2. Overlay of ChIPchip analysis and LIN9 kd RNA microarray

To see whether DREAM/LIN9 not only binds to promoter regions of those genes but also actively regulates their expression, an overlay of ChIPchip data with the LIN9 KD array was done. As listed in tab. 3.1, 25 of the up- and 32 of the downregulated genes were found by ChIPchip which is an indicator of direct regulation of expression by DREAM.

GO-term analysis showed that downregulated genes found both in KD array and ChIPchip function in cell cycle process and mitosis like *Aspm*, *Bub3*, *Plk1*, *CenpE* or *Gas2l3* which are also known DREAM target genes in differentiated mouse and human cells (fig. 3.10 **B**).

Genes that are upregulated in the LIN9 array and that are present in ChIPchip could not be clustered by Gene ontology.

3. Results

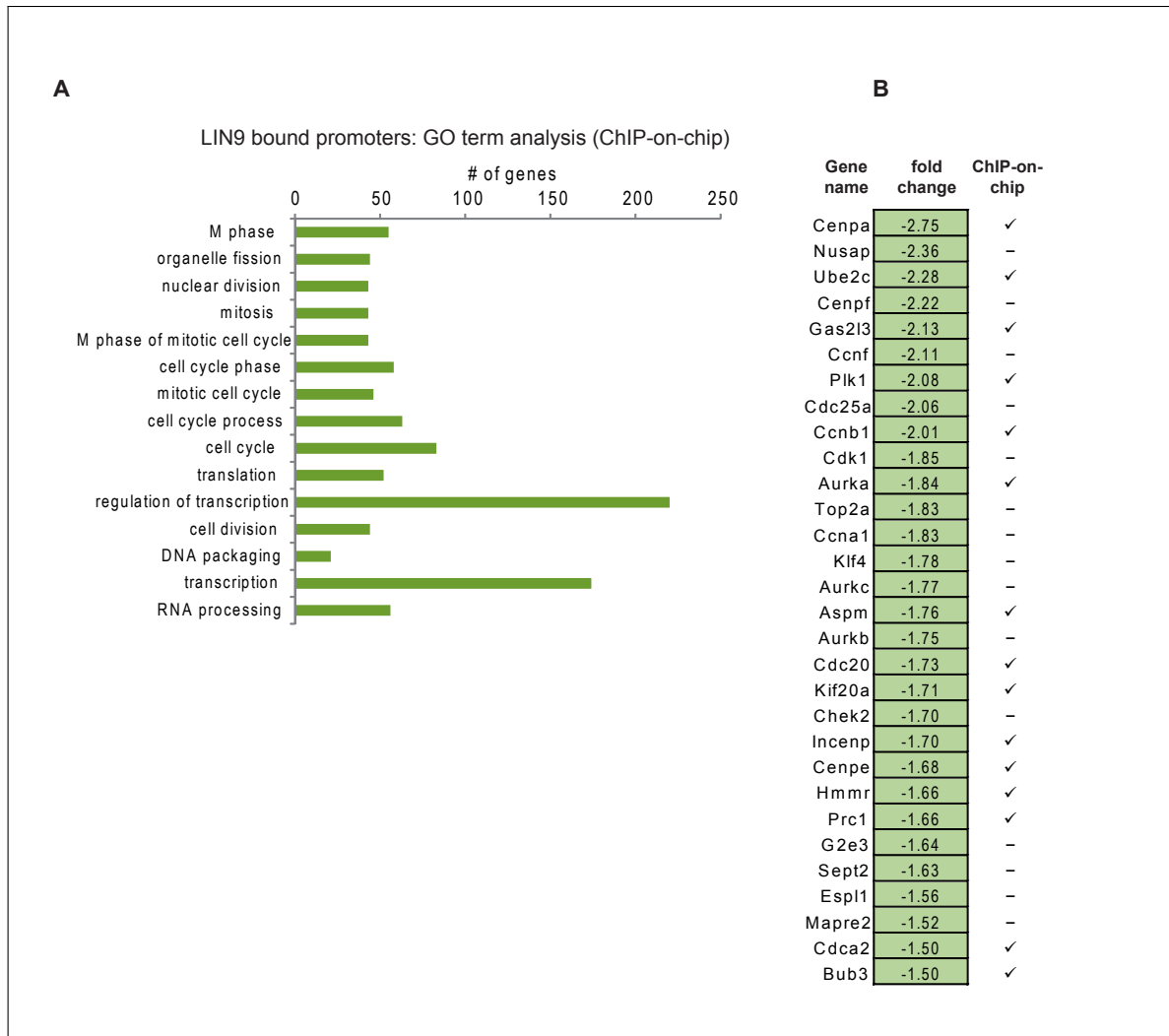


Figure 3.10.: **GO term analysis of BioLIN9 ChIPchip.** (A) Functional annotation of the ChIPchip data based on GO terms revealed that foremost promoters of genes involved in mitosis or transcription are bound by LIN9. Displayed are the top fifteen overrepresented GO terms according to the p-value. (B) Comparison of gene expression data and ChIPchip data confirmed that mitotic genes are direct targets of LIN9 in ES cells. Genes with a known function in mitosis and downregulated after depletion of LIN9 are shown. "✓" indicates that binding of LIN9 to the promoter was detected by ChIPchip. "-" indicates that no binding was detected.

3. Results

Table 3.1.: Direct target genes of LIN9 in ES cells as determined by microarray and ChIPchip

Gene name	Direction	Gene description
2900011O08Rik	down	RIKEN cDNA 2900011O08 gene
3300002I08Rik	up	RIKEN cDNA 3300002I08 gene
4930547N16Rik	down	RIKEN cDNA 4930547N16 gene
A430089I19Rik	up	RIKEN cDNA A430089I19 gene
Acpp	up	Acid phosphatase, prostate
Aspm	down	Asp (abnormal spindle)-like, microcephaly associated (Drosophila)
Aurka	down	Aurora kinase A
BC028528	up	CDNA sequence BC028528
Bub3	down	Budding uninhibited by benzimidazoles 3 homolog (S. cerevisiae)
Ccnb1	down	Cyclin B1
Cdc20	down	Cell division cycle 20 homolog (S. cerevisiae)
Cdca2	down	Cell division cycle associated 2
Cenpa	down	Centromere protein A
Cenpe	down	Centromere protein E
Cpne8	up	Copine VIII
Ctss	up	Cathepsin S
Cyp2d26	down	Cytochrome P450, family 2, subfamily d, polypeptide 26
D17H6S56E-5	down	DNA segment, Chr 17, human D6S56E 5
Depdc1b	down	DEP domain containing 1B
Dst	up	Dystonin
Fbp2	up	Fructose bisphosphatase 2
Gas2l3	down	Growth arrest-specific 2 like 3
Gm9	down	Gene model 9, (NCBI)
Grn	down	Granulin
H1f0	down	H1 histone family, member 0
Hist1h2bc	down	Histone cluster 1, H2bc
Hmga2	up	High mobility group AT-hook 2
Hmmr	down	Hyaluronan mediated motility receptor (RHAMM)

3. Results

Table 3.1.: Direct target genes of LIN9 (ChIPchip): continuation

Gene name	Direction	Gene description
Igfbp7	up	Insulin-like growth factor binding protein 7
Incenp	down	Inner centromere protein
Inhbc	up	Inhibin beta-C
Lmnb1	down	Lamin B1
Lrp4	up	Low density lipoprotein receptor-related protein 4
Ly6a	down	Lymphocyte antigen 6 complex, locus A
Matn3	up	Matrilin 3
Msc	down	Musculin
Oasl1	up	2'-5' oligoadenylate synthetase-like 1
Pipox	up	Pipecolic acid oxidase
Plk1	down	Polo-like kinase 1 (Drosophila)
Pnrc2	down	Proline-rich nuclear receptor coactivator 2
Polr3gl	up	Polymerase (RNA) III (DNA directed) polypeptide G like
Prc1	down	Protein regulator of cytokinesis 1
Prom1	up	Prominin 1
Prr11	down	Proline rich 11
Psat1	down	Phosphoserine aminotransferase 1
Rlbp1	down	Retinaldehyde binding protein 1
Slc30a9	up	Solute carrier family 30 (zinc transporter), member 9
Snap91	up	Synaptosomal-associated protein 91
Socs2	up	Suppressor of cytokine signaling 2
Speer4d	up	Spermatogenesis associated glutamate (E)-rich protein 4d
Spnb1	up	Spectrin beta 1
Syt10	down	Synaptotagmin X
Tax1bp1	up	Tax1 (human T-cell leukemia virus type I) binding protein 1
Tpm1	up	Tropomyosin 1, alpha
Ube2c	down	Ubiquitin-conjugating enzyme E2C
Zfp28	down	Zinc finger protein 28
Zfp521	up	Zinc finger protein 521

3.2. Identification and characterisation of new DREAM binding partners

3.2.1. Affinity purification reveals possible novel interaction partners of DREAM

The DREAM complex is highly conserved among species. It was first found in *Drosophila* (Korenjak et al., 2004; Lewis et al., 2004) and named dREAM (*Drosophila* RBF, dE2F2 and dMyb-interacting proteins). Later, ortholog complexes were found in *C.elegans* (Harrison et al., 2006) as well as in human and mouse (Litovchick et al., 2007; Schmit et al., 2007; Pilkinton et al., 2007; Knight and Watson, 2009). Thereby, the core subunits LIN9, LIN37, LIN52, LIN54, RBBP4 as well as the associating proteins p130, E2F4 and B-MYB were found in the mammalian complexes. Schmit *et al.* (Schmit et al., 2007) performed affinity purification followed by mass spectrometry analysis which led to the discovery of the different DREAM subunits. Because not all protein bands of the analysed silver gel could be identified, it is likely that additional subunits exist. As shown in section 3.1.2 the DREAM complex exists in its activating conformation (DREAM-B-MYB) with bound B-MYB in mouse ES cells. The repressing DREAM complex could not be detected. So it might be, that other proteins are incorporated in order to repress gene expression. Also it is still unclear how the DREAM complex can perform its gene activating function as none of the members bear a catalytic domain. It is likely that there are more proteins or co-factors that bind to DREAM, maybe in a cell cycle dependent manner. In this work 'stable isotope labeling in cell culture' (SILAC) of mouse ES cells was combined with affinity purification and followed by mass spectrometry to identify proteins which might interact with DREAM. The high sensitivity of this method also allows the detection of just weak protein-protein bindings.

For the conducting of those experiments, the BioLIN9 and BioB-MYB ES cell lines (3.1.2.1) were used that express biotinylated LIN9 or B-MYB. By the use of those cells, the DREAM complex can be immunoprecipitated with streptavidin dynabeads from nuclear extracts and further analysed by mass spectrometry.

3.2.2. SILAC and MassSpec analysis reveals several potential binding partners

To increase the sensitivity of the identification of DREAM bound proteins by affinity purification and mass spectrometry, mass spectrometry (MS)-based quantitative proteomics (MassSpec) was coupled with the SILAC approach. SILAC relies on metabolic incorporation of a given 'light' or 'heavy' form of the amino acid into the proteins. To do so, the Biotag cell lines (either LIN9- or B-MYB-tagged) were cultured in 'heavy' medium containing ^{13}C -labeled L-Lysine and $^{13}\text{C}^{15}\text{N}$ -labeled L-Arginine whereas control cells were grown in unlabeled 'light' medium. To achieve complete incorporation of the isotope labeled amino acid cells underwent 4 passages before they were propagated to a scale needed for the experiment. After preclearing and streptavidin-IP of equal amounts of nuclear extracts, protein eluates from the beads were mixed and sent for mass spectrometry analysis in collaboration with Prof. Henning Urlaub from the Max Planck Institute for Biophysical Chemistry in Goettingen. As shown in fig. 3.11 **A**, the DREAM core complex members RBAP48, LIN54, LIN37 and also B-MYB could be detected in both the LIN9 and the B-MYB MassSpec samples. Furthermore, a long list of proteins could be identified which were enriched in the Biotag-LIN9 and -B-MYB sample compared to control (see supplementary S8). Proteins with function in transcription or RNA processing are listed in fig. 3.11 **B**. In this work I focused on the zona occludens protein 2 (ZO-2) also known as tight junction protein 2 (TJP2). This protein is mostly found at the tight junctions of cells. It belongs to a family of membrane-associated *guanylate kinases* (MAGUK) homologs. ZO proteins, consisting of the family members ZO-1-3, play an important role in the assembly of tight junctions and cell polarity. Tight junction proteins not only execute functions related to their barrier role at the plasma membrane but also are involved in signal transduction to modulate cell proliferation and differentiation (Balda and Anderson, 1993; Sourisseau et al., 2006). ZO-1 and ZO-2 also shuttle to the nucleus and are reported to associate with proteins involved in the regulation of cell proliferation such as the transcription factors Jun, Fos, C/EBP (Betanzos et al., 2004). AP-1 regulated gene transcription can also be modulated by ZO-2 (Betanzos et al., 2004). Because of the reported functions of ZO-2 in gene transcription and cell proliferation it was analysed whether ZO-2 associates with the DREAM complex. RNA interference (RNAi) experiments were used to investigate the effects of ZO-2 depletion onto cell proliferation, cell cycle and gene expression.

3. Results

A

known interacting proteins

protein name	fold enrichment	
	B-MYB	LIN9
RBAP48	12.4	2
LIN54	10.2	1.2
B-MYB	4.5	4.3
LIN37	2.4	-

B

candidate interacting proteins

protein name	fold enrichment		process
	B-MYB	LIN9	
TOP2A	6.7	-	DDR, transcription
TOP1	3.2	-	DDR, transcription
NAT10	3	-	transcription/ chromatin structure
RFP (TRIM27)	4	2	DNA binding/ transcription
LZTS2	5.1	2.2	microtubule stability/ wnt-signalling
TRAF4	3.6	2.7	signal transduction
ZO-1	3	1.4	tight junction/ transcription
ZO-2	4.7	3.2	tight junction/ transcription
Cingulin	2.5	1.9	tight junction/ transcription
PES1	4.5	1.3	ribosome RNA biogenesis/ PeBoW complex
BOP1	3.4	1.2	ribosome RNA biogenesis/ PeBoW complex
WDR12	3.2	-	ribosome RNA biogenesis/ PeBoW complex
DDX27	4.3	1.4	RNA helicase/ mRNA processing
DDX49	4	-	RNA helicase/ mRNA processing
Nop10	4.2	2.5	ribosome biogenesis
Nucleolin	3	-	ribosome biogenesis
MYBBP1A	2.8	-	RNA processing/ transcription
NPM1	2.8	-	ribosome biogenesis/ regulation of p53/ARF

Figure 3.11.: **List of proteins found in MassSpec analysis (A)** With MassSpec analyses of immunoprecipitated DREAM-complexes from BioB-MYB and BioLIN9 ES cells known DREAM subunits were found. **(B)** Part of the list of identified proteins found with MassSpec analysis. Proteins are listed which were enriched >2fold compared to control cells and are involved in transcriptional pathways.

3. Results

3.2.3. ZO-2 also binds to DREAM in differentiated cells

After choosing ZO-2 as candidate protein the results of the MassSpec analysis had to be validated to see whether the binding is true. To test ZO-2 binding in differentiated cells, HEK293T cells, a human embryonal kidney cell line, were transfected with an expression plasmid encoding Flag-tag alone or Flag-tagged LIN9. After immunoprecipitation with anti-flag antibodies, the binding of endogenous ZO-2 was detected by immunoblotting (fig. 3.12). Thus, the binding of ZO-2 to the LIN9 could be verified.

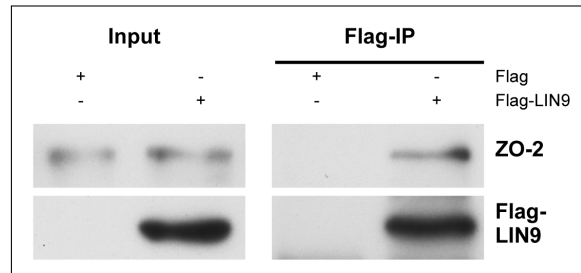


Figure 3.12.: **ZO-2 binding to DREAM in human HEK293T cells** Cells were transfected with vectors expressing either Flag-tag alone or Flag-tagged LIN9. Flag-IP and immunoblotting against ZO-2 confirms the binding of endogenous ZO-2 to Flag-tagged LIN9.

3.2.4. Binding of ZO-2 to DREAM is cell cycle dependent

The DREAM complex is an important regulator of cell proliferation as the DREAM-B-MYB complex activates the expression of genes required for entry into and through mitosis. To investigate whether ZO-2 associates during S-phase to DREAM when the DREAM-B-MYB complex is active, binding assays with synchronised cells were performed. The human glioblastoma cell line T98G was used and cells synchronised in G0/G1 by serum starvation for 72 hours. Cells re-entered the cell cycle after addition of 20% serum. To monitor progression of cells through cell cycle PI-FACS was performed for each time point (fig. 3.13 A). After 18 h cells enter S-phase and reach G2/M phase at about 24 h. Progression through mitosis is completed 32 h after releasing. With cell lysates of each time point Co-immunoprecipitations were performed with antibodies directed against LIN9 or B-MYB. IPs were immunoblotted with antibodies specific for ZO-2. As displayed in fig. 3.13 B ZO-2 binding to LIN9 is not detectable in G0/G1 phase when ZO-2 protein levels are low. DREAM-ZO-2 binding enhances and is strongest after cells enter S-phase. The conclusion that ZO-2 binding to DREAM is strongest in S-phase is confirmed by Co-

3. Results

IPs with B-MYB antibody. Here ZO-2 shows also the most clear binding during S-phase

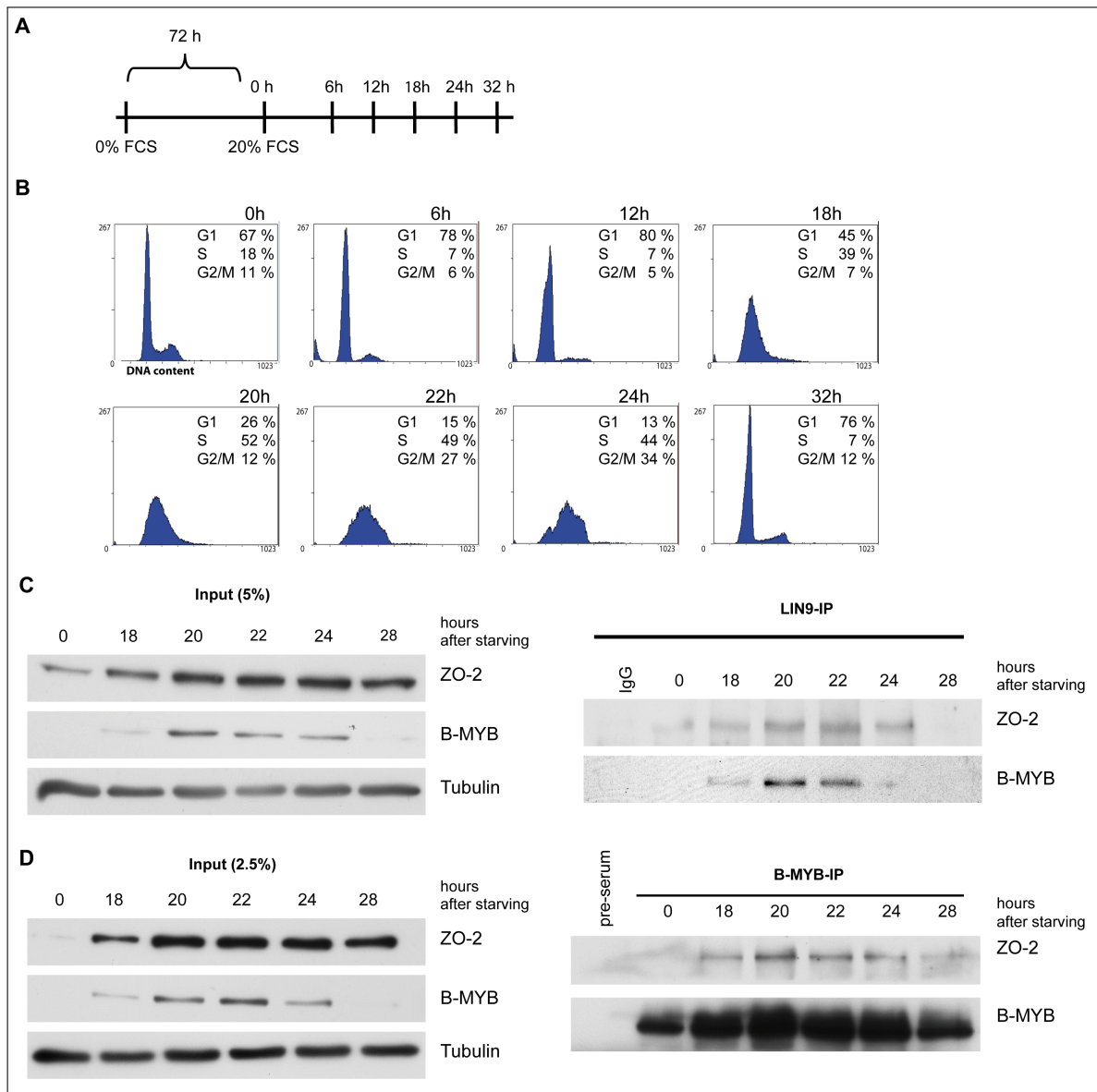


Figure 3.13.: **DREAM-ZO-2 binding in synchronised T98G cells** (A) Scheme of synchronisation experiments in T98G cells. (B) PI-FACS profiles of serum starved T98G cells. 0 h marks the time point when cells re-enter the cell cycle. Cells enter S-phase at 18 h, progress into G2/M at about 24 h. 32 h after release cells reach G1 again. Co-IPs were done with LIN9- (C) or B-MYB-antibody (D) and binding of ZO-2 confirmed by immunoblotting. ZO-2 binding is strongest after 20 h when cells are progressing through S-phase. Inputs on the left show that ZO-2 protein levels are low when cells are in G0/G1 phase.

(fig. 3.13 C) when the DREAM-B-MYB complex is formed and active.

3.2.5. Effects of ZO-2 depletion

3.2.5.1. ZO-2 depletion leads to proliferation defects

As shown in 3.1.1, depletion of LIN9 leads to proliferation defects, G2/M cell cycle arrest and downregulation of G2/M genes. To investigate whether knock down of ZO-2 results in similar phenotypes, RNAi experiments with sequences against ZO-2 RNA were performed. T98G cells were treated with siRNA against ZO-2 and cell proliferation was monitored by generating a growth curve. Compared to control transfected cells, ZO-2 reduction by 50% led to a significant reduction of cell growth (fig. 3.14 A). This effect is not cell type specific as a reduced proliferation was also observed in the human osteosarcoma cell line U2OS after ZO-2 depletion by 75%. However, despite the greater knock down the effect on proliferation was weaker in U2OS cells (fig. 3.14 B).

3.2.5.2. G1 but not G2/M gene expression is affected by ZO-2 depletion

As described in 3.2.5.1, depletion of ZO-2 led to slower proliferation. To examine whether this might be the result of a diminished G2/M gene expression, mRNA levels of several DREAM target genes were determined after ZO-2 depletion. T98G cells were serum starved in G0/G1 for 72 h followed by siRNA transfection. After 48 h cells were allowed to re-enter the cell cycle by adding 20% FCS and were collected for mRNA expression analysis after different time points (fig. 3.15). Passage through the cell cycle was monitored by PI-FACS analysis. To compare gene expression in cells treated with siZO-2 with cells having a non functional DREAM complex, cells were transfected with siRNA against B-Myb.

Reduction of B-MYB resulted in reduced expression of the G2/M genes Birc5 and (to a lesser extent) cyclinB1 (Ccnb1) that are all direct target genes of the DREAM complex. Knock down of ZO-2 expression did not lead to a significant decrease in Birc5 gene expression and an effect similar to B-MYB reduction on cyclinB. As seen in fig. 3.15 A, ZO-2 depletion resulted in a significant decrease of B-Myb mRNA levels. Since B-MYB is expressed in G1 phase, the expression of other G1 genes was determined. Therefore cells were starved and transfected as described but only mRNA levels of two time points (15 h and 24 h after release into cell cycle) were examined. As depicted in fig 3.15 B, expression of the G1 genes Cdc6, CycA, RR1 and B-MYB (Mybl2) were reduced especially at the 24h time point.

3. Results

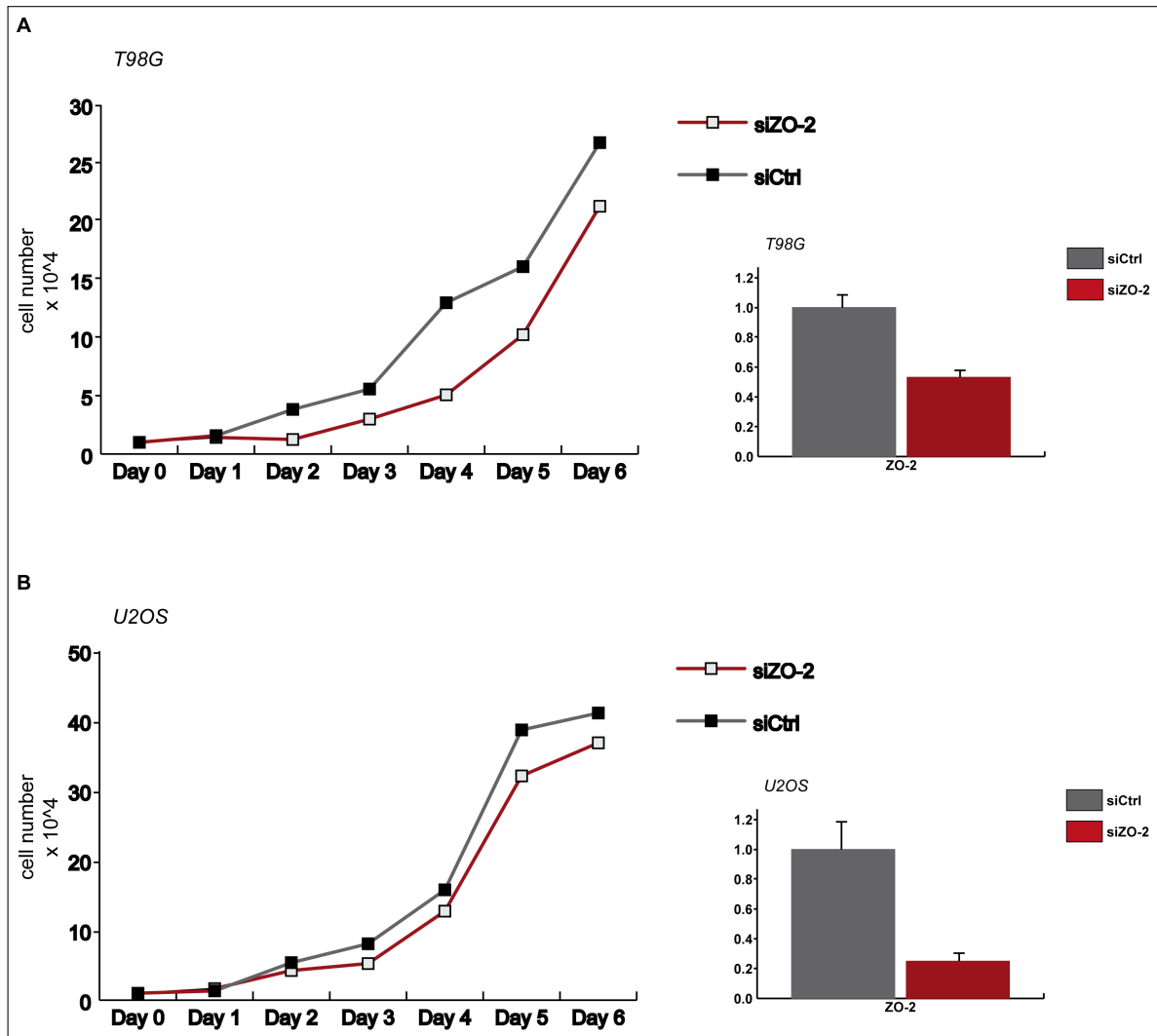


Figure 3.14.: **Growth curves of cells after ZO-2 depletion (A)** T98G cells were treated with siZO-2 or siCtrl and counted daily in triplicates to monitor cell growth. Mean values of the cell number were plotted against time. ZO-2 mRNA reduction by 50% leads to a strong decrease in proliferation in T98G cells. This effect is also observed in U2OS cells but to a weaker extent despite the higher mRNA knock down efficiency in those cells (**B**).

3. Results

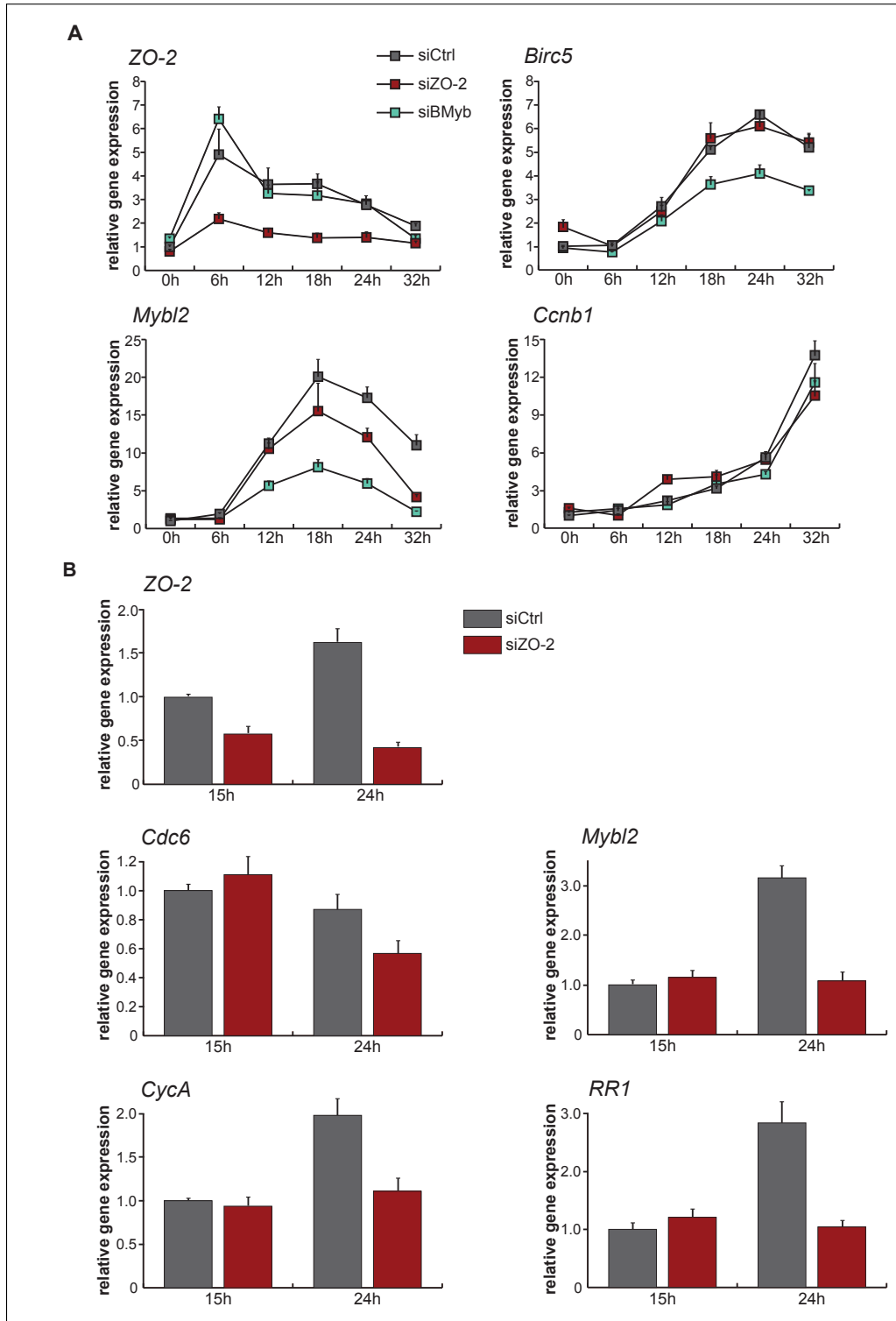


Figure 3.15.: **Expression analysis after ZO-2 knock down (A)** T98G cells were starved and transfected with siRNA against ZO-2, B-MYB or siCtrl. RNA was extracted at several time points and expression levels of several genes determined by qRT-PCR. Depletion of ZO-2 does not influence G2/M genes but B-Myb (*Mybl2*) mRNA levels. **(B)** Further gene expression analyses demonstrate decreased mRNA levels of G1 genes upon ZO-2 knock down.

3. Results

3.2.5.3. ZO-2 depletion results in mitotic delay

As described in 3.2.5.1 and 3.2.5.2, the depletion of ZO-2 leads to defects in proliferation and the reduction of G1 gene expression. Tapia et al., 2009 report that ZO-2 overexpression inhibits proliferation of epithelial Madin-Darby canine kidney (MDCK) cells by blocking cell progression at the G1/S border. It was reported that this is due to the inhibition of cyclinD1 expression and function which is essential for the proper transit of cells into S-phase. Knock down of ZO-2 therefore might lead to the opposite effect, the faster progression through G1 phase. As shown in 3.2.5.1, depletion of ZO-2 also led to a slower proliferation. FACS analysis was performed to clarify whether reduction of ZO-2 expression leads to a cell cycle block at a specific cell cycle phase.

To determine the amount of cells in S-phase after siZO-2 transfection, cells were treated as described in 3.2.5.2 and analysed with BrdU-FACS. To do so, 10 μ M bromodeoxyuridine (BrdU) was added 30 min before collecting the cells.

BrdU-FACS of control cells showed that incorporation of BrdU is high (75-80 %) after 18 - 24 hours after releasing cells from G0/G1 block and almost absent after 32 hours where only 3 % of cells are BrdU positive (fig. 3.16 **A**). At that time point cells are already in G1 of the next cell cycle as seen in the PI-FACS profiles in fig. 3.16 **B**. Depletion of ZO-2 by RNAi had no strong effect on early time points as the amount of BrdU positive cells after 18 - 24 h also reaches 73 %. However, 32 h after release, the cells seem to progress slower into and through G2/M phase as seen in the PI FACS. Also the percentage of BrdU positive cells stays high at 76 % indicating that cells still are in late S-phase.

For MPM2-FACS, the transfected cells were synchronised at the border of G1 and S-phase by a thymidine block with 2 mM thymidine for 24 h. Cells were followed up to 13 h after re-entering the cell cycle and analysed by MPM2-staining for mitotic cells. Additionally, standard PI-FACS were performed at the tested time points. As seen in fig. 3.17 **C**, 8 hours after release from cell cycle block the majority of cells are in G2/M. 2 hours later many cells passed through mitosis and enter G1 phase. Whereas, in ZO-2 depleted cells only few cells reach G1 phase. Even at the latest analysed time point (13 hours post release) there is no enrichment of cells in G1 phase in contrast to control (fig. 3.17 **D**). MPM2-staining showed that up to 16.1 % of cells accumulate in mitosis after ZO-2 depletion whereas in control cells the amount of MPM2 positive cells reaches only 6.3 % 13 hours after release from cell cycle block (fig. 3.17 **A** & **B**).

3. Results

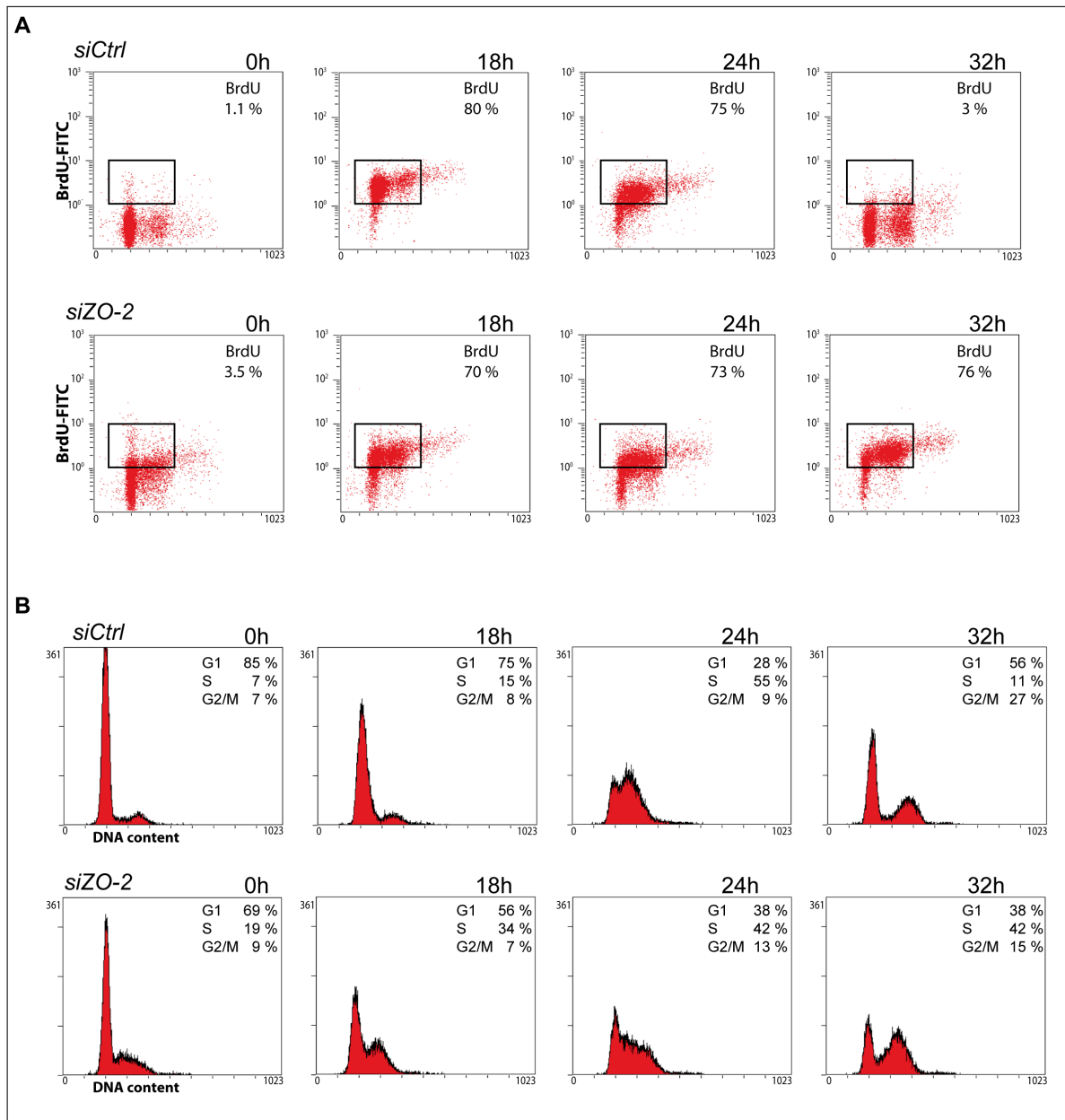


Figure 3.16.: **BrdU-FACS analysis after ZO-2 depletion (A)** Synchronised cells were treated with siCtrl or siZO-2 and analysed for S-phase cells by BrdU-FACS. FACS profiles indicate an accumulation of BrdU-positive cells after ZO-2 depletion. **(B)** PI-FACS profiles point to a delay in S-G2/M progression upon ZO-2 reduction.

3. Results

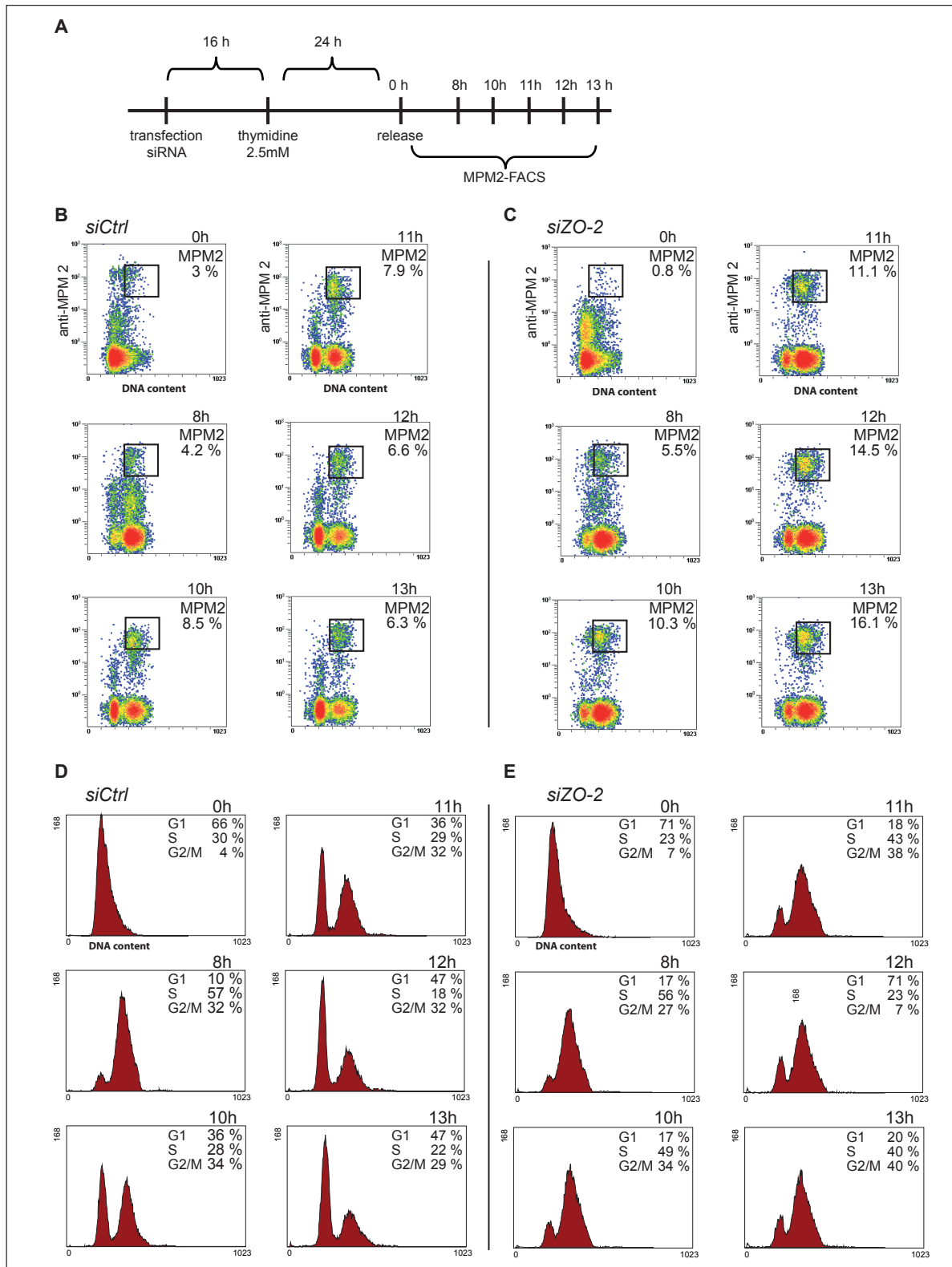


Figure 3.17.: **MPM2-FACS analysis after ZO-2 depletion** (A) Scheme of the MPM2 experiment. (B) (C) Synchronised cells were treated with siCtrl or siZO-2 and analysed for mitotic cells by MPM2-staining. MPM2-FACS profiles show an accumulation of MPM2-positive cells upon ZO-2 depletion. PI-FACS analysis confirms the delay of cell progression through mitosis (D) (E).

4. Discussion

The first part of this work dealt with the question which functions LIN9 and the DREAM-B-MYB complex play in mouse embryonic stem cells. Using RNAi approaches the influence on cell proliferation, gene regulation and a possible role in differentiation and pluripotency was analysed.

The second part focused on the identification DREAM interacting proteins that might contribute to DREAM-mediated gene activation.

4.1. Only DREAM-B-MYB found in ES cells

In this work I examined which proteins are associated to the DREAM core unit in ES cells. Both Co-immunoprecipitation with antibodies against LIN9 and MassSpec analysis identified DREAM-B-MYB as the only variant in mouse ES cells (fig. 3.3, 3.11 A). In somatic mammalian cells the DREAM complex exists in two conformations, dependent on the cell cycle phase. DREAM-p130/E2F4 in G0/G1 and DREAM-B-MYB which is formed upon S-phase entry (Schmit et al., 2007; Litovchick et al., 2007; Pilkinton et al., 2007). The binding of RBAP48 and E2F4 could not be verified by Co-IP since there were no working antibodies against RBAP48 in mouse cells or the protein band for E2F4 was overlaid by the heavy IgG heavy chain signal. But Masspec analysis could confirm RBAP48 as a subunit of DREAM (fig. 3.11 A), whereas E2F4 could not be identified (list of MassSpec results see supplementary S8). Since the pocket protein p130 is not expressed in ES cells (LeCouter et al., 1996), it is not surprising that it is not part of the DREAM complex. Whereas p107, which also is reported to bind to DREAM (Pilkinton et al., 2007; Schmit et al., 2007) is detectable in the Input of nuclear extracts of ES cells but does not associate to the complex as binding of p107 could not be verified by Co-IPs or Masspec analysis.

These findings lead to the assumption that pluripotent cells only build one DREAM variant. This is affirmed by a LIN9 study in embryonal carcinoma (EC) F9 cells that feature attributes of ES cells. In EC cells also only DREAM-B-MYB was verified (Knight

and Watson, 2009). The cell cycle structure of EC cells resembles that of ES cells with very short G1 and hyperphosphorylated pocket proteins, which might explain the lack of binding of p130 and E2F4 to DREAM. RBAP48 was not identified as subunit in EC cells, other than in ES cells, where it was detected by Masspec analysis. This suggests a different complex composition among the pluripotent cell types and an ES cell specific DREAM variety.

4.2. DREAM-B-MYB responsible for G2/M progression, genomic stability and integrity in ES cells

In this work, genome wide RNA expression analysis after LIN9 depletion demonstrated the influence of DREAM on the expression of mitotic genes in ES cells as the majority of genes with reduced expression after LIN9 kd are involved in cell cycle progression and mitotic processes (fig. 3.7 B, tab. 3.1).

Genome wide promoter binding analysis (ChIPchip) proved that LIN9 directly regulates the activation of these genes as it prevalently binds to promoters of mitotic genes (fig. 3.10) and the overlay of microarray and ChIPchip data revealed that many promoters of the downregulated mitotic genes are bound by LIN9 (fig. 3.10 B, tab. 3.1).

For example, at the onset of mitosis, cyclin B1 accumulates in the nucleus and binds to CDK1 which leads to the activation its kinase activity (reviewed in Porter and Donoghue, 2003). The cyclinB-CDK1 complex then controls the activation of different proteins needed for chromosome segregation and mitotic spindle formation (reviewed in Morgan, 1999). BUB3, a members of the 'spindle assembly checkpoint' (SAC), controlling chromosome segregation in early mitosis (Li and Nicklas, 1995), and Gas2l3, a protein involved in chromosome segregation and cytokinesis (Wolter et al., 2012), were also found to be directly regulated by DREAM. The DREAM target AURORA-A is critical in various steps of mitosis, e.g it is necessary for proper organisation of the mitotic spindle and the separation of the centromers after the mitotic spindle has been formed (reviewed in Barr and Gergely, 2007; Carmena and Earnshaw, 2003). These data from ES cells are consistent with studies from somatic cells where DREAM-B-MYB also was found to activate corresponding genes particularly needed for G2/M progression and mitosis (Osterloh et al., 2007; Pilkinton et al., 2007; Schmit et al., 2007).

4. Discussion

As LIN9 and B-MYB were shown to be required for the activation cell cycle progression genes, their depletion presumably affects cell proliferation. Indeed, LIN9 and B-MYB knock down in ES cells resulted in an increased fraction of cells in G2/M and polyploidy as shown by FACS analysis (fig. 3.1 C). To determine whether cells fail to progress into mitosis (and therefore accumulate in G2) or whether they delay during mitosis, FACS stainings with e.g. MPM-2 antibodies could be performed to calculate the amount of mitotic cells. Additionally, immunostainings against mitotic proteins or the mitotic spindle in ES cells could help to further demonstrate the effect of LIN9 and B-MYB depletion on mitosis and genomic stability.

The results found in ES cells are concordant with human (Osterloh et al., 2007) or mouse fibroblasts (Reichert et al., 2010) and embryonic carcinoma cells (Knight and Watson, 2009) where LIN9 depletion also resulted in cell cycle arrest at the G2/M border and polyploidy. These effects are based on the regulatory functions of DREAM on many genes needed for proper mitosis.

Lin9 knockout in MEFs leads to binucleated and tetraploid cells with abnormal shaped nuclei, multipolar spindles and numerous centrosomes. As consequence of these serious defects in mitosis, MEFs undergo premature senescence to avoid further progression through the cell cycle (Reichert et al., 2010). By introducing the SV40 LT antigen, cells can adopt to the loss of LIN9. These highly aneuploid cells are able to overcome senescence and grow anchorage-independently in soft agar, a hallmark of oncogenic transformation (Hauser et al., 2012).

Likewise, the depletion of dMyb, the *Drosophila* homologue of B-MYB leads to defective cell cycle progression and genome instability (Okada et al., 2002; Katzen et al., 1998; Manak et al., 2002; Fung et al., 2002). B-MYB was also reported to be part of the Myb-Clafi complex which is needed for the stabilisation of kinetochores and the localisation of clathrin at the mitotic spindle (Yamauchi et al., 2008). The disruption of the Myb-Clafi complex by inserting a point mutation into B-MYB caused genomic instability in form of aneuploidy. It is not determined whether the Myb-Clafi complex also exists in ES cells, but for ES it was also described that B-MYB depletion causes G2/M, arrest mitotic spindle and centrosome defects leading to aneuploidy (Tarasov et al., 2008).

In ES cells, it was earlier described that B-MYB depletion causes G2/M, arrest mitotic spindle and centrosome defects leading to aneuploidy (Tarasov et al., 2008).

The obtained data in ES cells affirm that DREAM is responsible for the regulation of a variety of genes needed for proper G2/M progression and cytokinesis by activating a set

of key mitotic genes. This underlines the importance of a functional DREAM-B-MYB complex for the maintenance of genome stability in ES cells.

4.3. DREAM is important for early embryonic development

To examine the influence of LIN9/B-MYB on embryonic development, I conducted embryoid body formation experiments. EB formation assays are often carried out to test whether genes execute functions in the development of the embryo by resembling the stages of gastrulation *in vitro* (Doetschman et al., 1985; Desbaillets et al., 2000).

Strikingly, EB formation is heavily impaired upon LIN9 and even stronger after B-MYB depletion (fig. 3.2). The resulting EBs consist of loosely attached cells with an irregular outer shape that grow very slowly compared to normal developing EBs. This observation is consistent with a study from Iwai et al., 2001. They found out that inhibition of B-MYB function by inserting an inducible dominant interfering Myb protein (MERT) into ES cells led to retarded EB formation due to reduced expression of E-cadherin, which functions as a homophilic intercellular adhesion molecule.

Besides a possible reduced E-cadherin expression, the monitored effect can be explained by the defective proliferation caused by the induced G2/M arrest of LIN9 or B-MYB depleted cells.

The role of DREAM-B-MYB as a regulator of ES cells proliferation is consistent with *in vivo* studies (Reichert et al., 2010; Tarasov et al., 2008). They describe that Lin9 and B-Myb ko embryos develop to the blastocyst stage but die shortly after implantation because the inner cell mass (ICM) cannot be maintained. The results from the conducted experiments in the work at hand suggest that the embryonic lethal phenotype is due to proliferation defects of the ICM caused by the reduction of mitotic gene expression.

This assumption is supported by the fact that deletion of several mitotic DREAM target genes results in a similar phenotype. Thus, knock out of Survivin (Birc5), Bub1, Plk1, CenpE or cyclinA2 all lead to an early embryonic lethality around 4.5 dpc caused by severe defects in cell cycle progression and mitosis (Uren et al., 2000; Perera et al., 2007; Lu et al., 2008; Putkey et al., 2002; Murphy et al., 1997). As ES cells undergo rapid cell cycles with no regulated cyclin-CDK activity (except for cyclinB-CDK1), an efficient cell cycle relies on a functioning mechanism that regulates progression from S-phase into mitosis.

4. Discussion

Disturbances in the expression of genes needed for G2/M transition or mitosis have a severe impact on stem cell proliferation. Since ES cells do display only reduced or no cell cycle controls (like the restriction point R), the outcome of such mitosis failures is cell death. However, besides the impact on cell proliferation it cannot be excluded that DREAM execute so far unknown functions in cell differentiation (4.4.2).

Taken together, the effect of LIN9 and B-MYB depletion on EB formation underlines the importance of a functional DREAM complex for the development and proliferation of the early embryo.

4.4. DREAM-B-MYB in Pluripotency and Differentiation

4.4.1. DREAM does not influence pluripotency in ES cells

Since the knock out of either Lin9 or B-Myb results in early embryonic lethality and B-MYB acting together with the DREAM complex, in this work a possible role of DREAM-B-MYB in pluripotency was investigated. But none of the conducted experiments delivered hints that DREAM might be involved in the regulation of pluripotency markers such as Sox2 or Oct4. LIN9 was not found to bind the promoters of these genes (fig. 3.3 B, ChIPchip data see supplementary S4) which contradicts the assumption of a direct gene regulation.

OCT4 and SOX2 levels must be maintained at a certain level, as downregulation of SOX2 or heavily unstable OCT4 protein levels induce differentiation (Niwa2000; Li et al., 2007). But no deregulated expression of Sox2 or Oct4 were observed after LIN9 depletion in ES cells by qRT-PCR (fig. 3.6 A) or genome wide RNA expression analysis (supplementary S1) which does not point to a disturbance in pluripotency.

Another feature of pluripotent cells is the high alkaline phosphatase (AP) activity which rapidly declines upon differentiation. Depletion of LIN9 or B-MYB did not result in decreased AP staining of ES cell (fig. 3.6 B) but led to the formation of noticeable smaller colonies than control cells which might be the outcome of proliferation defects.

The findings lead to the assumption that LIN9, DREAM respectively, is not needed for the maintenance of pluripotency.

Whether B-MYB, independently of DREAM, is involved in pluripotency, is not solved.

There are controversial studies concerning B-MYB and pluripotency. Tarasov *et al.* reported in 2008 that depletion of B-Myb by RNAi led to the transient increase of early differentiation markers such as CoupTF, Sox17 or Hand1 and to a slight reduction of

4. Discussion

mRNA and protein levels of the pluripotency markers Oct4 and Sox2. In their studies B-MYB binds to the Pou5f1 (Oct4) and Sox2 promoters. Depletion of B-MYB modestly affected Pou5f1 promoter activity suggesting a direct role in Oct4 regulation. They also observed morphological changes like the flattening of cell colonies and the emerging of spindle formed cells which is a characteristic of differentiation.

Genome wide binding studies using an antibody with higher specificity (Zhan et al., 2012) could not confirm the binding of B-MYB to Pou5f1 but to Sox2 and Nanog. They suggest that the role of B-MYB in maintaining pluripotency is secondary to its effects on cell cycle and that B-MYB exerts its effects on pluripotency indirectly through the regulation of other critical pluripotency factors like Sall4.

However, there are studies which oppose a role of B-MYB in the maintenance of pluripotency. In 2001, Iwai *et al.* report that inhibition of B-MYB did not change expression profiles of differentiation markers. Likewise, conditional gene deletion and therefore complete knock out of B-Myb did not affect pluripotency (Lorvellec et al., 2010) nor caused any alteration of Sox2 or Oct4 levels. An explanation for the diverging results might be that B-Myb was only partially depleted by RNAi in the studies by Tarasov *et al.* which probably did not abolish all B-MYB functions.

Further experiments are necessary to elucidate the role of B-MYB in ES cells. It is possible that the achieved depletion by shRNA is not enough to detect possible effects on pluripotency genes. For this purpose, an ES cell line with an inducible shRNA construct targeting B-Myb could be generated. Dose-dependent depletion (from low to complete B-MYB ablation) can be used to examine B-MYB function. Furthermore, genome wide RNA expression analyses after different times of B-MYB depletion also would provide information which genes are regulated by B-MYB together or independently of DREAM.

Thus, in this work a role for DREAM-B-MYB or B-MYB alone in the maintenance of pluripotency of ES cells could not be proven and it is suggested that the main role of B-MYB lies in its cell cycle regulating function.

4.4.2. Differentiation genes indirectly affected by DREAM

Unlike pluripotency genes, which were not affected upon LIN9 depletion, several developmental genes were found upregulated (fig. 3.7).

GO analysis of the array data indicate that genes associated with neuron -, lung development or angiogenesis are overrepresented among the upregulated genes. For instance, increased mRNA levels of early differentiation markers such as NeuroD1, Id4, Stmn3 or

4. Discussion

Vax2 after LIN9 depletion could be validated by qRT-PCR (fig. 3.8 A), but a direct binding of LIN9 on those promoters was not confirmed by ChIP analysis (fig. 3.8 B). Further ChIP experiments, e.g. further genome wide promoter binding assays for LIN9 or other DREAM subunits as LIN54, are necessary to gain information whether the regulatory influence on differentiation genes is of direct or indirect nature.

A specific function in development can not be completely excluded. This speculation is however possible because it is known that the *Drosophila* Myb-MuvB (MMB)/dREAM complex participates in the repression and activation of cell cycle-specific and developmentally regulated genes (Korenjak et al., 2004; Wen et al., 2008; Lewis et al., 2004; Georgette et al., 2007). A recent study reported that MMB/dREAM plays an important role in mediating neuron-specific expression of the carbon dioxide receptor genes (Gr63a/Gr21a) in *Drosophila* (Sim et al., 2012).

In 2011, it was described for the first time in human cells that DREAM holds a functional role in repressing a developmentally regulated gene (Flowers et al., 2011).

In osteoblast precursors, the alkaline phosphatase gene *Alpl* is essential for bone matrix mineralisation and a key marker gene for osteoblast differentiation (reviewed in Golub et al., 1992). *Alpl* is induced early in osteoblast differentiation concomitantly with differentiation-associated cell cycle arrest. ChIP analysis revealed that p130 targets the promoter in undifferentiated progenitors when *Alpl* is repressed, whereas pRB and p130 occupy the promoter specifically during *Alpl* activation after p130 dissociates from the promoter (Flowers et al., 2010). In the study of 2011, Flowers and colleagues also could verify that the DREAM components LIN9, RBAP48, DP1 and E2F4 as well as HDAC1 and HDAC2 bind to the *Alpl* promoter in proliferating osteoblast precursor cells. This promoter association is maintained by the BRM-SWI/SNF complex, a chromatin remodeling complex that exerts gene repressing function directly opposing the activating effect of BRG1-SWI/SNF (reviewed in Reisman et al., 2009) and helps to maintain the pre-osteoblast state until appropriate signals for terminal differentiation (Flowers et al., 2009).

Depletion of BRM or p130 caused the dissociation of DREAM and permitted BRG1-containing SWI/SNF to occupy the promoter prematurely. The resulting activation of *Alpl* leads to constitutive elevated AP activity and accelerated progression to mature osteoblast phenotype (Flowers et al., 2011). This indicates that DREAM contributes substantially to the repression of tissue-specific gene expression and differentiation in precursor cells.

To determine other tissue-specific genes regulated by DREAM, promoter analyses should be performed in different lineages and at different developmental stages.

Since many neuronal genes were found upregulated following LIN9 depletion, it could

4. Discussion

be further analysed whether the observed influence is restricted to special lineages in the developing embryo. This could be addressed by directed differentiation of ES cells into special developmental lineages after LIN9 or B-MYB depletion to see whether particular genes involved in neuronal development or angiogenesis are affected.

However, it seems that the observed deregulation of developmental genes is mostly based on an indirect effect which might be connected with the LIN9 kd mediated G2/M cell cycle arrest.

During differentiation, the cell cycle structure gets remodeled resulting in the prolongation of G1 and the establishment of a robust G1/S checkpoint (White et al., 2005). So, it is possible that the cell cycle delay caused by DREAM depletion is the reason for the upregulation of developmental genes. Indeed, the artificial prolongation of the cell cycle by trapping ES cells in G1 or mitosis, both lead to the induction of developmental genes such as *Flk1*, *NeuroD1* or *Pdgfra*, which were deregulated to a similar amount after LIN9 depletion (fig. 3.9 B,C). Upon withdrawal of the blocking agents and re-release into a normal ES cell cycle, mRNA levels dropped back to levels comparable of asynchronous growing ES cells (fig. 3.9 D) which indicates a direct connection between cell cycle delay and (reversible) induction of differentiation genes.

It is discussed controversially whether the cell cycle structure gets remodeled during or before cells begin to differentiate. Models are proposed for mammalian embryonal, neuronal and haemopoietic stem cells that G1 lengthening is the cause rather than the consequence of differentiation. The "Cell cycle length hypothesis" (Calegari and Huttner, 2003) suggests that a long G1 phase allows the accumulation of factors needed for differentiation to occur which a short G1 may not. This model is difficult to demonstrate as factors contributing to differentiation also often alter the cell cycle. Therefore, studies concentrate on the manipulation of genes only affecting G1 such as G1 specific cyclin-CDK complexes.

In neuronal stem cells (NSC) the crucial role of G1 lengthening in differentiation is accepted. It is shown that G1 length plays a central role in the switch from symmetric to asymmetric division of apical precursor cells resulting in postmitotic neurons. Lange et al., 2009 report that overexpression of cyclinD1-CDK4 in NSC inhibited lengthening of G1 which resulted in decreased neurogenesis and triggered a greater expansion of NSC. The inhibition of cyclinE-CDK2 led to the prolongation of G1 followed by differentiation of NSC whereas the outcome of overexpression was an increased generation and expansion of basal progenitors (Orford and Scadden, 2008).

4. Discussion

But, looking at embryonic stem cells there are controversial studies.

2009, Kim et al. (Kim et al., 2009) induced a construct into ES cells overexpressing a constitutively active CDK2. This led to elevated CDK2 activity which resulted in persistent pluripotency and defective differentiation (due to a loss of its binding protein Cdk2ap1). Knock down of CDK2 or antagonising its activity by pRB overexpression induced differentiation. Similar results were observed by Koledova et al., 2010 who claimed that decreasing CDK2 activity, caused by RNAi, leads to G1 lengthening and establishment of a canonical cell cycle profile in ES cells and differentiation.

A recent study (Coronado et al., 2013) showed that LIF withdrawal leads to a G1 lengthening. This G1 expansion is an early reversible response prior to the commitment to differentiation. This response occurs shortly before or concomitantly with the transient activation of early lineage specific markers. A short G1 results from LIF signaling. Upregulation or overexpression of cyclinE enhances self renewal whereas the depletion of cyclinE lengthens G1 and leads to spontaneous differentiation.

However, antagonising studies could not confirm these effects. Though the induced overexpression of the CDKi p21 and p27 did lengthen G1 in ES cells, this did not induce differentiation as RNA levels of the pluripotency markers Nanog, Oct4 and stage specific embryonic antigen 1 (SSEA1) did not alter (Li and Sousa, 2012). Additionally, no significant increase in genes used to characterise differentiation lineages such as Gata4 (endoderm), Brachyury (mesoderm) or Fgf5 (ectoderm) could be observed. Also Cdk2 knockout mice are viable and Cdk2 seems dispensable for differentiation (Berthet et al., 2003).

Thus, it is unlikely that in ES cells, contrary to NSC, G1 elongation alone is sufficient to induce differentiation.

Hence, it is most likely that depletion of LIN9 or B-MYB indirectly influence the upregulation of differentiation genes possibly by causing a cell cycle arrest in G2/M. This might be a transient and reversible effect as LIN9 or B-MYB depleted ES cells maintain their pluripotent character and do not undergo differentiation.

4.5. Identification of possible DREAM interactors

The function of the mammalian DREAM complex as regulator of G2/M gene expression is well documented. However, the mechanistic of activating or repressing gene activity is

4. Discussion

unknown as none of the DREAM members bear a catalytic domain which could mediate gene activation. Since none of the DREAM subunits contains a catalytically active domain, the exact mechanisms underlying the activation of gene expression are unknown. It is feasible that the association, maybe in a cell cycle dependent manner, of further proteins or co-factors is needed for the proper function of DREAM. This assumption is affirmed by a study of Schmit et al., 2007, in which mass spectrometry analysis of cell extracts after Co-IP with antibodies directed against the DREAM subunit LIN37 was conducted. Not all of the proteins that were bound to LIN37, and therefore are possible DREAM interactors, could be identified.

SILAC and MassSpec analyses of ES cells expressing a biotinylated version of LIN9 or B-MYB revealed a long list of potential interacting proteins (fig. 3.11 B). The candidate ZO-2 was chosen for further experiments as its binding to DREAM could be validated in different cell lines with Co-IPs against overexpressed and endogenous protein.

4.5.1. The tight junction protein ZO-2

Zona occludens proteins (ZOPs) are members of the membrane-associated guanylate kinase (MAGUK) homologous. As all known MAGUK members ZO-2 contains characteristic postsynaptic density 95/disc-large/zona occludens (PDZ), Src homology 3 (SH3) and guanylate kinase-like (GK) domains (fig. 4.1) which are all involved in protein-protein interactions (González-Mariscal et al., 2000). However, the GK domain which is located at the C-terminus in ZOPs has been reported to be enzymatically inactive.

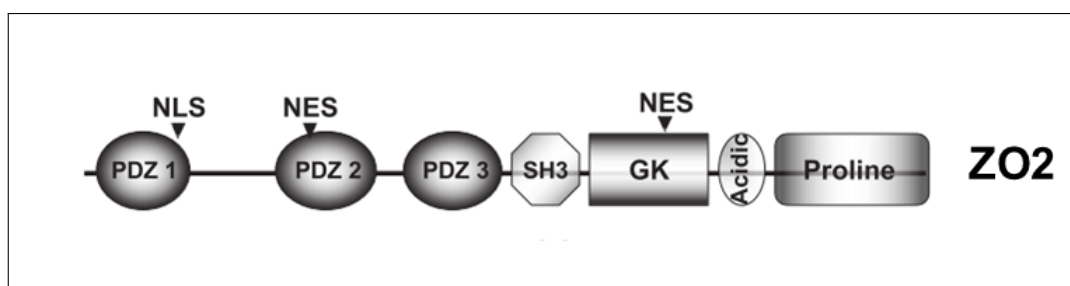


Figure 4.1.: **Schematic representation of ZO-2.** The localization of PDZ, SH3, GK, acidic and proline-rich domains, nuclear localization (NLS) and exportation (NES) signals is indicated (Adapted from Betanzos et al., 2004).

ZOPs localise to the cytoplasmatic surface of tight intercellular contacts (tight junctions) in endothelial and epithelial cells. They act as scaffold proteins to recruit additional structural and signaling proteins.

4. Discussion

Three members of Zona occludens proteins are known, ZO-1, ZO-2 and ZO-3.

The 160 kDa phosphoprotein ZO-2 shows a high homology to ZO-1, both proteins can form a heterodimeric complex (Wittchen et al., 1999). ZO-2 mainly localises to the region of tight junctions (TJ) but it was also found to translocate to the nucleus of epithelial cells (Islas et al., 2002). As the protein carries several functional nuclear import and export signals, its nucleo-cytoplasmic shuttling appears plausible (Traweger et al., 2003; Jaramillo et al., 2004).

The distribution of ZO-2 is influenced by the degree of cell-cell-contact. Thus, in confluent monolayers ZO-2 localises to the TJ whereas, in sparse cultures with high proliferative state a significant amount of ZO-2 is found in the nucleus (Islas et al., 2002).

4.5.2. ZO-2 binding to DREAM is strongest in S-phase

ZO-2 was identified as potential binding partner of DREAM in ES cells with MassSpec analyses. Co-immunoprecipitations in ES cells confirmed the binding which also was found in overexpression experiments in human 293T cells and endogenously with human T98G cells (fig. 3.12 and fig. 3.13). These results demonstrate that ZO-2 binding is not specific for ES cells but occurs in cell types of different origin. It is possible that the intensity of the interaction is influenced by the proliferative state of cells since nuclear localization of ZO-2 is increased in cells with high proliferation (Islas et al., 2002).

Experiments with synchronised T98G cells showed that binding of ZO-2 to DREAM happens in a cell cycle dependent manner. Consistent with Traweger (Traweger et al., 2008) ZO-2 could not be detected in G0 in the nucleus and therefore no binding to LIN9 was observed. Upon progression through G1, ZO-2 protein levels increase and stay constant. Binding to LIN9 was detected in late G1, during S-phase strongest signals were found which decreased in intensity along further progression through G2/M (fig. 3.13 B). The same binding pattern was found when nuclear cell extracts were immunoprecipitated with B-MYB antibody. The strongest binding between ZO-2 and B-MYB was detected in S-phase (fig. 3.13 C).

Thus, this leads to the suggestion that ZO-2 associates to DREAM during the switch from the repressive DREAM-p130/E2F4 to the activating DREAM-B-MYB complex.

4.5.2.1. ZO-2 affects G1 rather than G2/M gene expression

The interaction to the DREAM-B-MYB complex suggests a participation of ZO-2 in the activation of G2/M genes. However, depletion of ZO-2 with RNAi in starved T98G cells

4. Discussion

and re-release of cells into the cell cycle did not affect the expression of typical DREAM target genes such as Birc5 or cyclinB1 (fig. 3.15 A). Whereas, for G1 expressed genes like Cdc6 or Mybl2 (B-Myb), decreased mRNA levels could be detected after release from cell cycle block (fig. 3.15 B). This indicates that ZO-2 is involved in the regulation of G1 genes but possibly not required for G2/M gene expression. Several studies indicate an influence of ZO-2 on gene regulation. Thus, ZO-2 associates with the transcription factors Jun, Fos and C/EPB (Betanzos et al., 2004). Jun and Fos are known to form a transcriptional activator complex named AP-1 (reviewed in Karin et al., 1997) which is reported to be involved in cellular proliferation, transformation and death (Shaulian and Karin, 2002). By using reporter gene assays, Betanzos *et al.* observed that ZO-2 modulates the transcriptional activity of AP-1-controlled promoters as ZO-2 overexpression resulted in a diminished promoter activity. Since ZO-2 was found to co-localise with AP-1 at TJ of MDCK cells, it is speculated that this triggers a sequestration effect of AP-1 out of the nucleus and that the resulting decreased amount of AP-1 effects its activity upon gene regulation (Betanzos et al., 2004).

ZO-2 also interacts with the scaffold attachment factor B (SAF-B) (Traweger et al., 2003), a ribonucleoprotein that is involved in chromatin organisation, assembly of transcriptosome complexes and RNA splicing (Renz and Fackelmayer, 1996).

In 2007, Huerta *et al.* examined the impact of ZO-2 on the transcription of cyclinD1 and found that ZO-2 downregulates cyclinD1 transcription by interacting with the c-Myc/E box element and by recruiting the histone deacetylase HDAC1 for repression (Huerta et al., 2007).

Since there is no evidence that ZO-2 can directly bind to DNA it is probable that it influences gene expression indirectly by regulating transcription factors such as mentioned or other proteins controlling gene expression.

The finding that G1 but no G2/M genes, like the DREAM targets cyclinB1 or Birc5, were found to be deregulated upon ZO-2 knock down, suggests that ZO-2 is not needed for DREAM-mediated gene activation but might be involved in G1 gene regulation.

4.5.2.2. Reduced proliferation after ZO-2 depletion due to delayed progression through mitosis

Besides its importance at tight junctions, ZO-2 fulfils functions in cell proliferation. In this work it could be shown that ZO-2 reduction by RNAi results in decreased proliferation in T98G and - to a lesser extent- in U2OS cells (fig. 3.14). Former studies also documented that ZO-2 knock out mice showed reduced proliferation 6.5 dpc and increased apoptosis

4. Discussion

at 7.5 dpc resulting in embryonic lethality shortly after implantation due to an arrest in early gastrulation (Xu et al., 2008). In vascular smooth muscle cells (VSMC), the silencing of ZO-2 resulted in decreased proliferation in VSMC caused by increased Stat1 expression and transcriptional activity (Kusch et al., 2009). But not only decreased ZO-2 levels but also its overexpression inhibits cell proliferation (Huerta et al., 2007) and leads to arrest at the G1/S boundary in canine epithelial cells (Tapia et al., 2009). This is explained by reduced cyclinD1 protein levels due to diminished protein transcription and increased proteasomal degradation (Huerta et al., 2007). CyclinD1 assembles with CDK4/6 in early G1. Accumulation of this complex leads to the activation of the kinases that phosphorylate and inactivate the tumor suppressor retinoblastoma, a necessary step for cell cycle progression through G1-to-S phases (Harbour and Dean, 2000)

Unlike ZO-2 overexpression its depletion does not result in G1/S arrest. BrdU stainings of RNAi treated, synchronised T98G cells revealed that entry into S-phase is not affected, but it seems that progression into G2/M is delayed (fig. 3.16). FACS staining with the mitotic marker MPM2 showed that ZO-2 depleted cells stay longer in mitosis than control cells (fig. 3.17). Thus, decreased ZO-2 levels might lead to a slower cell progression into and through mitosis. Since ZO-2 depletion does not affect G2/M gene expression the observed effect might not be connected with DREAM mediated function. The reason for the prolonged mitosis could not be resolved in this work. It is also suggested that ZO-2 serves as a platform for transcriptosome assembly (González-Mariscal et al., 2012). Thus, it is possible that reduced ZO-2 levels affect transcription of non-DREAM target genes involved in mitosis which results in the observed cell cycle delay. Therefore, it might be that ZO-2 participate in the regulation of genes needed for progression through the cell cycle.

4.5.3. ZO-2 might act as scaffold protein to support DREAM assembly

As described in fig. 4.5, ZO-2 binding to DREAM was found during the switch from the repressing DREAM to the gene activating DREAM-B-MYB complex. However, since ZO-2 often acts as a scaffold protein (González-Mariscal et al., 2012) it is possible that it is needed for the assembly of the DREAM-B-MYB complex. Its absence might lead to an diminished assembly of the complex.

It also is feasible that ZO-2 influences the stability of B-MYB as it is reported that overexpression of ZO-2 leads to an increased proteasomal degradation of cyclinD1 in ca-

4. Discussion

nine epithelial cells (Huerta et al., 2007). This could be investigated by experiments with cycloheximid (CHX), an agent that inhibits protein synthesis. CHX is often used to study the half-life of proteins. If ZO-2 affects B-MYB stability it should be degraded faster upon ZO-2 depletion.

Furthermore a role for ZO-2 as a nucleo-cytoplasmic shuttle for YAP2, one of the effectors of the Hippo pathways, was proposed in 2010 by Oka and his colleagues. They describe that ZO-2 uses its first PDZ domain to build a complex with YAP2 and facilitates the nuclear localisation of YAP2 and that this activity of ZO-2 is PDZ-domain-dependent (Oka et al., 2010).

To better understand the function of ZO-2 binding to DREAM-B-MYB it would be interesting to know which ZO-2 domains and which DREAM subunits are involved in the association. ZO-2 features several protein-protein binding domains. This could be achieved by using pulldown assays with GST-fusion constructs. Thus, it was demonstrated that the transcription factors Jun, Fos and C/EBP bind to the proline rich C-terminus of ZO-2 (Betanzos et al., 2004), whereas the transcriptional coactivators TAZ/YAP or the DNA-binding protein SAF-B interact with the N-terminal PDZ1 domain (Remue et al., 2010; Traweger et al., 2003).

4.5.4. The mechanism of DREAM mediated gene regulation is still unclear

MassSpec analyses from nuclear extracts after streptavidin pulldown of LIN9- and B-MYB-biotinylated ES cells identified many proteins that possibly bind to DREAM. The conducted experiments did not reveal any participation of ZO-2 in DREAM mediated gene regulation. Hence, further proteins from the MassSpec list could be validated and investigated whether they assist the DREAM complex in the activation of genes.

It is feasible that activation of gene expression is mediated by epigenetic control. In *Drosophila*, several studies suggest a role for the MMB/dREAM complex in genomewide epigenetic control. Wen et al., 2008 demonstrated that the expression of Polo kinase, a gene expressed in G2, was controlled in a switch-like manner by dREAM/MMB and suggested a role for the complex in the epigenetic regulation of gene expression. The absence of both Myb and Mip130/Lin9, or of both Myb and E2F2, caused altered expression in which high or low levels of Polo were stably inherited through successive cell divisions in imaginal wing discs of *Drosophila*. Restoration of Myb resulted in a uniformly high level of Polo expression similar to that seen in wild-type tissue, whereas restoration of Mip130 or

4. Discussion

E2F2 extinguished Polo expression which indicates the activating function of Myb in contrast to the repression by Mip130 or E2F2 in MMB/dREAM. Lee et al., 2010 also describe a role for MMB/dREAM in two mechanisms involved in repression of group D/E genes: the deacetylation of histones at promoters, a mechanism shared with cell cycle-regulated genes, and the dimethylation of histone H3K27, a feature unique to differentiation-specific E2F/RB targets. Lee and his colleagues suggest that MMB/DREAM components serve as a scaffold to assemble distinct activities at different promoters and in different cellular states, thereby mediating the epigenetic regulation of RB target genes. Another role for MMB/dREAM in epigenetic control in *Drosophila* was reported for the neuron-specific expression of the carbon-dioxide receptor genes (*Gr63a/Gr21a*) (Sim et al., 2012).

Several chromatin-modifying proteins were found to associate with MMB/dREAM.

p55/Caf1 is a histone chaperone and also member of the nucleosome remodeling factor (NuRF) and the nucleosome remodeling and deacetylating factor (NuRD) (Tyler et al., 1996; Song et al., 2008; Martínez-Balbás et al., 1998). Furthermore, the histone deacetylase Rpd3 and L(3)mbt, which binds H4K20me1 (Trojer et al., 2007), were suggested to be part of the MMB/dREAM complex (Lewis et al., 2004). Whether these proteins contribute to the epigenetic control of MMB/dREAM regulated genes is so far unknown.

However, one might speculate that also in mammalian cells DREAM might recruit histone modifying or chromatin remodeling proteins in order to regulate gene expression.

But no proteins with such function could be detected to bind to LIN9 or B-MYB by MassSpec analysis in this work. It is possible that during the many steps of the experiment weakly bound proteins are lost. This could be the case if they do not directly bind to LIN9 or B-MYB but to other DREAM subunits. Hence, analogue experiments could be performed for the other DREAM subunits to obtain additional potential interacting proteins.

4.6. Conclusion

The mammalian DREAM complex acts as an important regulator of G2/M gene transcription. But the molecular mechanisms behind the activation of genes are still unclear. Possibly, co-factors or other interacting proteins are involved in DREAM-mediated transcriptional regulation. In the work at hand various potential DREAM interacting proteins were identified by mass spectrometry analysis. The focus was laid at the tight junction protein ZO-2 which is reported fulfil functions in proliferation and transcription. ZO-2 binding to DREAM-B-MYB is strongest in S-phase but is probably not contributing to DREAM mediated G2/M gene regulation. It might be that ZO-2 acts as scaffold protein, needed for the assembly of the DREAM-B-MYB complex. Further experiments are necessary to elucidate the role of the ZO-2/DREAM-B-MYB binding.

DREAM function is relatively well understood in differentiated cells. However, this study describes the first genome-wide analysis of genes regulated by the DREAM subunit LIN9 in mouse ES cells by using a combination of RNAi mediated depletion of Lin9 and microarray experiments. I could validate that DREAM is required for the activation of key mitotic genes such as AuroraA, Plk1 or cyclinB. The consequences of the depletion of either LIN9 or B-MYB in pluripotent ES cells are reduced proliferation, increased polyploidy and strongly impaired embryoid body formation. The hypothesis that the DREAM complex might be involved in the maintenance of pluripotency as it is suggested for B-MYB could not be confirmed in this study. Neither resulted the depletion of LIN9 or B-MYB in a decrease of pluripotency markers such as Oct4 or Sox2 nor did ES cells undergo differentiation. Altogether, the findings in this work underline the important role of the DREAM-B-MYB complex as master regulator of G2/M gene transcription and point out its requirement for proliferation and genome stability in ES cells.

References

- Attwooll, C., S. Oddi, P. Cartwright, E. Prosperini, K. Agger, P. Steensgaard, C. Wagener, C. Sardet, M. Moroni, and K. Helin (2005). 'A novel repressive E2F6 complex containing the polycomb group protein, EPC1, that interacts with EZH2 in a proliferation-specific manner.' In: *J. Biol. Chem.* 280, pp. 1199–1208.
- Avilion, A, S Nicolis, L Pevny, L Perez, N Vivian, and R Lovell-Badge (2003). 'Multipotent cell lineages in early mouse development depend on SOX2 function.' In: *Genes Dev* 1, pp. 126–40.
- Azuara, V., P. Perry, S. Sauer, M. Spivakov, H. J. R. John, M. Gouti, M. Casanova, G. Warnes, M. Merkenschlager, and A. Fisher (2006). 'Chromatin signatures of pluripotent cell lines.' In: *Nat. Cell Biol.* 8, pp. 532–538.
- Balda, M and J Anderson (1993). '2 Classes of Tight Junctions are revealed by ZO-1 Isoforms'. In: *Am. J. Physiol.* 264, pp. C918–C924.
- Barr, A. and F. Gergely (2007). 'Aurora-A: the maker and breaker of spindle poles.' In: *J. Cell Sci.* 120. Ed. by N. Martínez-Editors, pp. 2987–2996.
- Bartek, J and J Lukas (2001). 'Pathways governing G1/S transition and their response to DNA damage.' In: *FEBS Lett.* 490, pp. 117–122.
- Beijersbergen, R, R Kerkhoven, L Zhu, L Carlee, P Voorhoeve, and R Bernards (1994). 'E2F-4, a new member of the E2F gene family, has oncogenic activity and associates with p107 in vivo.' In: *Genes Dev.* 8, pp. 2680–2690.
- Beitel, G., E. Lambie, and H. Horvitz (2000). 'The *C. elegans* gene *lin-9*, which acts in an Rb-related pathway, is required for gonadal sheath cell development and encodes a novel protein.' In: *Gene* 254, pp. 253–263.
- Bender, T., C. Kremer, M. Kraus, T. Buch, and K. Rajewsky (2004). 'Critical functions for c-Myb at three checkpoints during thymocyte development.' In: *Nature Immunology* 5, pp. 721–729.
- Bernstein, B., T. Mikkelsen, X. Xie, M. Kamal, D. Huebert, J. Cuff, B. Fry, A. Meissner, M. Wernig, K. Plath, and et al. (2006). 'A bivalent chromatin structure marks key developmental genes in embryonic stem cells.' In: *Cell* 125, pp. 315–326.
- Berthet, C., E. Aleem, V. Coppola, L. Tessarollo, and P. Kaldis (2003). 'Cdk2 Knockout Mice Are Viable'. In: *Current Biology* 13, pp. 1775–1785.
- Betanzos, A., M. Huerta, E. Lopez-Bayghen, E. Azuara, J. Amerena, and L. González-Mariscal (2004). 'The tight junction protein ZO-2 associates with Jun, Fos and C/EBP transcription factors in epithelial cells'. In: *Exp. Cell Res.* 292, pp. 51–66.
- Bhatt, A., Q. Zhang, S. Harris, H. White-Cooper, and H. Dickinson (2004). 'Gene structure and molecular analysis of *Arabidopsis thaliana* ALWAYS EARLY homologs.' In: *Gene* 336, pp. 219–229.

References

- Boheler, K (2002). 'Differentiation of Pluripotent Embryonic Stem Cells Into Cardiomyocytes'. In: *Circulation Research* 91, pp. 189–201.
- Boyer, L., T. I. Lee, M. Cole, S. Johnstone, S. Levine, J. Zucker, M. Guenther, R. Kumar, H. Murray, R. Jenner, and et al. (2005). 'Core transcriptional regulatory circuitry in human embryonic stem cells.' In: *Cell* 122, pp. 947–956.
- Boyer, L., K. Plath, J. Zeitlinger, T. Brambrink, L. Medeiros, T. I. Lee, S. Levine, M. Wernig, A. Tajonar, M. Ray, G Bell, A Otte, M Vidal, D. Gifford, Y. RA, and R. Jaenisch (2006). 'Polycomb complexes repress developmental regulators in murine embryonic stem cells.' In: *Nature* 441, pp. 349–353.
- Bracken, A., M. Ciro, A. Cocito, and K. Helin (2004). 'E2F target genes: unraveling the biology.' In: *Trends Biochem. Sci.* 29, pp. 409–417.
- Bradford, M (1976). 'A rapid and sensitive method for the quantitation of microgram quantities of protein using the principle of protein dye binding'. In: *Anal. Biochem.* 72, pp. 248–254.
- Bruin, A. de, B. Maiti, L. Jakoi, C. Timmers, R. Buerki, and G. Leone (2003). 'Identification and characterization of E2F7, a novel mammalian E2F family member capable of blocking cellular proliferation.' In: *J Biol Chem* 278, pp. 42041–9.
- Bunz, F, A Dutriaux, C Lengauer, T Waldman, S Zhou, J Brown, J Sedivy, K Kinzler, and B Vogelstein (1998). 'Requirement for p53 and p21 to Sustain G2 Arrest After DNA Damage'. In: *Science* 282, pp. 1497–1501.
- Burdon, T, A Smith, and P Savatier (2002). 'Signalling, cell cycle and pluripotency in embryonic stem cells.' In: *Trends Cell Biol.* 12, pp. 432–438.
- Calegari, F. and W. Huttner (2003). 'An inhibition of cyclin-dependent kinases that lengthens, but does not arrest, neuroepithelial cell cycle induces premature neurogenesis.' In: *J. Cell Sci.* 116, pp. 4947–4955.
- Carmena, M. and W. Earnshaw (2003). 'The cellular geography of Aurora kinases'. In: *Nat. Rev. Mol. Cell Biol.* 4, pp. 842–854.
- Cartwright, P, H MÄller, C Wagener, K Holm, and K Helin (1998). 'E2F-6: a novel member of the E2F family is an inhibitor of E2F-dependent transcription.' In: *Oncogene* 17, pp. 611–623.
- Chambers, I., D. Colby, M. Robertson, J. Nichols, S. Lee, S. Tweedie, and A. Smith (2003). 'Functional Expression Cloning of Nanog, a Pluripotency Sustaining Factor in Embryonic Stem Cells.' In: *Cell* 113, pp. 643–55.
- Chen, P, D Riley, Y Chen, and W Lee (1996). 'Retinoblastoma protein positively regulates terminal adipocyte differentiation through direct interaction with C/EBPs.' In: *Genes Dev.* 10, pp. 2794–2804.
- Christensen, J., P. Cloos, U. Toftegaard, D. Klinkenberg, A. Bracken, E. Trinh, M. Heeran, L. Di Stefano, and K. Helin (2005). 'Characterization of E2F8, a novel E2F-like cell-cycle regulated repressor of E2F-activated transcription'. In: *Nucleic Acids Res.* 33, pp. 5458–5470.
- Coller, H. (2007). 'Whats taking so long? S-phase entry from quiescence versus proliferation.' In: *Nat. Rev. Mol. Cell Biol.* 8, pp. 667–670.
- Coronado, D., M. Godet, P.-Y. Bourillot, Y. Taponnier, A. Bernat, M. Petit, M. Afanassieff, S. Markossian, A. Malashicheva, R. Iacone, K. Anastassiadis, and P. Savatier (2013).

References

- 'A short G1 phase is an intrinsic determinant of naïve embryonic stem cell pluripotency.' In: *Stem cell research* 10, pp. 118–31.
- Dai, B. and T. Rasmussen (2007). 'Global epiproteomic signatures distinguish embryonic stem cells from differentiated cells.' In: *Stem Cells* 25, pp. 2567–2574.
- Dang, S. and M. Kyba (2002). 'Efficiency of embryoid body formation and hematopoietic development from embryonic stem cells in different culture systems'. In: *Biotechnol. Bioeng.* 78, pp. 442–453.
- Den Haese, G, N Walworth, A Carr, and K Gould (1995). 'The Wee1 protein kinase regulates T14 phosphorylation of fission yeast Cdc2.' In: *Mol. Biol. Cell* 6, pp. 371–385.
- Desbaillets, I., U. Ziegler, P. Groscurth, and M. Gassmann (2000). 'Embryoid bodies : an in vitro model of mouse embryogenesis'. In: *Exp. Physiol.* 85, pp. 645–651.
- Di Stefano, L., M. R. Jensen, and K. Helin (2003). 'E2F7, a novel E2F featuring DP-independent repression of a subset of E2F-regulated genes'. In: *EMBO J* 22, pp. 6289–6298.
- Doetschman, T, H Eistetter, M Katz, W Schmidt, and R Kemler (1985). 'The in vitro development of blastocyst-derived embryonic stem cell lines: formation of visceral yolk sac, blood islands and myocardium.' In: *J. Embryol. Exp. Morphol.* 87, pp. 27–45.
- Doree, M. and S. Galas (1994). 'The cyclin-dependent protein kinases and the control of cell division'. In: *FASEB J.* 8, pp. 1114–1121.
- Driegen, S., R. Ferreira, A. Van Zon, J. Strouboulis, M. Jaegle, F. Grosveld, S. Philipsen, and D. Meijer (2005). 'A generic tool for biotinylation of tagged proteins in transgenic mice.' In: *Transgenic Res.* 14, pp. 477–482.
- Dyson, N (1998). 'The regulation of E2F by pRB-family proteins.' In: *Genes Dev.* 12, pp. 2245–2262.
- Efroni, S., R. Duttagupta, J. Cheng, H. Dehghani, D. Hoepfner, C. Dash, D. Bazett-Jones, S. Le Grice, R. McKay, K. Buetow, T. Gingeras, T. Misteli, and E. Meshorer (2008). 'Global transcription in pluripotent embryonic stem cells.' In: *Cell stem cell* 2, pp. 437–447.
- Evans, M. J. and M Kaufman (1981). 'Establishment in culture of pluripotential cells from mouse embryos.' In: *Nature* 292, pp. 154–156.
- Faast, R., J. White, P. Cartwright, L. Crocker, B. Sarcevic, and S. Dalton (2004). 'Cdk6-cyclin D3 activity in murine ES cells is resistant to inhibition by p16(INK4a).' In: *Oncogene* 23, pp. 491–502.
- Felsani, A, A Mileo, and M Paggi (2006). 'Retinoblastoma family proteins as key targets of the small DNA virus oncoproteins.' In: *Oncogene* 25, pp. 5277–5285.
- Ferguson, E. and H. Horvitz (1989). 'The multivulva phenotype of certain *Caenorhabditis elegans* mutants results from defects in two functionally redundant pathways.' In: *Genetics* 123, pp. 109–121.
- Flowers, S., N. Nagl, G. Beck, and E. Moran (2009). 'Antagonistic Roles for BRM and BRG1 SWI/SNF Complexes in Differentiation'. In: *J. Biol. Chem.* 284, pp. 10067–10075.
- Flowers, S., G. Beck, and E. Moran (2010). 'Transcriptional activation by pRB and its coordination with SWI/SNF recruitment.' In: *Cancer Res.* 70, pp. 8282–8287.
- (2011). 'Tissue-specific Gene Targeting by the Multiprotein Mammalian DREAM Complex.' In: *J. Biol. Chem.* 286, pp. 27867–27871.

References

- Fung, S.-M., G. Ramsay, and A. Katzen (2002). 'Mutations in *Drosophila myb* lead to centrosome amplification and genomic instability.' In: *Development* 129, pp. 347–359.
- Gangaraju, V. and B. Bartholomew (2007). 'Mechanisms of ATP dependent chromatin remodeling.' In: *Mutat. Res.* 618, pp. 3–17.
- Gaubatz, S., J. Wood, and D. Livingston (1998). 'Unusual proliferation arrest and transcriptional control properties of a newly discovered E2F family member, E2F-6'. In: *Proc. Natl. Acad. Sci. U. S. A.* 95, pp. 9190–9195.
- Gaubatz, S., J. Lees, G. Lindeman, and D. Livingston (2001). 'E2F4 Is Exported from the Nucleus in a CRM1-Dependent Manner'. In: *Mol. Cell. Biol.* 21, pp. 1384–1392.
- Georgette, D., S. Ahn, D. MacAlpine, E. Cheung, P. Lewis, E. Beall, S. Bell, T. Speed, R. Manak, and M. Botchan (2007). 'Genomic profiling and expression studies reveal both positive and negative activities for the *Drosophila Myb MuvB/dREAM* complex in proliferating cells.' In: *Genes Dev.* 21, pp. 2880–2896.
- Giacinti, C and A Giordano (2006). 'RB and cell cycle progression.' In: *Oncogene* 25, pp. 5220–5227.
- Giangrande, P., W. Zhu, S. Schlisio, X. Sun, S. Mori, S. Gaubatz, and J. Nevins (2004). 'A role for E2F6 in distinguishing G1 / S- and G2 / M-specific transcription'. In: *Genes Dev* 18, pp. 2941–2951.
- Ginsberg, D, G Vairo, T Chittenden, Z Xiao, G Xu, K Wydner, J DeCaprio, J Lawrence, and D Livingston (1994). 'E2F-4, a new member of the E2F transcription factor family, interacts with p107.' In: *Genes Dev.* 8, pp. 2665–2679.
- Girard, F, U Strausfeld, A Fernandez, and N Lamb (1991). 'Cyclin A is required for the onset of DNA replication in mammalian fibroblasts.' In: *Cell* 67, pp. 1169–1179.
- Golub, E, G Harrison, and A Taylor (1992). 'The role of alkaline phosphatase in cartilage mineralization'. In: *Bone Miner.* 17, pp. 273–278.
- Gonda, T and D Metcalf (1984). 'Expression of *myb*, *myc* and *fos* proto-oncogenes during the differentiation of a murine myeloid leukaemia.' In: *Nature* 310, pp. 249–251.
- González-Mariscal, L, A Betanzos, and A Avila-Flores (2000). 'MAGUK proteins: structure and role in the tight junction.' In: *Seminars in cell developmental biology* 11, pp. 315–324.
- González-Mariscal, L., P. Bautista, S. Lechuga, and M. Quiros (2012). 'ZO-2, a tight junction scaffold protein involved in the regulation of cell proliferation and apoptosis.' In: *Ann. N. Y. Acad. Sci.* 1257, pp. 133–41.
- Graf, T (1992). 'Myb: a transcriptional activator linking proliferation and differentiation in hematopoietic cells.' In: *Curr. Opin. Genet. Dev.* 2, pp. 249–255.
- Gu, W, J Schneider, G Condorelli, S Kaushal, V Mahdavi, and B Nadal-Ginard (1993). 'Interaction of myogenic factors and the retinoblastoma protein mediates muscle cell commitment and differentiation.' In: *Cell* 72, pp. 309–324.
- Guan, K, J Rohwedel, and a. M. Wobus (1999). 'Embryonic stem cell differentiation models: cardiogenesis, myogenesis, neurogenesis, epithelial and vascular smooth muscle cell differentiation in vitro.' In: *Cytotechnology* 30, pp. 211–26.
- Harbour, J. and D. Dean (2000). 'The Rb/E2F pathway: expanding roles and emerging paradigms.' In: *Genes Dev.* 14, pp. 2393–2409.

References

- Harbour, J, R Luo, A Dei Santi, A Postigo, and D Dean (1999). 'Cdk phosphorylation triggers sequential intramolecular interactions that progressively block Rb functions as cells move through G1.' In: *Cell* 98, pp. 859–869.
- Harrison, M., C. Ceol, X Lu, and H Horvitz (2006). 'Some *C. elegans* class B synthetic multivulva proteins encode a conserved LIN-35 Rb-containing complex distinct from a NuRD-like complex.' In: *Proc. Natl. Acad. Sci. U. S. A.* 103, pp. 16782–16787.
- Hauser, S, T Ulrich, S Wurster, K Schmitt, N Reichert, and S Gaubatz (2012). 'Loss of LIN9, a member of the DREAM complex, cooperates with SV40 large T antigen to induce genomic instability and anchorage-independent growth.' In: *Oncogene* 31, pp. 1859–68.
- Hijmans, E, P Voorhoeve, R Beijersbergen, L Van T Veer, and R Bernards (1995). 'E2F-5, a new E2F family member that interacts with p130 in vivo.' In: *Mol. Cell. Biol.* 15, pp. 3082–3089.
- Horn, P. and C. Peterson (2006). 'Heterochromatin assembly: a new twist on an old model.' In: *Chromosome Res.* 14, pp. 83–94.
- Huerta, M., R. Munoz, R. Tapia, E. Soto-Reyes, L. Ramirez, F. Recillas-Targa, L. González-Mariscal, and E. Lopez-Bayghen (2007). 'Cyclin D1 is transcriptionally down-regulated by ZO-2 via an E box and the transcription factor c-Myc.' In: *Mol. Biol. Cell* 18. Ed. by A. Nusrat, pp. 4826–4836.
- Hunter, P and J Pines (1994). 'Cyclins and cancer II: Cyclin D and CDK inhibitors come of age.' In: *Cell* 79, pp. 573–582.
- Hurford, R, D Cobrinik, M Lee, and N Dyson (1997). 'pRB and p107/p130 are required for the regulated expression of different sets of E2F responsive genes.' In: *Genes Dev* 11, pp. 1447–1463.
- Islas, S., J. Vega, L. Ponce, and L. González-Mariscal (2002). 'Nuclear localization of the tight junction protein ZO-2 in epithelial cells.' In: *Exp. Cell Res.* 274, pp. 138–148.
- Iwai, N, K Kitajima, K Sakai, T Kimura, and T Nakano (2001). 'Alteration of cell adhesion and cell cycle properties of ES cells by an inducible dominant interfering Myb mutant.' In: *Oncogene* 20, pp. 1425–1434.
- Jaramillo, B., A. Ponce, J. Moreno, A. Betanzos, M. Huerta, E. Lopez-Bayghen, and L. González-Mariscal (2004). 'Characterization of the tight junction protein ZO-2 localized at the nucleus of epithelial cells'. In: *Exp. Cell Res.* 297, pp. 247–258.
- Kamb, A, N Gruis, J Weaver-Feldhaus, Q Liu, K Harshman, S Tavtigian, E Stockert, R Day, B Johnson, and M Skolnick (1994). 'A cell cycle regulator potentially involved in genesis of many tumor types.' In: *Science* 264, pp. 436–440.
- Karin, M, L. Zg, and E Zandi (1997). 'AP-1 function and regulation'. In: *Curr. Opin. Cell Biol.* 9, pp. 240–246.
- Katzen, A., J. Jackson, B. Harmon, S.-M. Fung, G. Ramsay, and J Bishop (1998). 'Drosophila myb is required for the G2/M transition and maintenance of diploidy.' In: *Genes Dev.* 12, pp. 831–843.
- Kim, J., A. Cantor, S. Orkin, and J. Wang (2009). 'Use of in vivo biotinylation to study protein-protein and protein-DNA interactions in mouse embryonic stem cells.' In: *Nature protocols* 4, pp. 506–17.

References

- Kimura, M., C. Uchida, Y. Takano, M. Kitagawa, and Y. Okano (2004). 'Cell cycle-dependent regulation of the human aurora B promoter.' In: *Biochem. Biophys. Res. Commun.* 316, pp. 930–936.
- Knight A Sand Notaridou, M and R Watson (2009). 'A Lin-9 complex is recruited by B-Myb to activate transcription of G2/M genes in undifferentiated embryonal carcinoma cells.' In: *Oncogene* 28, pp. 1737–47.
- Koledova, Z., L. Kafkova, L. Calabkova, V. Krystof, P. Dolezel, and V. Divoky (2010). 'Cdk2 inhibition prolongs G1 phase progression in mouse embryonic stem cells.' In: *Stem Cells Dev.* 19, pp. 181–194.
- Korenjak, M., B. Taylor-Harding, U. Binné, J. Satterlee, O. Stevaux, R. Aasland, H. White-Cooper, N. Dyson, and A. Brehm (2004). 'Native E2F/RBF complexes contain Myb-interacting proteins and repress transcription of developmentally controlled E2F target genes.' In: *Cell* 119, pp. 181–193.
- Kouzarides, T. (2007). 'Chromatin modifications and their function.' In: *Cell* 128, pp. 693–705.
- Kusch, A., S. Tkachuk, N. Tkachuk, M. Patecki, J.-K. Park, R. Dietz, H. Haller, and I. Dumler (2009). 'The tight junction protein ZO-2 mediates proliferation of vascular smooth muscle cells via regulation of Stat1.' In: *Cardiovasc. Res.* 83, pp. 115–22.
- Laemmli, U (1970). 'Cleavage of structural proteins during the assembly of the head of bacteriophage T4.' In: *Nature* 227, pp. 680–685.
- Lam, E and R Watson (1993). 'An E2F-binding site mediates cell-cycle regulated repression of mouse B-myb transcription.' In: *EMBO J.* 12, pp. 2705–2713.
- Lam, E, J Bennett, and R Watson (1995). 'Cell-cycle regulation of human B-myb transcription.' In: *Gene* 160, pp. 277–281.
- Lange, C., W. B. Huttner, and F. Calegari (2009). 'Cdk4/cyclinD1 overexpression in neural stem cells shortens G1, delays neurogenesis, and promotes the generation and expansion of basal progenitors.' In: *Cell stem cell* 5, pp. 320–31.
- LeCouter, J, P Whyte, and M Rudnicki (1996). 'Cloning and expression of the Rb-related mouse p130 mRNA.' In: *Oncogene* 12, pp. 1433–1440.
- Lee, H., K. Ohno, Y. Voskoboynik, L. Ragusano, A. Martinez, and D. Dimova (2010). 'Drosophila RB proteins repress differentiation-specific genes via two different mechanisms.' In: *Mol. Cell. Biol.* 30, pp. 2563–2577.
- Lee, T., R. Jenner, L. Boyer, M. Guenther, S. Levine, R. Kumar, B. Chevalier, S. Johnstone, M. Cole, K.-i. Isono, and et al. (2006). 'Control of developmental regulators by Polycomb in human embryonic stem cells.' In: *Cell* 125, pp. 301–313.
- Lewis, P., E. Beall, T. Fleischer, D. Georgette, A. Link, and M. Botchan (2004). 'Identification of a Drosophila Myb-E2F2/RBF transcriptional repressor complex'. In: *Genes Dev.* 18, pp. 2929–2940.
- Li, J., G. Pan, K. Cui, Y. Liu, S. Xu, and D. Pei (2007). 'A dominant-negative form of mouse SOX2 induces trophectoderm differentiation and progressive polyploidy in mouse embryonic stem cells.' In: *J. Biol. Chem.* 282, pp. 19481–19492.
- Li, X and R Nicklas (1995). 'Mitotic forces control a cell-cycle checkpoint.' In: *Nature* 373, pp. 630–632.

References

- Li, Y. and R. Sousa (2012). 'Expression and purification of E. coli BirA biotin ligase for in vitro biotinylation.' In: *Protein Expr. Purif.* 82, pp. 162–7.
- Lipinski, M and T Jacks (1999). 'The retinoblastoma gene family in differentiation and development.' In: *Oncogene* 18, pp. 7873–82.
- Litovchick, L., S. Sadasivam, L. Florens, X. Zhu, S. Swanson, S. Velmurugan, R. Chen, M. Washburn, X Liu, and J. DeCaprio (2007). 'Evolutionarily conserved multisubunit RBL2/p130 and E2F4 protein complex represses human cell cycle-dependent genes in quiescence.' In: *Mol. Cell* 26, pp. 539–51.
- Loh, Y.-H., Q. Wu, J.-L. Chew, V. Vega, W. Zhang, X. Chen, G. Bourque, J. George, B. Leong, J. Liu, and et al. (2006). 'The Oct4 and Nanog transcription network regulates pluripotency in mouse embryonic stem cells.' In: *Nat. Genet.* 38, pp. 431–440.
- Lorvellec, M., S. Dumon, A. Maya-Mendoza, D. Jackson, J. Frampton, and P. García (2010). 'B-Myb is critical for proper DNA duplication during an unperturbed S phase in mouse embryonic stem cells.' In: *Stem Cells* 28, pp. 1751–9.
- Lu, L.-Y., J. Wood, K. Minter-Dykhouse, L. Ye, T. Saunders, X. Yu, and J. Chen (2008). 'Polo-like kinase 1 is essential for early embryonic development and tumor suppression.' In: *Mol. Cell. Biol.* 28, pp. 6870–6876.
- Lucibello, F, M Truss, J Zwicker, F Ehlert, M Beato, and R Müller (1995). 'Periodic cdc25C transcription is mediated by a novel cell cycle-regulated repressor element (CDE).' In: *EMBO J* 14, pp. 132–142.
- Mac Auley, A, Z Werb, and P Mirkes (1993). 'Characterization of the unusually rapid cell cycles during rat gastrulation.' In: *Development* 117, pp. 873–883.
- Malumbres, M and M Barbacid (2001). 'To cycle or not to cycle: a critical decision in cancer.' In: *Nat. Rev. Cancer* 1, pp. 222–231.
- Manak, J, N. Mitiku, and J. Lipsick (2002). 'Mutation of the Drosophila homologue of the Myb protooncogene causes genomic instability.' In: *Proc. Natl. Acad. Sci. U. S. A.* 99, pp. 7438–7443.
- Mannefeld, M., E. Klassen, and S. Gaubatz (2009). 'B-MYB is required for recovery from the DNA damage-induced G2 checkpoint in p53 mutant cells.' In: *Cancer Res* 69, pp. 4073–80.
- Mao, X., G. Orchard, D. Lillington, R. Russell-Jones, B. Young, and S. Whittaker (2003). 'Amplification and overexpression of JUNB is associated with primary cutaneous T-cell lymphomas.' In: *Blood* 101, pp. 1513–1519.
- Margueron, R. and D. Reinberg (2011). 'The Polycomb complex PRC2 and its mark in life.' In: *Nature* 469, pp. 343–349.
- Martin, G (1981). 'Isolation of a pluripotent cell line from early mouse embryos cultured in medium conditioned by teratocarcinoma stem cells.' In: *Proc. Natl. Acad. Sci. U. S. A.* 78, pp. 7634–7638.
- Martínez-Balbás, M., T. Tsukiyama, D. Gdula, and C. Wu (1998). 'Drosophila NURF-55, a WD repeat protein involved in histone metabolism'. In: *Proc. Natl. Acad. Sci. U. S. A.* 95, pp. 132–137.
- Matsuda, T, T Nakamura, K Nakao, T Arai, M Katsuki, T Heike, and T Yokota (1999). 'STAT3 activation is sufficient to maintain an undifferentiated state of mouse embryonic stem cells.' In: *EMBO J* 18, pp. 4261–4269.

References

- Matsushime, H, M Ewen, D Strom, J Kato, S Hanks, M Roussel, and C Sherr (1992). 'Identification and properties of an atypical catalytic subunit (p34PSK-J3/cdk4) for mammalian D type G1 cyclins.' In: *Cell* 71, pp. 323–334.
- Meshorer, E. and T. Misteli (2006). 'Chromatin in pluripotent embryonic stem cells and differentiation.' In: *Nat. Rev. Mol. Cell Biol.* 7, pp. 540–546.
- Meshorer, E., D. Yellajoshula, E. George, P. Scambler, D. Brown, and T. Misteli (2006). 'Hyperdynamic plasticity in pluripotent embryonic of chromatin proteins stem cells'. In: *Dev. Cell* 10, pp. 105–116.
- Meyerson, M and E Harlow (1994). 'Identification of G1 kinase activity for cdk6, a novel cyclin D partner.' In: *Mol. Cell. Biol.* 14, pp. 2077–2086.
- Mikkelsen, T., M. Ku, D. Jaffe, B. Issac, E. Lieberman, G. Giannoukos, P. Alvarez, W. Brockman, T.-K. Kim, R. Koche, and et al. (2007). 'Genome-wide maps of chromatin state in pluripotent and lineage-committed cells.' In: *Nature* 448, pp. 553–560.
- Mitsui, K, Y Tokuzawa, H. Itoh, K Segawa, M. Murakami, K Takahashi, M Maruyama, M Maeda, and S Yamanaka (2003). 'The homeoprotein Nanog is required for maintenance of pluripotency in mouse epiblast and ES cells.' In: *Cell* 113, pp. 631–642.
- Moberg, K, M Starz, and J Lees (1996). 'E2F-4 switches from p130 to p107 and pRB in response to cell cycle reentry.' In: *Mol. Cell. Biol.* 16, pp. 1436–1449.
- Morgan, D. (1995). 'Principles of CDK regulation.' In: *Nature* 374, pp. 131 –134.
- Morgan, D (1999). 'Regulation of the APC and the exit from mitosis.' In: *Nat. Cell Biol.* 1, E47–E53.
- Morgan, D. (1997). 'Cyclin-dependant kinases : Engines , Clocks , and Microprocessors'. In: *Cell* 13, pp. 261–91.
- Morgan, D. (2007). *The Cell Cycle: Principles of Control*. Primers in biology. New Science Press. ISBN: 9780878935086.
- Mucenski, M, K McLain, A Kier, S Swerdlow, C Schreiner, T Miller, D Pietryga, W Scott, and S Potter (1991). 'A functional c-myb gene is required for normal murine fetal hepatic hematopoiesis.' In: *Cell* 65, pp. 677–689.
- Müller, G, M. Quaas, M Schümann, E Krause, M Padi, M Fischer, L Litovchick, J Decaprio, and K Engeland (2011). 'The CHR promoter element controls cell cycle-dependent gene transcription and binds the DREAM and MMB complexes.' In: *Nucleic Acids Res.* 40, pp. 1561–1578.
- Murphy, M, M Stinnakre, C Senamaud-Beaufort, N Winston, C Sweeney, M Kubelka, M Carrington, C Bréchet, and J Sobczak-Thépot (1997). 'Delayed early embryonic lethality following disruption of the murine cyclin A2 gene.' In: *Nat. Genet.* 15, pp. 83–86.
- Nichols, J, B Zevnik, K Anastasiadis, H Niwa, D Klewe-Nebenius, I Chambers, H Schöler, and A Smith (1998). 'Formation of pluripotent stem cells in the mammalian embryo depends on the POU transcription factor Oct4.' In: *Cell* 95, pp. 379–391.
- Niwa, H., J. Miyazaki, and A. Smith (2000). 'Quantitative expression of Oct-3/4 defines differentiation, dedifferentiation or self-renewal of ES cells.' In: *Nat Genet* 24, pp. 372–6.
- Niwa, H., T. Burdon, I. Chambers, and A. G. Smith (1998). 'Self-renewal of pluripotent embryonic stem cells is mediated via activation of STAT3.' In: *Genes Dev.* 12, pp. 2048–2060.

References

- Nomura, N, M Takahashi, M Matsui, S Ishii, T Date, S Sasamoto, and R Ishizaki (1988). 'Isolation of human cDNA clones of myb-related genes, A-myb and B-myb.' In: *Nucleic Acids Res.* 16, pp. 11075–11089.
- Novitch, B, D Spicer, P Kim, W Cheung, and A Lassar (1999). 'pRb is required for MEF2-dependent gene expression as well as cell-cycle arrest during skeletal muscle differentiation.' In: *Curr. Biol.* 9, pp. 449–459.
- Ogawa, H., K.-I. Ishiguro, S. Gaubatz, D. Livingston, and Y. Nakatani (2002). 'A complex with chromatin modifiers that occupies E2F- and Myc-responsive genes in G0 cells.' In: *Science* 296, pp. 1132–6.
- Oh, I and E Reddy (1998). 'The C-terminal domain of B-Myb acts as a positive regulator of transcription and modulates its biological functions.' In: *Mol. Cell. Biol.* 18, pp. 499–511.
- Oka, T., E. Remue, K. Meerschaert, B. Vanloo, C. Boucherie, D. Gfeller, G. Bader, S. Sidhu, J. Vandekerckhove, J. Gettemans, and et al. (2010). 'Functional complexes between YAP2 and ZO-2 are PDZ domain-dependent, and regulate YAP2 nuclear localization and signalling.' In: *Biochem. J.* 432, pp. 461–472.
- Okada, M., H. Akimaru, D.-X. Hou, T. Takahashi, and S. Ishii (2002). 'Myb controls G2/M progression by inducing cyclin B expression in the Drosophila eye imaginal disc'. In: *EMBO J.* 21, pp. 675–684.
- Orford, K. and D. Scadden (2008). 'Deconstructing stem cell self-renewal: genetic insights into cell-cycle regulation.' In: *Nature Reviews Genetics* 9, pp. 115–128.
- O'Shea, K (2004). 'Self-renewal vs. differentiation of mouse embryonic stem cells.' In: *Biology of reproduction* 71, pp. 1755–65.
- Osterloh, L., B. von Eyss, F. Schmit, L. Rein, D. Hübner, B. Samans, S. Hauser, and S. Gaubatz (2007). 'The human synMuv-like protein LIN-9 is required for transcription of G2/M genes and for entry into mitosis.' In: *EMBO J.* 26, pp. 144–57.
- Palmieri, S, W Peter, H Hess, and H Schöler (1994). 'Oct-4 transcription factor is differentially expressed in the mouse embryo during establishment of the first two extraembryonic cell lineages involved in implantation.' In: *Dev Biol* 166, pp. 259–267.
- Pardee, A. (1974). 'A restriction point for control of normal animal cell proliferation.' In: *Proc. Natl. Acad. Sci. U. S. A.* 71, pp. 1286–1290.
- Patterton, D and A Wolffe (1996). 'Developmental roles for chromatin and chromosomal structure.' In: *Dev. Biol.* 173, pp. 2–13.
- Pavletich, N (1999). 'Mechanisms of cyclin-dependent kinase regulation: structures of Cdks, their cyclin activators, and Cip and INK4 inhibitors.' In: *J. Mol. Biol.* 287, pp. 821–828.
- Perera, D., V. Tilston, J. Hopwood, M. Barchi, R. Boot-Handford, and S. Taylor (2007). 'Bub1 maintains centromeric cohesion by activation of the spindle checkpoint.' In: *Dev. Cell* 13, pp. 566–579.
- Pesce, M and H Schöler (2001). 'Oct-4: gatekeeper in the beginnings of mammalian development.' In: *Stem Cells* 19, pp. 271–278.
- Pilkinton, M, R Sandoval, and O Colamonici (2007). 'Mammalian Mip/LIN-9 interacts with either the p107, p130/E2F4 repressor complex or B-Myb in a cell cycle-phase-

References

- dependent context distinct from the Drosophila dREAM complex.' In: *Oncogene* 26, pp. 7535–7543.
- Planas-Silva, M and R Weinberg (1997). 'The restriction point and control of cell proliferation.' In: *Curr. Opin. Cell Biol.* 9, pp. 768–772.
- Porter, L. and D. Donoghue (2003). 'Cyclin B1 and CDK1: nuclear localization and upstream regulators.' In: *Prog. Cell Cycle Res.* 5, pp. 335–347.
- Putkey, F., T. Cramer, M. Morphew, A. Silk, R. Johnson, J McIntosh, and D. Cleveland (2002). 'Unstable kinetochore-microtubule capture and chromosomal instability following deletion of CENP-E.' In: *Dev. Cell* 3, pp. 351–365.
- Raschella, G, A Negroni, A Sala, S Pucci, A Romeo, and B Calabretta (1995). 'Requirement of b-myb function for survival and differentiative potential of human neuroblastoma cells'. In: *J. Biol. Chem.* 270, pp. 8540–8545.
- Raschella, G, V Cesi, R Amendola, A Negroni, B Tanno, P Altavista, G Tonini, B De Bernardi, and B Calabretta (1999). 'Expression of B-myb in neuroblastoma tumors is a poor prognostic factor independent from MYCN amplification.' In: *Cancer Research* 59, pp. 3365–3368.
- Rayman, J., Y. Takahashi, V. Indjeian, J.-H. Dannenberg, S. Catchpole, R. Watson, H. Te Riele, and B. Dynlacht (2002). 'E2F mediates cell cycle-dependent transcriptional repression in vivo by recruitment of an HDAC1/mSin3B corepressor complex'. In: *Genes Dev* 16, pp. 933–947.
- Reichert, N., S. Wurster, T. Ulrich, K. Schmitt, S. Hauser, L. Probst, R. Götz, F. Ceteci, R. Moll, U. Rapp, and S. Gaubatz (2010). 'Lin9, a subunit of the mammalian DREAM complex, is essential for embryonic development, for survival of adult mice, and for tumor suppression.' In: *Mol. Cell. Biol.* 30, pp. 2896–908.
- Reisman, D, S Glaros, and E Thompson (2009). 'The SWI/SNF complex and cancer.' In: *Oncogene* 28, pp. 1653–1668.
- Remue, E., K. Meerschaert, T. Oka, C. Boucherie, J. Vandekerckhove, M. Sudol, and J. Gettemans (2010). 'TAZ interacts with zonula occludens-1 and -2 proteins in a PDZ-1 dependent manner.' In: *FEBS Lett.* 584, pp. 4175–80.
- Renz, A and F Fackelmayer (1996). 'Purification and molecular cloning of the scaffold attachment factor B (SAF-B), a novel human nuclear protein that specifically binds to S/MAR-DNA.' In: *Nucleic Acids Res.* 24, pp. 843–849.
- Ringrose, L., H. Ehret, and R. Paro (2004). 'Distinct contributions of histone H3 lysine 9 and 27 methylation to locus-specific stability of polycomb complexes.' In: *Mol. Cell* 16, pp. 641–653.
- Robinson, C, Y Light, R Groves, D Mann, R Marias, and R Watson (1996). 'Cell-cycle regulation of B-Myb protein expression: specific phosphorylation during the S phase of the cell cycle.' In: *Oncogene* 12, pp. 1855–1864.
- Russo, A, P Jeffrey, and N Pavletich (1996). 'Structural basis of cyclin-dependent kinase activation by phosphorylation.' In: *Nat. Struct. Biol.* 3, pp. 696–700.
- Savatier, P, S Huang, L Szekely, K Wiman, and J Samarut (1994). 'Contrasting patterns of retinoblastoma protein expression in mouse embryonic stem cells and embryonic fibroblasts.' In: *Oncogene* 9, pp. 809–818.

References

- Savatier, P, H Lapillonne, L Van Grunsven, B Rudkin, and J Samarut (1996). 'Mutational analysis of the p16 family cyclin-dependent kinase inhibitors p15INK4b and p18INK4c in tumor-derived cell lines and primary tumors.' In: *Oncogene* 12, pp. 309–322.
- Saville, M and R Watson (1998). 'The cell-cycle regulated transcription factor B-Myb is phosphorylated by cyclin A/Cdk2 at sites that enhance its transactivation properties.' In: *Oncogene* 17, pp. 2679–89.
- Schmit, F., M. Korenjak, M. Mannefeld, K. Schmitt, C. Franke, B. von Eyss, S. Gargica, F. Hänel, A. Brehm, and S. Gaubatz (2007). 'LINC, a human complex that is related to pRB-containing complexes in invertebrates regulates the expression of G2/M genes.' In: *Cell cycle (Georgetown, Tex.)* 6, pp. 1903–13.
- Schmit, F., S. Cremer, and S. Gaubatz (2009). 'LIN54 is an essential core subunit of the DREAM/LINC complex that binds to the cdc2 promoter in a sequence-specific manner.' In: *The FEBS journal* 276, pp. 5703–5716.
- Shaulian, E. and M. Karin (2002). 'AP-1 as a regulator of cell life and death.' In: *Nat. Cell Biol.* 4, E131–6.
- Sherr, C (1994). 'The ins and outs of RB: coupling gene expression to the cell cycle clock.' In: *Trends Cell Biol.* 4, pp. 15–18.
- Sherr, C and J Roberts (1999). 'CDK inhibitors: positive and negative regulators of G1-phase progression.' In: *Genes Dev.* 13, pp. 1501–1512.
- Sim, C., S. Perry, S. Tharadra, J. Lipsick, and A. Ray (2012). 'Epigenetic regulation of olfactory receptor gene expression by the Myb-MuvB/dREAM complex.' In: *Genes Dev* 26, pp. 2483–2498.
- Sitzmann, J, K Noben-Trauth, H Kamano, and K Klempnauer (1996). 'Expression of B-Myb during mouse embryogenesis.' In: *Oncogene* 12, pp. 1889–1894.
- Smith, A, J Heath, D Donaldson, G Wong, J Moreau, M Stahl, and D Rogers (1988). 'Inhibition of pluripotential embryonic stem cell differentiation by purified polypeptides.' In: *Nature* 336, pp. 688–690.
- Song, J.-J., J. Garlick, and R. Kingston (2008). 'Structural basis of histone H4 recognition by p55.' In: *Genes Dev.* 22, pp. 1313–1318.
- Sourisseau, T., A. Georgiadis, A. Tsapara, R. Ali, R. Pestell, K. Matter, and M. Balda (2006). 'Regulation of PCNA and Cyclin D1 Expression and Epithelial Morphogenesis by the ZO-1-Regulated Transcription Factor ZONAB/DbpA'. In: *Mol. Cell. Biol.* 26, pp. 2387–2398.
- Stead, E., J. White, R. Faast, S. Conn, S. Goldstone, J. Rathjen, U. Dhingra, P. Rathjen, D. Walker, and S. Dalton (2002). 'Pluripotent cell division cycles are driven by ectopic Cdk2, cyclin A/E and E2F activities.' In: *Oncogene* 21, pp. 8320–33.
- Tanaka, Y, N Patestos, T Maekawa, and S Ishii (1999). 'B-myb is required for inner cell mass formation at an early stage of development.' In: *J. Biol. Chem.* 274, pp. 28067–28070.
- Tanner, M, S Grenman, A Koul, O Johannsson, P Meltzer, T Pejovic, A Borg, and J Isola (2000). 'Frequent amplification of chromosomal region 20q12-q13 in ovarian cancer.' In: *Clin. Cancer Res.* 6, pp. 1833–1839.
- Tapia, R., M. Huerta, S. Islas, A. Avila-flores, E. Lopez-bayghen, O. Huber, and L. González-Mariscal (2009). 'Zona Occludens-2 Inhibits Cyclin D1 Expression and Cell Prolifera-

References

- tion and Exhibits Changes in Localization along the Cell Cycle.' In: *Mol. Biol. Cell* 20, pp. 1102–1117.
- Tarasov, K., Y. Tarasova, W. Tam, D. Riordon, S. Elliott, G. Kania, J. Li, S. Yamanaka, D. Crider, G. Testa, R. Li, B. Lim, C. Stewart, Y. Liu, J. Van Eyk, R. Wersto, A. Wobus, and K. Boheler (2008). 'B-MYB is essential for normal cell cycle progression and chromosomal stability of embryonic stem cells.' In: *PLoS one* 3, e2478.
- Thorner, A, K Hoadley, J Parker, S Winkel, R Millikan, and C Perou (2009). 'In vitro and in vivo analysis of B-Myb in basal-like breast cancer.' In: *Oncogene* 28, pp. 742–751.
- Tommasi, S and G Pfeifer (1995). 'In vivo structure of the human cdc2 promoter: release of a p130-E2F-4 complex from sequences immediately upstream of the transcription initiation site coincides with induction of cdc2 expression.' In: *Mol. Cell. Biol.* 15, pp. 6901–6913.
- Toscani, A, R Mettus, R Coupland, H Simpkins, J Litvin, J Orth, K Hatton, and E Reddy (1997). 'Arrest of spermatogenesis and defective breast development in mice lacking A-myb.' In: *Nature* 386, pp. 713–717.
- Trauth, K, B Mutschler, N Jenkins, D Gilbert, N Copeland, and K Klempnauer (1994). 'Mouse A-myb encodes a trans-activator and is expressed in mitotically active cells of the developing central nervous system, adult testis and B lymphocytes.' In: *EMBO J* 13, pp. 5994–6005.
- Traweger, A., R. Fuchs, I. Krizbai, T. M. Weiger, H.-C. Bauer, and H. Bauer (2003). 'The tight junction protein ZO-2 localizes to the nucleus and interacts with the heterogeneous nuclear ribonucleoprotein scaffold attachment factor-B.' In: *J. Biol. Chem.* 278, pp. 2692–700.
- Traweger, A., C. Lehner, A. Farkas, I. Krizbai, H. Tempfer, E. Klement, B. Guenther, H.-C. Bauer, and H. Bauer (2008). 'Nuclear Zonula occludens-2 alters gene expression and junctional stability in epithelial and endothelial cells.' In: *Differentiation* 76, pp. 99–106.
- Trimarchi, J., B. Fairchild, R. Verona, K. Moberg, N. Andon, and J. Lees (1998). 'E2F-6, a member of the E2F family that can behave as a transcriptional repressor.' In: *Proc. Natl. Acad. Sci. U. S. A.* 95, pp. 2850–2855.
- Trimarchi, J., B. Fairchild, J. Wen, and J. Lees (2001). 'The E2F6 transcription factor is a component of the mammalian Bmi1-containing polycomb complex'. In: *Proc. Natl. Acad. Sci. U. S. A.* 98, pp. 1519–1524.
- Trojer, P., G. Li, R. Sims, A. Vaquero, N. Kalakonda, P. Boccuni, D. Lee, H. Erdjument-Bromage, P. Tempst, S. Nimer, and et al. (2007). 'L3MBTL1, a histone-methylation-dependent chromatin lock.' In: *Cell* 129, pp. 915–928.
- Tyers, M and P Jorgensen (2000). 'Proteolysis and the cell cycle: with this RING I do thee destroy.' In: *Current opinion in genetics development* 10, pp. 54–64.
- Tyler, J, M Bulger, R Kamakaka, R Kobayashi, and J Kadonaga (1996). 'The p55 subunit of Drosophila chromatin assembly factor 1 is homologous to a histone deacetylase-associated protein.' In: *Mol. Cell. Biol.* 16, pp. 6149–6159.
- Uren, A, L Wong, M Pakusch, K Fowler, F Burrows, D Vaux, and K Choo (2000). 'Survivin and the inner centromere protein INCENP show similar cell-cycle localization and gene knockout phenotype.' In: *Curr. Biol.* 10, pp. 1319–1328.

References

- Verona, R, K Moberg, S Estes, M Starz, J Vernon, and J Lees (1997). 'E2F activity is regulated by cell cycle-dependent changes in subcellular localization.' In: *Mol. Cell. Biol.* 17, pp. 7268–7282.
- Vidal, A and A Koff (2000). 'Cell-cycle inhibitors: three families united by a common cause.' In: *Gene* 247, pp. 1–15.
- Walker, D and J Maller (1991). 'Role for cyclin A in the dependence of mitosis on completion of DNA replication.' In: *Nature* 354, pp. 314–317.
- Wang, X. and P. Yang (2008). 'In vitro differentiation of mouse embryonic stem (mES) cells using the hanging drop method.' In: *J vis exp* 48, pp. 2008–2008.
- Weitzer, G (2006). 'Embryonic stem cell-derived embryoid bodies: an in vitro model of eutherian pregastrulation development and early gastrulation.' In: *Handb Exp Pharmacol* 174, pp. 21–51.
- Wen, H., L. Andrejka, J. Ashton, R. Karess, and J. Lipsick (2008). 'Epigenetic regulation of gene expression by Drosophila Myb and E2F2-RBF via the Myb-MuvB/dREAM complex.' In: *Genes Dev.* 22, pp. 601–614.
- White, J., E. Stead, R. Faast, S. Conn, P. Cartwright, and S. Dalton (2005). 'Developmental Activation of the Rb and E2F Pathway and Establishment of Cell Cycle-regulated Cyclin-dependent Kinase Activity during Embryonic Stem Cell Differentiation'. In: *Mol. Biol. Cell* 16, pp. 2018–2027.
- Wittchen, E, J Haskins, and B Stevenson (1999). 'Protein interactions at the tight junction. Actin has multiple binding partners, and ZO-1 forms independent complexes with ZO-2 and ZO-3.' In: *J. Biol. Chem.* 274, pp. 35179–35185.
- Wobus, A. and K. Boheler (2005). 'Embryonic stem cells: prospects for developmental biology and cell therapy.' In: *Physiol Rev* 85, pp. 635–678.
- Wolter, P., K. Schmitt, M. Fackler, H. Kremling, L. Probst, S. Hauser, O. Gruss, and S. Gaubatz (2012). 'GAS2L3, a novel target gene of the dream complex, is required for proper cytokinesis and genomic stability.' In: *J. Cell Sci.* 125, pp. 2393–2406.
- Xu, J., P Kausalya, D. Phua, Z. Ali Safiahand Hossain, and W. Hunziker (2008). 'Early embryonic lethality of mice lacking ZO-2, but Not ZO-3, reveals critical and nonredundant roles for individual zonula occludens proteins in mammalian development.' In: *Mol. Cell. Biol.* 28, pp. 1669–1678.
- Yamanaka, S, J Li, G Kania, S Elliott, R Wersto, J Van Eyk, A Wobus, and K Boheler (2008). 'Pluripotency of embryonic stem cells.' In: *Cell Tissue Res.* 331, pp. 5–22.
- Yamauchi, T., T. Ishidao, T. Nomura, T. Shinagawa, Y. Tanaka, S. Yonemura, and S. Ishii (2008). 'A B-Myb complex containing clathrin and filamin is required for mitotic spindle function.' In: *The EMBO journal* 27, pp. 1852–62.
- Ying, Q., J. Nichols, I. Chambers, and A. Smith (2003). 'BMP induction of Id proteins suppresses differentiation and sustains embryonic stem cell self-renewal in collaboration with STAT3.' In: *Cell* 115, pp. 281–292.
- Zhan, M., D. Riordon, B. Yan, Y. Tarasova, S. Bruweleit, K. Tarasov, R. Li, R. Wersto, and K. Boheler (2012). 'The B-MYB Transcriptional Network Guides Cell Cycle Progression and Fate Decisions to Sustain Self-Renewal and the Identity of Pluripotent Stem Cells.' In: *PloS one* 7, e42350.

References

- Zhu, W., P. Giangrande, and J. Nevins (2004). 'E2Fs link the control of G1/S and G2/M transcription.' In: *EMBO J* 23, pp. 4615–4626.
- Zondervan, P, J Wink, J Alers, J IJzermans, S Schalm, R De Man, and H Van Dekken (2000). 'Molecular cytogenetic evaluation of virus-associated and non-viral hepatocellular carcinoma: analysis of 26 carcinomas and 12 concurrent dysplasias.' In: *J. Pathol.* 192, pp. 207–215.
- Zwicker, J, F Lucibello, L Wolfrain, C Gross, M Truss, K Engeland, and R Müller (1995). 'Cell cycle regulation of the cyclin A, cdc25C and cdc2 genes is based on a common mechanism of transcriptional repression.' In: *EMBO J* 14, pp. 4514–4522.

A. Appendix

A.1. Supplementary Data

See attached CD-ROM:

- Table S1. LIN9 regulated genes in ES cells
- Table S2. GO terms of downregulated genes after LIN9 kd
- Table S3. GO terms of upregulated genes after LIN9 kd
- Table S4. ChIP-on-chip peaks
- Table S5. Overlay LIN9 array and ChIPchip
- Table S6. GO terms: Overlap ChIPchip with downregulated genes from LIN9 array
- Table S7. Mass spectrometry data for BioLIN9 and BioB-MYB

A.2. Abbreviations

AP	Alkaline phosphatase
BioB-MYB	Biotag-B-MYB
BioLIN9	Biotag-LIN9
BrdU	Bromodeoxyuridine
CDE	Cell cycle-dependent element
CDK	Cyclin-dependent kinase
CDKi	CDK inhibitor
ChIP	Chromatin immunoprecipitation
ChIPchip	ChIP-on-chip
CHR	Cell cycle genes homology
CHX	Cycloheximid
Co-IP	Co-immunoprecipitation
Ctrl	Control

A. Appendix

DNA	Deoxyribonucleic acid
dpc	Days post coitum
DREAM	Drosophila RBF, dE2F2 and dMyb-interacting proteins
EB	Embryoid body
EC	Embryonic carcinoma
EG	Embryonic germ
ES	Embryonic stem
ESB	Electrophoresis sample buffer
ESC	Embryonic stem cell
FCS	Fetal calf serum
FDR	False discovery rate
fig	Figure
G	Gap phase
GO	Gene Ontology
h	Hours
HDAC	Histone deacetylase
hpt	Hours past transfection
HU	Hydroxyurea
ICM	Inner cell mass
IP	Immunoprecipitation
kd	knock down
LB	Luria Bertani
MAGUK	Membrane-associated guanylate kinase
MassSpec	Mass spectrometry
MDCK	Madin-Darby canine kidney
me3	Trimethylation
MEF	Mouse embryonic fibroblasts
MMB	Myb-MuvB
MPF	Mitosis-promoting factor
M-phase	Mitosis
MPM2	Mitotic protein #2
Myb	Myeloblastosis
MS	Massenspektrometrie
NEAA	Non essential amino acids
Neb	Nuclear extract buffer
NSC	Neuronal stem cell

A. Appendix

NuRD	Nucleosome remodeling and deacetylating factor
NuRF	Nucleosome remodeling factor
PBS	Phosphate buffered saline
PcG	Polycomb group
PCR	Polymerase chain reaction
PDZ	Post synaptic density 95/disc-large/zona occludens
PI	Propidium-iodide
poly-HEMA	poly(2-hydroxyethyl methacrylate)
pRB	Retinoblastoma
PRC	Polycomb repressor complex
qRT-PCR	Quantitative real-time PCR
RNA	Ribonucleic acid
RNAi	RNA interference
RT	Room temperature/Reverse transcriptase
SAFB	Scaffold attachment factor-B
SDS-PAGE	SDS-polyacrylamide gel electrophoresis
shRNA	Short-hairpin RNA
SILAC	Stable isotope labeling by amino acids in cell culture
siRNA	Small interfering RNA
S-phase	Synthesis phase
tab	Table
TJ	Tight junction
TJP	Tight junction protein
VSMC	vascular smooth muscle cells
ZO-2	Zona occludens protein 2
ZOP	Zona occludens protein

A.3. Own publications

- 2013 Esterlechner J, Reichert N, Iltzsche, Krause M, Finke F, Gaubatz S. LIN9, a Subunit of the DREAM Complex, Regulates Mitotic Gene Expression and Proliferation of Embryonic Stem Cells. PLoS One. 2013 May 7;8(5):e62882.
- 2010 Scrivano L, Esterlechner J, Mühlbacher H, Ettischer N, Hagen C, Grünewald K, Mohr CA, Ruzsics Z, Koszinowski U, Adler B. The m74 gene product of murine cytomegalovirus (MCMV) is a functional homolog of human CMV gO and determines the entry pathway of MCMV. J Virol. 2010 May;84(9):4469-80.

Conference contributions (Talks & Posters)

- 2012 Meeting Integrated Graduate College of the SFB Transregio 17, Kloster Schöntal
Talk Esterlechner J. DREAM complex: Finding new Binding Partners
- 2011 Joint Meeting of the SFB-Transregio 17 "Ras-dependent pathways in human cancer" with the LOEWE Research Cluster "Tumor and Inflammation"
Poster Esterlechner J, Nikolov M, Urlaub H, Gaubatz S. Characterization of the DREAM complex in mouse stem cells
- 2010 Meeting "The Puzzling World of Cancer", Integrated Graduate College of the SFB Transregio 17, Universität Würzburg
Poster Esterlechner J, Gaubatz S. Role of LIN9 in murine embryonal stem cells

A.4. Curriculum Vitae

Persönliche Angaben

Name	Jasmina Esterlechner
Adresse	Kaiserweg 4 97947 Grünsfeld
Geburtsdatum	01.12.1982
Geburtsort	Starnberg
Nationalität	Deutsch

Ausbildung

2008 - 2012	Dissertation im Labor von Prof. Dr. Stefan Gaubatz Institut für Physiologische Chemie I, Julius-Maximilians-Universität Würzburg Titel: Role of the DREAM complex in mouse embryonic stem cells and identification of ZO-2 as a new LIN9 interacting protein
2008	Master of Science Master Thesis am Lehrstuhl für Virologie der LMU München Titel: Vergleich der Genprodukte des humanen UL74 Leserahmens und des m74 Leserahmens des murinen Cytomegalievirus
2005-2008	Masterstudium Molekulare Biotechnologie an der Technischen Universität München
2005	Bachelor of Science Bachelor Thesis am Lehrstuhl für Physiologie der Technischen Universität München Titel: Establishment of a cholesterol efflux assay in cell culture
2002-2005	Bachelorstudium Molekulare Biotechnologie an der Technischen Universität München
1994-2002	Allgemeine Hochschulreife Max-Born-Gymnasium, Germering Gymnasium Weilheim in Obb.

A.5. Acknowledgments

First of all I want to thank Prof. Stefan Gaubatz for giving me the opportunity to work in his lab and for supervising my PhD thesis. I appreciate all the scientific support and helpful suggestions.

I also want to thank Prof. Krohne and Prof. Stigloher for being my supervisor from the faculty of biology.

Thanks to my lab members who made the every day work life so pleasant. Thanks for the motivation, help and advice: Tanja Ulrich, Piero Ocone, Kathrin Schmitt, Miriam Mannefeld, Fabian Iltzsche, Marc Fackler, Geeta Kumari, Patrick Wolter, Adelgunde Wolpert, Susi Spahr, Leona Probst. I am also grateful to Dr. Elmar Wolf from PCII, who helped me a lot with all the ChIPseq experiments.

A special thanks to my boyfriend Jochen, my sister Roswitha and my best friend Therese for supporting me in all situations, for cheering me up when I was down and giving me great feedback.

Last but not least I want to thank my parents who always believed in me and who I could always rely on.

A.6. Eidesstattliche Erklärung

Hiermit erkläre ich, Jasmina Esterlechner, geboren am 1. Dezember 1982 in Starnberg, an Eides statt, dass ich die vorliegende Dissertation selbständig verfasst habe und dabei keine anderen als die von mir angegebenen Hilfsmittel und Quellen benutzt habe. Zitate sind als solche gekennzeichnet.

Ich erkläre außerdem, dass die vorliegende Dissertation weder in gleicher noch in ähnlicher Form bereits in anderem Prüfungsverfahren vorgelegen hat.

Ich habe früher, außer den mit dem Zulassungsantrag urkundlich vorgelegten Graden, keine weiteren akademischen Grade erworben oder zu erwerben versucht.

Würzburg, 01. Juli 2013

.....
Jasmina Esterlechner